2023

UNRAVELING THE REGULATORY BASIS OF THE DESICCATION TOLERANCE TRAIT IN Selaginella lepidophylla

Madhavi Anuradha Ariyarathne Hewa Babarandhage

UNRAVELING THE REGULATORY BASIS OF THE DESICCATION TOLERANCE TRAIT IN *Selaginella lepidophylla*

By

Hewa Babarandhage Madhavi Anuradha Ariyarathne

B. S., Plant Biology, University of Sri Jayewardenepura, 2015

A Dissertation Submitted in Partial Fulfillment of
the Requirements for the Degree of Doctor of Philosophy

Department of Biology

Biological Sciences Program
In the Graduate School
The University of South Dakota
August 2023

The members of the Committee appointed to examine
the _Dissertation of Hewa Babarandhage Madhavi Anuradha Ariyarathne
find it satisfactory and recommend that it be accepted.

DocuSigned by:
Bernard W. M. Wone
F1C640F1C9D24D9...
Chairperson

DocuSigned by:
Karen L. Koster
6123132952CF48E...

DocuSigned by:
Mark D. Dixon
1C4CF6FFB73E4A8...

DocuSigned by:
Dr. Grigoriy Sereda
C05E271B3A6642B...

DocuSigned by:
0552F3745F6E47D...

Abstract

Desiccation tolerance was a crucial adaptation for plants during their transition to terrestrial environments. Some spike mosses, including *S. lepidophylla*, have evolved the remarkable ability to tolerate extreme desiccation, enabling survival in arid regions of the world. However, the regulatory basis of this trait remains unknown. This dissertation aims to unravel the genetic basis of desiccation tolerance in *Selaginella lepidophylla* and its potential for improving crop abiotic stress tolerance. To achieve this goal, three objectives were pursued. Objective 1 focused on determining the regulatory role of the *SlbHLH* transcription factor (TF) by overexpressing it in *Arabidopsis thaliana* to assess its impact on water-use efficiency, abiotic stress tolerance, growth, and development. Objective 2 aimed to develop a genetic transformation protocol for *Selaginella* species, enabling the study of regulatory genes in *S. lepidophylla* and other *Selaginella* species. Objective 3 involved identifying dehydration responsive genes from transcriptome of *S. lepidophylla* during dehydration, providing insights into the desiccation mechanism and potential candidate genes for improving drought tolerance in crops. Our findings as the first to functionally characterize a TF from the spike moss, *S. lepidophylla*, revealed that the *SlbHLH* TF plays a crucial regulatory role in plant growth, development, abiotic stress tolerance, and water-use efficiency. Moreover, the development of a transformation system for *Selaginella moellendorffii* enables the study of regulatory genes in desiccation-tolerant spike mosses, including *S. lepidophylla*, thereby enhancing our understanding of desiccation tolerance mechanisms. Furthermore, the identification of dehydration responsive genes associated with desiccation tolerance of *S. lepidophylla* provides valuable genomic resources for improving abiotic stress tolerance in crop plants. Altogether, this dissertation advances our understanding of the genetic basis of desiccation tolerance in *S. lepidophylla* and proposes practical approaches for enhancing crop abiotic stress tolerance. Furthermore, the development of a genetic transformation system for *Selaginella* and the transcriptomic analysis of *S. lepidophylla* provide essential tools and insights for studying desiccation tolerance mechanisms and regulatory networks, thus paving the way for future advancements in crop improvements and sustainable agriculture.

Dissertation Advisor 

Dr. Bernard W. M. Wone

Acknowledgment

Numerous individuals have played an indispensable role in the realization of this dissertation, providing invaluable support and unwavering encouragement throughout the entire process. First, I am deeply grateful for the exceptional support and guidance provided by my advisor, Dr. Bernie Wone, throughout my Ph.D. journey. From the very beginning, Dr. Wone demonstrated an unwavering belief in my potential, which opened numerous doors for me and allowed me to thrive as a researcher. His invaluable mentorship has played a pivotal role in both my academic and personal growth. Dr. Wone consistently encouraged me to explore my capabilities and step outside my comfort zone, always valuing and nurturing my ideas. I am very grateful to him for securing assistantships during my studies, which further enriched my experience. Being a part of Dr. Wone's lab is a true honor, and the transformative experiences and memories from this chapter of my life will be cherished forever.

I would like to thank Beate Wone for her kind support over the last five years. Throughout my Ph.D. journey, she was always there for me providing kind support during the most challenging moments. Moreover, I am grateful for her kind assistance me with my experiment plants.

I am sincerely grateful to Dr. Karen Koster, Dr. Jose Gonzalez, Dr. Mark Dixon, and Dr. Grigoriy Sereda for their investment of time and expertise as members of my dissertation committee. They have not only provided guidance and expertise for my research projects but have also contributed significantly to my career development. I cannot thank them enough for the profound impact they have had on my academic journey and professional path. All of their exceptional support is truly appreciated.

I am immensely grateful to Dr. Jake Kerby and the entire biology department for their support and resources that have facilitated my research and academic pursuits. The opportunities for growth that the department provided have been crucial in shaping my development as a researcher.

I'm deeply grateful for University of South Dakota, for providing me with endless opportunities, wonderful memories, and a transformative education. I am grateful for the remarkable experiences and cherish the time spent at University of South Dakota. I will carry the values and lessons learned here with me as I embark on the next chapter of my journey. Thank you, University of South Dakota.

I would like to express gratitude to the Cushman Lab at the University of Nevada, Reno, for their provision of transcription factor sequences in *Selaginella lepidophylla* and *Selaginella moellendorffii*. I am immensely grateful to Dr. Miyuraj Harishchandra and Dr. Pasan Fernando for their assistance with the RNA-seq analyses, which greatly enhanced the quality of my work. I would also like to extend my thanks to Kelly Graber, senior research associate of Sanford Research Imaging Core, for her invaluable support with confocal microscopy imaging. I am also thankful to my colleagues for supporting me and making the lab environment vibrant and enjoyable. Lastly, my sincere appreciation goes to the undergraduate students in the lab for their assistance with my experiments. I am deeply grateful for the collaborative efforts and contributions of all those involved in my research journey.

I would like to express my deepest appreciation to my husband Nisitha Wijewantha, who has been my rock and unwavering support throughout this entire process. Your love, patience, understanding, and belief in me and your constant reminders of my capabilities have been a driving force behind my achievements. This dissertation would not have been possible without your

presence by my side, and I am truly fortunate to have you by my side. I would also like to acknowledge the immense motivation and inspiration provided by our precious daughter, Chloe Wijewantha. Your presence in my life has brought immense joy and purpose, and you have been my biggest motivation to excel in my research and strive for success.

I am at a loss for words when it comes to expressing my immense gratitude to my parents, Nalani Samarakkodi and Muditha Ariyarathne. The love, unwavering support, and sacrifices you have made on my behalf are beyond measure. Your unconditional love, constant encouragement, and unwavering support have given me the strength and confidence to overcome challenges and pursue my dreams. You sacrificed so much to give me every opportunity to succeed, and I'm truly grateful for everything you both have done for me. Thank you will never be enough.

I would also like to extend my gratitude to my siblings Gangani Ariyarathne and Isuru Ariyarathne, in-laws, relatives, and friends for their continuous support, encouragement, and understanding throughout this journey. Finally, I would like to express my gratitude to all those who have directly or indirectly contributed to my research, provided valuable insights, or offered their support in any form. Your contributions have played a significant role in the completion of this dissertation.

Thank you all for being an integral part of my PhD journey and for making this achievement possible.

Table of Contents

COMMITTEE SIGNATURE PAGE----------**I**

ABSTRACT ---------- **II**

ACKNOWLEDGMENT---------- **III**

TABLE OF CONTENTS----------**VI**

LIST OF TABLES ---------- **XI**

LIST OF FIGURES----------**XII**

LIST OF EQUATIONS ----------**XVII**

CHAPTER 1----------**1**

INTRODUCTION ---------- 1

CHAPTER 2 : OVEREXPRESSION OF THE *SELAGINELLA LEPIDOPHYLLA* BHLH TRANSCRIPTION FACTOR ENHANCES WATER-USE EFFICIENCY, GROWTH, AND DEVELOPMENT IN *ARABIDOPSIS* ----------**4**

ABSTRACT----------4

2.1 INTRODUCTION ---------- 5

2.2 MATERIALS AND METHODS ---------- 8

2.2.1 Sequence analysis of SlbHLH$_{opt}$----------*8*

2.2.2 Subcloning the codon-optimized SlbHLH gene into plasmid vectors ---------- *9*

2.2.3 Transformation of Arabidopsis and identification of homozygous SlbHLH$_{opt}$ overexpressing lines ---------- *10*

2.2.4 Analysis of SlbHLH$_{opt}$ gene expression ---------- *10*

2.2.5 Plant growth conditions and phenotypic characterization ---------- *11*

2.2.6 Determination of subcellular localization of SlbHLH$_{opt}$-sGFP expression ---------- *12*

2.2.7 Analysis of integrated water-use efficiency ---------- *12*

2.2.8 Assays of in vitro seed germination in SlbHLH$_{opt}$-overexpressing lines under abiotic stress conditions ---------- *13*

2.2.9 Assay of in vitro NaCl stress in SlbHLH$_{opt}$-overexpressing lines ---------- *14*

2.2.10 Determination of total flavonoid content ---------- *14*

2.3 RESULTS ---------- 15

2.3.1 Phylogenetic analysis of the SlbHLH$_{opt}$ protein ---------- *15*

2.3.2 SlbHLH$_{opt}$ protein is localized to the nucleus ---------- *15*

2.3.3 SlbHLH$_{opt}$ overexpression enhances plant growth and development ---------- *19*

2.3.4 SlbHLHopt overexpression increases integrated water-use efficiency ---------- *19*

2.3.5 SlbHLH$_{opt}$ overexpression improves rates of seed germination and green cotyledon emergence under water-deficit stress and salinity stress ---------- *21*

2.3.6 SlbHLHopt overexpression results in enhanced tolerance to salinity stress conditions at the seedling stage ---------- *23*

2.3.7 SlbHLH$_{opt}$ overexpression enhances flavonoid accumulation ---------- *24*

2.4. DISCUSSION ---------- 25

2.5 CONCLUSIONS ---------- 30

2.6 FUNDING ---------- 30

2.7 ACKNOWLEDGEMENTS ---------- 31

CHAPTER 3 : DEVELOPING A GENETIC TRANSFORMATION SYSTEM FOR THE *SELAGINELLA MOELLENDORFFII* USING NANOHYDROXYAPATITE RODS ------ 32

ABSTRACT ---------- 32

3.1 INTRODUCTION ---------- 33

3.2 MATERIALS AND METHODS ---------- 35

3.2.1 Synthesis of arginine-functionalized nanohydroxyapatite particles ---------- 35

3.2.2 Plant growth ---------- 36

3.2.3 Arginine-functionalized nanohydroxyapatite particle–mediated delivery of GFP and GUS reporter genes in S. moellendofii sporophylls ---------- 36

3.2.4 Arginine-functionalized nanohydroxyapatite particle – mediated delivery of eYGFPuv reporter gene in S. moellendofii sporophylls ---------- 38

3.2.5 Characterization of Conjugates and sample preparation ---------- 39

3.2.6 Agarobacterium mediated delivery of GUS reporter gene ---------- 41

3.3 RESULTS ---------- 43

3.3.1 Arginine-functionalized nanohydroxyapatite particle – mediated expression of GFP and GUS reporter genes in S. moellendorffii sporophylls ---------- 43

3.3.2 Arginine-functionalized nanohydroxyapatite particle-mediated expression of eYGFPuv reporter gene in S. moellendorffii sporophylls ---------- 43

3.3.3 Agrobacterium-mediated transient expression of GUS in S. meollendorffii sporophylls ---------- 45

3.3.4 Characterization of conjugates ---------- 46

3.4 DISCUSSION ---------- 47

3.5 CONCLUSIONS ---------- 51

3.6 FUNDING ---------- 52

3.7 ACKNOWLEDGEMENTS ---------- 52

CHAPTER 4 : IDENTIFICATION OF DEHYDRATION RESPONSIVE GENES FROM THE TRANSCRIPTOME OF *SELAGINELLA LEPIDOPHYLLA* DURING DEHYDRATION TIME COURSE---------- 53

ABSTRACT---------- 53

4.1 INTRODUCTION ---------- 54

4.2 MATERIALS AND METHODS ---------- 57

4.2.1 Plant material maintenance and water-deficit stress treatments ---------- 57

4.2.2 Sample collection and RNA extraction from S. lepidophylla tissues ---------- 58

4.2.3 Library construction and sequencing ---------- 58

4.2.4 RNA-Seq data analysis ---------- 58

4.3 RESULTS ---------- 61

4.3.1 Dehydration rates in S. lepidophylla ---------- 61

4.3.2 Read alignment with HISAT and Transcript assembly and quantification with StringTie ---------- 62

4.3.3 Screening of differentially expressed genes (DEGs) ---------- 64

4.4.4 Identification of dehydration responsive genes ---------- 65

4.3.5 Gene ontology (GO) analysis of DEGs ---------- 66

4.4 DISCUSSION---------- 67

4.5 CONCLUSIONS AND FUTURE DIRECTIONS ---------- 72

4.6 FUNDING ---------- 73

4.7 ACKNOWLEDGEMENTS ---------- 73

CHAPTER 5 : CONCLUSIONS AND FUTURE DIRECTIONS ---------- 74

REFERENCES ---------- 76

APPENDIX: SUPPORTING MATERIALS FOR CHAPTER 4 ---------- 92

List of Tables

TABLE 4.1 - SELECTED DIFFERENTIALLY EXPRESSED GENES (DEGS) UNDER DEHYDRATION STRESS WITH KNOWN STRESS RESPONSIVE FUNCTIONS. GENE ID - SELAGINELLA MOELLENDORFFII AND ARABIDOPSIS THALIANA ANNOTATIONS FOR DIFFERENTIALLY EXPRESSED GENES RESULTED FROM THE BLASTN. 67

List of Figures

FIGURE 2.1- GENE EXPRESSION LEVELS OF THE SLBHLH TF AT 4% AND 100% RCW. SLBHLH TF SHOWED SIGNIFICANT DIFFERENCE ($P < 0.001$) IN ITS TRANSCRIPT ABUNDANCE BETWEEN 4% RWC AND 100% RWC (CUSHMAN ET AL., UNPUBL. DATA). 7

FIGURE 2.2- PHYLOGENETIC ANALYSIS OF THE SLBHLH$_{OPT}$ PROTEIN. (A) PHYLOGENETIC TREE SHOWING EVOLUTIONARY RELATIONSHIP OF SLBHLH$_{OPT}$ AND OTHER PLANT BHLH PROTEINS. PHYLOGENETIC TREE WAS MADE BY NEIGHBOR JOINING METHOD USING MEGA X SOFTWARE (KUMAR ET AL., 2018). [ATBHLH 122 – *ARABIDOPSIS THALIANA* BHLH122, VVCEB1 – *VITIS VINIFERA* BHLH, VVBHLH1 – *VITIS VINIFERA* BHLH1, PEBHLH35 – *POPULUS EUPHRATICA* BHLH35, HANBHLH – *HELIANTHUS ANNUUS* BHLH, SMICE1 – *SELAGINELLA MOELLENDORFFII* ICE1, SMSCREAM2 – *SELAGINELLA MOELLENDORFFII* SCREAM2**, SLBHLH$_{OPT}$ – *SELAGINELLA LEPIDOPHYLLA* CODON-OPTIMIZED *BHLH***, PPBHLH – *PRUNUS PERSICA* BHLH, ONIBHLH – *ORYZA NIVARA* BHLH, OSBHLH – *ORYZA SATIVA* SUBSP. *INDICA* BHLH, OSJBHLH – *ORYZA SATIVA* SUBSP. *JAPONICA* BHLH, ZMBHLH – *ZEA MAYS* BHLH, SOBHLH – *SACCHARUM OFFICINARUM* BHLH, SBSCREAM2 – *SORGHUM BICOLOR* SCREAM2, TUBHHLH – *TRITICUM URARTU* BHLH, HBICE1-X1 – *HEVEA BRASILIENSIS* ICE1-LIKE ISOFORM X1, MEICE1 – *MANIHOT ESCULENTA* ICE1, POTRIICE1 – *POPULUS TRICHOCARPA* ICE1, POTRIBHLH – *POPULUS TRICHOCARPA* BHLH, RCICE1 – *RICINUS COM- MUNIS* ICE1, JRICE1 – *JUGLANS REGIA ICE1,* ITRBHLH – *IPOMOEA TRIFIDA* BHLH, CRBHLH – *CATHARANTHUS ROSEUS* BHLH, NIBENBHLH – *NICOTIANA BENTHAMIANA* BHLH, NTBHLH – *NICOTIANA TABACUM* BHLH, CABHLH – *CAPSICUM ANNUUM* BHLH, STBHLH – *SOLANUM TUBEROSUM* BHLH, KMBHLH – *KALANCHOE MARNIERIANA* BHLH, PYBHLH – *PRUNUS YEDOENSIS* BHLH, GSICE1 – *GLYCINE SOJA* ICE1, LJBHLH – *LOTUS JAPONICUS* BHLH, CYSICE1-X1 – *CYMBIDIUM SINENSE* ICE1-LIKE ISOFORM X1, PBBHLH4 – *PHALAENOPSIS BELLINA* BHLH4, NCICE1 – *NYMPHAEA COLORATA* ICE1, AMTRICE1 – *AMBORELLA TRICHOPODA* ICE1, ACICE1 – *ANANAS COMOSUS* ICE1-LIKE ISOFORM X1, PSICE1 – *PAPAVER SOMNIFERUM* ICE1, CMICE1 – *CUCURBITA MAXIMA* ICE1, GMICE1 – *GLYCINE MAX* ICE1, PHVULBHLH – *PHASEOLUS VULGARIS* BHLH, CCBHLH – *COFFEA CANEPHORA* BHLH, AHICE1 – *ARACHIS HYPOGAEA* ICE1, BVBHLH – *BETA VULGARIS* BHLH, CICLEICE1 – *CITRUS CLEMENTINA* ICE1, BNSCREAM2 × 1 – *BRASSICA NAPUS* SCREAM2-LIKE ISOFORM X1, BRSCRREAM2 – *BRASSICA RAPA* SCREAM2, BNBHLH33-1 – *BRASSICA NAPUS* BHLH 33-1, TPBHLH – *THELLUNGIELLA PARVULA* BHLH, AT1G12860 – *ARABIDOPSIS THALIANA* 1G12860, BOICE1 – *BRASSICA OLERACEA* ICE1, CSABHLH – *CAMELINA SATIVA* BHLH, SMILBHLH – *SALVIA MILTIORRHIZA* BHLH, CUCMLCE1 – *CUCURBITA MAXIMA* ICE1, PAICE1 – *PROSOPIS ALBA* ICE1, CSBHLH – *CANNABIS SATIVA* BHLH, PRU- PEBHLH – *PRUNUS PERSICA* BHLH, CPICE1 – *CARICA PAPAYA* ICE1, HUICE1 – *HERRANIA UMBRATICAL* ICE1, TCBHLH – *THEOBROMA CACAO* BHLH DNA-BINDING SUPERFAMILY PROTEIN, PUTATIVE ISOFORM 1]. 16

FIGURE 2.3 - MULTIPLE SEQUENCE ALIGNMENT SHOWING CONSERVED MOTIFS AND NUCLEAR LOCALIZATION SIGNAL (NLS, BLACK LINE) IN THE C-TERMINUS OF SLBHLH$_{OPT}$ AND SEVERAL KNOWN ABIOTIC STRESS-RESPONSIVE BHLH PROTEINS. * = HIGHLY CONSERVED, : = MODERATELY CONSERVED, . = LESS CONSERVED. THE LOCALIZER WEB TOOL PREDICTED THE NLS OF THE BHLH PROTEIN AS GGKKGIPAKNLLAERRRRKK. 17

FIGURE 2.4 - ANALYSIS OF GENE EXPRESSION USING QUANTITATIVE REAL-TIME PCR. SLBHLH$_{OPT}$ TRANSCRIPT ABUNDANCE WAS DETERMINED IN COL-0 WT AND FOUR DIFFERENT INDEPENDENT SLBHLH$_{OPT}$-OVEREXPRESSING LINES (#22, #26, #29, AND #37) THAT WERE USED FOR ALL OF THE EXPERIMENTS THROUGHOUT THE PRESENT STUDY (#22, #26, #29, AND #37). TRANSCRIPT ABUNDANCES OF SLBHLH$_{OPT}$ IN EACH OF THESE FOUR SLBHLH$_{OPT}$-OVEREXPRESSING LINES WERE QUANTIFIED USING AN ACTIN-ENCODING GENE FROM A. THALIANA COL-0 WT AS AN INTERNAL CONTROL. VALUES REPRESENT MEANS ± S.D. OF THREE BIOLOGICAL REPLICATES..... 18

FIGURE 2.5 - ANALYSIS OF SUBCELLULAR LOCALIZATION OF SLBHLH$_{OPT}$-SGFP FUSION PROTEIN IN A. THALIANA. NUCLEAR LOCALIZATION OF THE SLBHLH$_{OPT}$-SGFP FUSION PROTEIN. TWO-WEEKS-OLD ROOTS OF TRANSGENIC HOMOZYGOUS 35S-3XHA-SLBHLH$_{OPT}$-SGFP T_3 SEEDLINGS WERE USED TO ANALYZE THE SUBCELLULAR LOCALIZATION OF OVEREXPRESSED SLBHLH$_{OPT}$-SGFP FUSION PROTEIN . THE IMAGES FOR A) OF SIGNALS FROM DAPI, (B) SLBHLH$_{OPT}$-SGFP,AND (C) MERGED SLBHLH$_{OPT}$-SGFP AND DAPI WERE TAKEN UNDER A DARK FIELD AT 60X MAGNIFICATION..... 18

FIGURE 2.6 - EFFECT OF SLBHLH$_{OPT}$ OVEREXPRESSION IN ARABIDOPSIS ON PLANT GROWTH AND DEVELOPMENT. (A) COMPARISON OF ROSETTE DIAMETERS OF FOUR SLBHLH$_{OPT}$-OVEREXPRESSING LINES (#22, #26, #29 AND #37) AND THE COL-0 WT CONTROL LINE. (N = 25). (B) REPRESENTATIVE IMAGE OF ABAXIAL SURFACES OF 6-WEEK-OLD COL-0 WT AND SLBHLH$_{OPT}$-OVEREXPRESSING T_3 A. THALIANA ROSETTES (LINES #22, #26, #29 AND #37) (6-WEEKS-OLD). (C) REPRESENTATIVE IMAGE OF ADAXIAL SURFACE OF 6-WEEK-OLD COL-0 WT AND SLBHLH$_{OPT}$-OVEREXPRESSING T_3 A. THALIANA ROSETTES (LINES #22, #26, #29 AND #37) (6-WEEKS-OLD). (D) COMPARISON OF THE NUMBER OF LEAVES PER MATURE ROSETTE IN PLANTS FROM FOUR SLBHLH$_{OPT}$-OVEREXPRESSING LINES (#22, #26, #29 AND #37) AND THE COL-0 WT CONTROL LINE (N = 25). (E) COMPARISON OF PLANT HEIGHT IN FOUR SLBHLH$_{OPT}$-OVEREXPRESSING LINES (#22, #26, #29 AND #37) AND THE COL-0 WT CONTROL LINE (N = 25). (F) REPRESENTATIVE IMAGE OF 6-WEEKS-OLD SLBHLH$_{OPT}$-OVEREXPRESSING T_3 A. THALIANA LINES (#22, #26, #29 AND #37) AND COL-0 WT CONTROL PLANTS. (G) COMPARISON OF THE NUMBER OF SILIQUES PER PRIMARY INFLORESCENCE OF PLANTS FROM FOUR SLBHLH$_{OPT}$-OVEREXPRESSING LINES (#22, #26, #29 AND #37) AND THE COL-0 WT CONTROL LINE (N = 25). VALUES REPRESENT MEANS ± S.D., *** ADJUSTED P < 0.001 COMPARED TO WT, ONE-WAY ANOVA WITH TUKEY'S MULTIPLE COMPARISON TEST..... 20

FIGURE 2.7 - EFFECT OF SLBHLH$_{OPT}$ OVEREXPRESSION IN ARABIDOPSIS ON INTEGRATED WATER-USE EFFICIENCY. (A) QUANTIFICATION OF INTEGRATED WUE (N = 25) OF FOUR SLBHLH$_{OPT}$-OVEREXPRESSING LINES (#22, #26, #29 AND #37) AND THE COL-0 WT CONTROL LINE, VALUES REPRESENT MEANS ± S.D., *** ADJUSTED P < 0.001 COMPARED TO WT, ONE-WAY ANOVA WITH TUKEY'S MULTIPLE COMPARISON TEST. (B) REPRESENTATIVE IMAGE OF WUE EXPERIMENTAL ARRANGEMENT OF LINE OXSLBHLH$_{OPT}$ – 29 21

FIGURE 2.8 - EFFECT OF SLBHLH$_{OPT}$ OVEREXPRESSION IN ARABIDOPSIS ON RATES OF SEED GERMINATION AND GREEN COTYLEDON EMERGENCE UNDER WATER-DEFICIT STRESS CONDITIONS. (A) SEED GERMINATION RATES WERE QUANTIFIED IN FOUR SLBHLH$_{OPT}$-OVEREXPRESSING LINES (#22, #26, #29 AND #37) AND THE COL-0 WT CONTROL LINE AT 12 D AFTER TREATMENTS WITH 0-, 300-, OR 400-MM MANNITOL (N = 5 REPLICATES WITH 30 SEEDS

per replicate). (B) Representative image of the Col-0 WT and SlbHLH$_{opt}$-overexpressing lines ((#22, #26, #29 and #37) grown on half-strength MS medium supplemented with 0-, 300-, or 400-mM mannitol at 12 d after treatments. (C) Quantification of the rate of green cotyledon emergence in seeds of four SlbHLH$_{opt}$-overexpressing lines (#22, #26, #29 and #37) and the Col-0 WTCol-0 control line at 12 d after treatments with 0-, 300-, or 400-mM mannitol (n = 5 replicates with 30 seeds per replicate). Values represent means ± S.D., *p < 0.1, **p < 0.01, and ***p < 0.001 compared to WT, one-way ANOVA with Tukey's multiple comparison test. 23

Figure 2.9 - Effect of SlbHLH$_{opt}$ overexpression in Arabidopsis on rates of seed germination and green cotyledon emergence under salinity stress conditions. (A) Seed germination rates were quantified in four SlbHLH$_{opt}$-overexpressing lines (#22, #26, #29 and #37) and the Col-0 WT control line at 12 d after NaCl salinity treatments (n = 5 replicates with 24 seeds per replicate). (B) Representative image of the Col-0 WT and SlbHLH$_{opt}$ overexpressing lines ((#22, #26, #29 and #37) grown on half-strength MS medium supplemented with 0, 100, or 150 mM NaCl at 12 d after treatments. (C) Quantification of the rate of green cotyledon emergence in four SlbHLH$_{opt}$-overexpressing lines (#22, #26, #29 and #37) and the Col-0 WT control line at 12 d after NaCl salinity treatments (n = 5 replicates with 24 seeds per replicate). Values represent means ± S.D., adjusted ***p < 0.001 compared to WT, one-way ANOVA with Tukey's multiple comparison test. 25

Figure 2.10 - Effect of SlbHLH$_{opt}$ overexpression in Arabidopsis on seedling response to salinity stress conditions. (A) Representative images at 12 d of plants from the Col-0 WT and SlbHLH$_{opt}$-overexpressing lines ((#22, #26, #29 and #37) grown on vertically on half-strength MS medium supplemented with 150 mM NaCl in vertically oriented plates. (B) Quantification of root elongation (= root length on the 12th day minus initial root length) in plants from four SlbHLH$_{opt}$-overexpressing lines (#22, #26, #29 and #37) and the Col-0 WT control line at 12 d after treatments (n = 30). (C) Quantification of the number of lateral roots on plants from four SlbHLH$_{opt}$-overexpressing lines (#22, #26, #29 and #37) and the Col-0 WT control line at 12 d after NaCl salinity treatments (n = 30). (D) Quantification of fresh weights of plants from four SlbHLH$_{opt}$-overexpressing lines (#22, #26, #29 and #37) and the Col-0 WT control line at 12 d after NaCl salinity treatments (n = 30). (E) Quantification of dry weights of plants from four SlbHLH$_{opt}$-overexpressing lines (#22, #26, #29 and #37) and the Col-0 WT control line at 12 d after NaCl salinity treatments (n = 30). Values represent means ± S.D., **p < 0.01, and ***p < 0.001 compared to WT, one-way ANOVA with Tukey's multiple comparison test. 27

Figure 2.11 - Effect of SlbHLH$_{opt}$ overexpression in Arabidopsis on flavonoid accumulation. Comparison of total flavonoid content of one month old four SlbHLH$_{opt}$-overexpressing lines (#22, #26, #29 and #37) and the Col-0 WT control line. Three biological replicates from each SlbHLH$_{opt}$-overexpressing line and Col-0 WT line and three technical replicates from each biological replicate.

VALUES REPRESENT MEANS ± S.D., **P < 0.01, AND ***P < 0.001 COMPARED TO WT, ONE-WAY ANOVA WITH TUKEY'S MULTIPLE COMPARISON TEST 28

FIGURE 3.1 - ARGININE-FUNCTIONALIZED NANO-HYDROXYAPATITES (R-NHAS)- MEDIATED TRANSIENT EXPRESSION OF GFP IN S. MEOLLENDORFFFII SPOROPHYLLS. GFP FLUORESCENCE WAS VISUALIZED USING A LEICA DMRA2 FLUORESCENCE MICROSCOPE WITH A LEICA DFC3000 G CAMERA (A-D) TRANSIENT GFP EXPRESSION IN S. MEOLLENDORFFII SPOROPHYLL 3D AFTER IN PLANTA R-NHAS- MEDIATED TRANSFORMATION. (E) SELAGINELLA MEOLLENDORFFII SPOROPHYLL 3D AFTER INCUBATING PLANTLETS IN R-NHAS SUSPENDED 0.5% LOW-VISCOSITY CARBOXYMETHYLCELLULOSE (CMC) SOLUTION (CONTROL) (F) CONTROL (UNTREATED – INCUBATED IN WATER) [(A-B) IMAGES ARE AT 100X MAGNIFICATION. (C-F) IMAGES ARE AT 200X MAGNIFICATION.] 42

FIGURE 3.2- ARGININE-FUNCTIONALIZED NANO-HYDROXYAPATITES (R-NHAS)-MEDIATED TRANSIENT EXPRESSION OF GUS IN *S. MEOLLENDORFFII* SPOROPHYLLS. (A-C) IMAGES WERE CAPTURED USING A LEICA EZ24 HD STEREO MICROSCOPE AND (D-F) IMAGES WERE CAPTURED USING A LEICA DM500 BINOCULAR MICROSCOPE. (A) CONTROL (UNTREATED – INCUBATED IN WATER) (B) *SELAGINELLA MEOLLENDORFFII* SPOROPHYLL 3D AFTER INCUBATING PLANTLETS IN R-NHA SUSPENDED 0.5% LOW-VISCOSITY CARBOXYMETHYLCELLULOSE (CMC) SOLUTION (CONTROL) (C-F) TRANSIENT GUS EXPRESSION IN *S. MEOLLENDORFFII* SPOROPHYLL 3D AFTER IN PLANTA R-NHAS-MEDIATED TRANSFORMATION. [(A-C) IMAGES ARE AT 35X MAGNIFICATION. (D) IMAGE IS AT 40X MAGNIFICATION. (E) IMAGE IS AT 100X MAGNIFICATION. (F) IMAGE IS AT 400X MAGNIFICATION. 44

FIGURE 3.3 - ARGININE-FUNCTIONALIZED NANO-HYDROXYAPATITES (R-NHAS)-MEDIATED TRANSIENT EXPRESSION OF EYGFPUV IN S. MEOLLENDORFFFII SPOROPHYLLS. (A) VISUALIZATION OF S. MEOLLENDORFFII SPOROPHYLL UNDER UV LIGHT 3D AFTER INCUBATING PLANTS IN R-NHA SUSPENDED 0.1% TRIMETHYL CHITOSAN (TMC) SOLUTION (CONTROL). (B) VISUALIZATION OF EYGFPUV IN S. MEOLLENDORFFFII SPOROPHYLL UNDER UV LIGHT 3D AFTER IN PLANTA R-NHAS-MEDIATED FOLIAR TRANSFORMATION. EYGFPUV-EXPRESSING SPOROPHYLLS SHOW GREEN FLUORESCENCE, WHILE NON-TRANSFORMED SPOROPHYLLSS SHOW RED AUTOFLUORESCENCE. 45

FIGURE 3.4 - AGROBACTERIUM-MEDIATED TRANSIENT EXPRESSION OF GUS IN S. MEOLLENDORFFII SPOROPHYLLS. (A-B) IMAGES WERE CAPTURED USING A LEICA EZ24 HD STEREO MICROSCOPE AND (C-D) IMAGES WERE CAPTURED USING A LEICA DM500 BINOCULAR MICROSCOPE. [(A) IMAGE IS AT 25X MAGNIFICATION. (B) IMAGE IS AT 35X MAGNIFICATION (C) IMAGE IS AT 40X MAGNIFICATION. (D) IMAGE IS AT 100X MAGNIFICATION. (F) IMAGE IS AT 400X MAGNIFICATION.] 46

FIGURE 3.5 - MORPHOLOGICAL CHARACTERIZATION OF CONJUGATES. TRANSMISSION ELECTRON MICROSCOPY IMAGES OF (A) PDNA|R-NHA (B) PDNA|R-NHA-CMC AND (C) PDNA|R-NHA-TMC. CONJUGATE MORPHOLOGIES WERE OBSERVED VIA FEI TECNAI G2 TWIN TEM WITH AN ACCELERATING VOLTAGE OF 200 KV. 47

FIGURE 3.6 - ZETA POTENTIAL MEASUREMENTS FOR NHA, R-NHA, PDNA|R-NHA, PDNA|R-NHA-CMC, AND PDNA|R-NHA-TMC PARTICLES AT PH 7.4. A MALVERN ZETASIZER NANO ZS WAS USED TO CONDUCT ZETA POTENTIAL MEASUREMENTS. 48

FIGURE 4.1 - SELAGINELLA LEPIDOPHYLLA DEHYDRATION CURVE. THE DEHYDRATION PROCESS WAS ASSESSED BY TRACKING THE PERCENTAGE OF RELATIVE WATER CONTENT (RWC) LOST OVER 24 H PERIOD. THE DATA PRESENTED IN THE GRAPH REPRESENT THE AVERAGE VALUES FROM SIX REPLICATES (N = 6). VALUES REPRESENT MEANS ± S.D. 61

FIGURE 4.2 - OVERVIEW TIME COURSE SAMPLING OF S. LEPIDOPHYLLA DURING DEHYDRATION PROCESS. (A) INITIAL DRY STAGE OF DESICCATED S. LEPIDOPHYLLA. SAMPLES WERE COLLECTED FROM **(B)** AT AT TIME 0 - FULLY HYDRATED (FULLY RECOVERED) – 100% RWC, 0.0T **(C)** AFTER 0.5H OF THE DEHYDRATION PROCESS – 85% RWC, 0.5T, **(D)** AFTER 1H OF THE DEHYDRATION PROCESS – 75% RWC, 1.0T, **(E)** AFTER 3.5H OF THE DEHYDRATION PROCESS – 50% RWC, 3.5T, AND **(F)** AFTER 7.5H OF THE DEHYDRATION PROCESS – 25% RWC, 7.5T OF S. LEPIDOPHYLLA. 62

FIGURE 4.3 – RELATIVE TRANSCRIPTS ABUNDANCE CHANGES OF DIFFERENT SAMPLES IN RESPONSE TO DEHYDRATION. (A) HIERARCHICAL CLUSTERING OF THE TOP 1000 GENES REVEALS PATTERNS OF RELATIVE TRANSCRIPT ABUNDANCE. IDEP.96 (GE ET AL., 2018) WAS UTILIZED TO VISUALIZE THE RESULTS. (B) PRINCIPAL COMPONENT ANALYSIS (PCA) PLOT OF TRANSCRIPTOMIC DATA AT DIFFERENT RWC. HIERARCHICAL CLUSTERING AND PCA ANALYSES INDICATE THE SUBSTANTIAL DIFFERENCE IN THOUSANDS OF GENES INDUCED BY DEHYDRATION. 64

FIGURE 4.4 - VOLCANO PLOT OF DEGS. RED DOTS ARE THE GENES THAT INCREASED IN RELATIVE ABUNDANCE (LOG2FOLD-CHANGE > 2), AND BLUE DOTS ARE THE GENES THAT DECREASED IN RELATIVE ABUNDANCE (LOG2FOLD-CHANGE < -2) IN 25% RWC COMPARED TO 100% RWC. IDEP.96 (GE ET AL., 2018) WAS UTILIZED TO VISUALIZE THE RESULTS. 65

FIGURE S.1 – PRECENT MAPPED. ALIGNMENT METRICS FROM SAMTOOLS STATS; MAPPED VS. UNMAPPED READS. 94

List of Equations

EQUATION 4.1- CALCULATION OF RWC 57

Chapter 1

Introduction

Early land plants, evolving from aquatic algal ancestors, faced the challenge of desiccation as they adapted to terrestrial environments. Desiccation, caused by rapid drying from heat, sunlight, or wind, posed a threat to vegetative tissues. Chlorophytic algae, specifically the Choleochetales group, served as precursors to terrestrial plants, and some acquired desiccation tolerance (Oliver et al., 2000). Desiccation tolerance is the ability to withstand and recover from almost complete loss of protoplasmic water (Giarola et al., 2017; Oliver et al., 2000). Desiccation tolerance is commonly observed in the reproductive structures of green plants, such as pollen, spores, and seeds (Gaff and Oliver, 2013). However, desiccation tolerance in the vegetative stage is less widespread in the plant kingdom. Vegetative desiccation tolerant plants are found among bryophytes, ferns, fern allies and a few angiosperms (Giarola et al., 2017).

During the evolution of land plants, vegetative desiccation tolerance was lost in favor of other developmental traits, such as increased growth rate and structural complexity (Farrant and Moore, 2011; Hilhorst et al., 2018; Silva Artur et al., 2019). However, the ability to survive periodic drying was crucial for the aquatic ancestors of terrestrial plants during their transition from water to land, and these protective mechanisms are believed to be ancestral and conserved in most land plants, serving as the foundation for modern seed and pollen desiccation tolerance pathways (Hilhorst et al., 2018; Silva Artur et al., 2019). The reacquisition of desiccation tolerance by vegetative tissues during prolonged drought stress may have involved the reactivation of this innate desiccation tolerance mechanism (Silva Artur et al., 2019).

Lycophytes, which include club mosses (Lycopodiaceae), quillworts (Isoetaceae), and spike mosses (Selaginellaceae), represents the earliest-diverging lineage of vascular plants,

emerging more than 400 million years ago. Selaginellaceae, commonly known as spike mosses, is a family of plants that encompasses a single genus called *Selaginella*, consisting of around 700 species (Banks, 2009). These diverse species have successfully adapted to various habitats, including arctic, temperate, tropical, and semi-arid environments (Banks, 2009; Yobi et al., 2013). While most spike moss species are susceptible to desiccation, a few species within the genus such as *Selaginella lepidophylla* (Iturriaga et al., 2006; VanBuren et al., 2018; Yobi et al., 2013), S. *bryopteris* (Deeba et al., 2016), *S. sellowii* (Alejo-Jacuinde et al., 2020), and *S. tamariscina* (Wang et al., 2010), have evolved the remarkable ability of vegetative desiccation tolerance (Tuba et al., 1998). The desiccation tolerance trait of those *Selaginella* species allows them to survive in extremely dry regions of the world. However, the underlying regulatory basis of the desiccation-tolerance trait is essentially unknown. I hypothesize that they have unique regulatory genes that can be bioengineered into drought-sensitive crop plants, and thus a better understanding of this desiccation tolerance adaptation could offer practical solutions for improving crop abiotic stress tolerance.

The goal of my dissertation research is to unravel the regulatory basis of the desiccation tolerance trait in one of desiccation tolerant *Selaginella* species, *S. lepidophylla*. To achieve this goal, I had three objectives.

Objective 1: Determine the regulatory role of the *SlbHLH* transcription factor (TF) in water-use efficiency (WUE), abiotic stress tolerance, growth, and development via overexpression in *Arabidopsis thaliana.*

Objective 2: Develop a genetic transformation protocol for *Selaginella* species using *S. moellendorffii*.

Objective 3: Identify dehydration responsive genes from the transcriptome of *Selaginella lepidophylla* during dehydration time course.

As the underlying regulatory basis of the *S. lepidophylla* desiccation tolerance trait is essentially unknown, this research provides a better understanding of the genetic basis of the *S. lepidophylla* desiccation tolerance trait. As part of the proposed work involves developing a transformation system in *Selaginella* spp., this will enable the ability to determine the function of regulatory genes in *S. lepidophylla* or other lycophytes. In addition, the collective results could be used to improve abiotic stress tolerance in crop and biofuel species if the identified dehydration responsive genes can be bioengineered into crop plants. The development of resilient crops with improved abiotic stress tolerance is of paramount importance, especially considering the projected climatic changes of the 21st century, characterized by hotter and drier conditions. By harnessing the unique adaptations and genetic insights gained from desiccation-tolerant species like *S. lepidophylla*, we can pave the way for innovative solutions that help mitigate the negative impacts of abiotic stresses on agriculture, ultimately contributing to food security and environmental sustainability in the face of a changing climate.

Chapter 2 : Overexpression of the *Selaginella lepidophylla* bHLH transcription factor enhances water-use efficiency, growth, and development in *Arabidopsis*[1]

Abstract

Abiotic stresses have the greatest impact on the growth and productivity of crops, especially under current and future extreme weather events due to climate change. Thus, it is vital to explore novel strategies to improve crop plant abiotic stress tolerance to feed an ever-growing world population. *Selaginella lepidophylla* is a desiccation-tolerant spike moss with specialized adaptations that allow it to tolerate water loss down to 4% relative water content. A candidate basic helix-loop-helix (bHLH) transcription factor was highly expressed at 4% relative water content in *S. lepidophylla* (*SlbHLH*). This *SlbHLH* gene was codon-optimized ($SlbHLH_{opt}$) and overexpressed in *Arabidopsis* for functional characterization. Overexpression of the $SlbHLH_{opt}$ gene not only significantly increased plant growth, development, and integrated water-use efficiency, but also significantly increased seed germination and green cotyledon emergence rates under water-deficit stress and salt stress conditions. Under a 150 mM NaCl salt stress condition, $SlbHLH_{opt}$-overexpressing lines increased primary root length, the number of lateral roots, and fresh and dry biomass at the seedling stage compared to control lines. Interestingly, $SlbHLH_{opt}$-overexpressing lines also have significantly higher flavonoid content. Altogether, these results suggest that SlbHLH functions as an important regulator of plant growth, development, abiotic stress tolerance, and water-use efficiency.

[1] This chapter is a reproduction of a published work, Plant Science Journal, Volume 315, 2022.

2.1 Introduction

The human population of the world is rapidly increasing and is expected to exceed 9 billion by 2050 (Oliver et al., 2000). A 70% increase in current agricultural production will be required to fulfill the demands of a growing population (Long et al., 2015). In particular, feeding will be an even greater challenge given limited amounts of water available for crop production. Among the world's available consumable water resources, 80% is used for irrigated agriculture (Condon, 2004). However, it is not realistic to allocate so much of our water resources to irrigate agriculture in view of an expanding human population coupled with climate change related to human activities. Increasing abiotic stresses including drought, high salinity, and high temperatures during extreme weather events that would be far less likely and frequent if not for anthropogenic climate change are major barriers to food production.

The growth and development of agricultural crops worldwide will be negatively impacted as extreme weather events influenced by anthropogenic climate change increase plant abiotic stresses. Accordingly, to diminish the negative impacts of limited water availability and abiotic stresses on global food production, it is essential to discover solutions to overcome these formidable challenges. In response to this challenge, the development of crop plants with improved water-use efficiency (WUE) and abiotic stress tolerance via regulatory genes from extremophytes might secure the environmental sustainability of food production (Amin et al., 2019). Some plants already express natural mechanisms that allow them to survive extreme conditions of drought, salinity, or heat. One example, the desiccation-tolerant spike moss *Selaginella lepidophylla* can survive a 96% loss of cellular water content (Yobi et al., 2012). Identifying candidate regulatory genes that coordinate the extreme desiccation tolerance response in *S. lepidophylla* could provide

an excellent opportunity to improve water-use efficiency and abiotic stress tolerance by applying the regulatory innovations of this extremophyte in crop plants (Amin et al., 2019).

Desiccation tolerance was a key innovation in the evolution of plants during their transition from an aquatic to a terrestrial environment (Dinakar and Bartels, 2013). This trait is defined as the ability to tolerate near-complete loss (80%–95%) of protoplasmic water and the ability to be "resurrected" from an air-dried state (Yobi et al., 2013). To compare, most vascular plants are unable to survive less than 60% relative water content (Giarola et al., 2017). *Selaginella lepidophylla* represents the earliest-diverging lineage of vascular plants and can withstand extremely dry conditions in its natural habitats (VanBuren et al., 2018). Desiccation tolerance is a complex trait that requires the expression of multiple regulatory genes (Dinakar and Bartels, 2013). Recent studies have improved our mechanistic understanding of the desiccation tolerance response. Non-biased, high-throughput metabolomics analysis at five stages of the rehydration/dehydration cycle of *S. lepidophylla* plants by Yobi et al. (2013) identified 251 metabolites that likely have a vital role in the desiccation tolerance response. These metabolites consist of constitutive, highly abundant sugars, inducible osmoprotectants, antioxidants, and UV-protective compounds (Yobi et al., 2013). However, the underlying regulatory basis of this resurrection trait is not yet completely understood.

Transcription Factors (TFs) function as regulators of the expression and function of clusters of other genes including stress-responsive ones (Amin et al., 2019). Thus, the TF-based genetic engineering approach involves identifying and manipulating a number of regulatory genes to achieve the desired global effect (Joshi et al., 2016) in an organism. With the recent advances in plant biotechnology and the availability of omics data, TF-based genetic manipulation has become

a relatively straightforward method for engineering crop plants with enhanced WUE and abiotic stress tolerance. *Selaginella lepidophylla* has 1079 TFs, among which 30 have been identified as candidate regulators of the desiccation tolerance response (Cushman et al., unpubl. data). One such TF is a basic helix-loop-helix (bHLH) protein that is highly expressed at 4% relative water content (Cushman et al., unpubl. data; Figure 2.1).

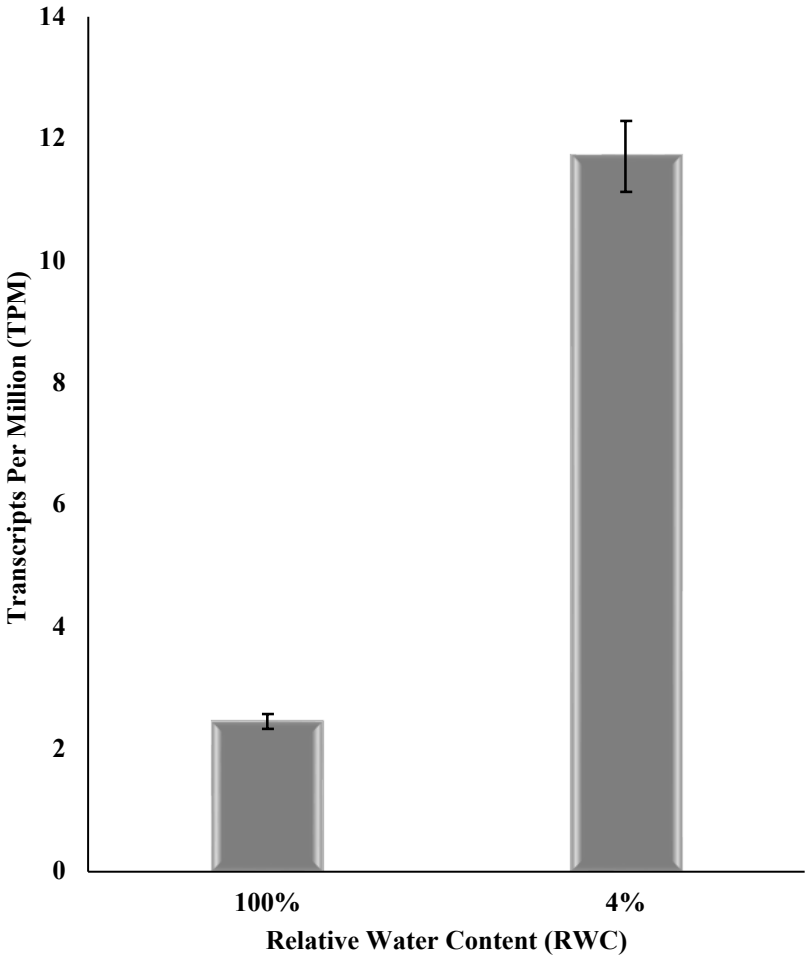

Figure 2.1- Gene expression levels of the SlbHLH TF at 4% and 100% RCW. *SlbHLH* TF showed significant difference ($p < 0.001$) in its transcript abundance between 4% RWC and 100% RWC (Cushman et al., unpubl. Data).

As part of a large TF family in the Eukaryota and one of the largest TF families in plants, the bHLH proteins are involved in a wide array of regulatory processes (Castilhos et al., 2014). A total of 167 bHLH members in *Arabidopsis thaliana* and 162 in rice are included in this family (Castilhos et al., 2014). Recent studies have shown that the bHLH TF functions in abiotic stress tolerance and water-use efficiency in plants. Overexpression of the codon-optimized bHLH *VvCEB1*$_{opt}$ from grape (*Vitis vinifera*) could improve WUE and salinity tolerance and attenuate water-deficit stress in *Arabidopsis* (Lim et al., 2020). Moreover, the overexpression of another codon-optimized bHLH from grape, *VvbHLH1* could enhance salt and drought tolerance in transgenic *Arabidopsis* (Wang et al., 2016). In tomato, overexpression of a tomato bHLH gene (*SlbHLH22*) improved tomato plant drought and salinity tolerance (Waseem et al., 2019). Further, overexpression of a *Populus euphratica* bHLH (*PebHLH35*) in *Arabidopsis* increased its drought stress tolerance (Dong et al., 2014). A native *Arabidopsis bHLH122* acts as a positive regulator of drought, NaCl, and osmotic signaling (Liu et al., 2014). Here, I describe the molecular cloning of a codon-optimized *S. lepidophylla* bHLH TF, *SlbHLH*$_{opt}$, and its functional characterization in the model plant *Arabidopsis*. I overexpressed *SlbHLH*$_{opt}$ in *Arabidopsis* and have confirmed that *SlbHLH* has regulatory roles in water-use efficiency, plant abiotic stress tolerance, plant growth, and development in *Arabidopsis*.

2.2 Materials and methods

2.2.1 Sequence analysis of *SlbHLH*$_{opt}$

The cDNA sequence of the *SlbHLH* gene was obtained from previous transcriptomic analyses of *S. lepidophylla* (Cushman et al. unpubl. data). Sequences homologous to the codon-optimized *SlbHLH* coding sequence (*SlbHLH*$_{opt}$) were retrieved from the *Arabidopsis* Information Resource (TAIR) (https://www.ncbi.nlm.nih.gov/) databases using Basic Local Alignment Search

Tool (BLAST). The TAIR (https://www.arabidopsis. org/) website was used to determine the putative functions of *SlbHLH$_{opt}$* orthologs.

Non-redundant homologous amino acid sequences were downloaded from the PlantTFDB (http://planttfdb.cbi.pku.edu.cn/) to construct the phylogenetic tree using Neighbor-Joining (NJ) method in MEGA X software (Kumar et al., 2018). Pairwise sequence alignments and multiple sequence alignment were performed using the Clustal Omega tool (https://www.ebi.ac.uk/Tools/msa/clustalo/)and the T-Coffee tool at the EMBL-EBI website (https://www.ebi.ac.uk/Tools/msa/tcoffee/). In addition, the machine learning prediction tool LOCALIZER was used to predict the subcellular localization of the SlbHLH$_{opt}$ protein (Sperschneider et al., 2017).

2.2.2 Subcloning the codon-optimized SlbHLH gene into plasmid vectors

The *SlbHLH$_{opt}$* sequence with flanking Att sites needed for LR cloning into Gateway™ vectors was synthesized (Gene Universal, Newark, DE, USA). Codon optimization was performed according to codon usage in *Arabidopsis* ecotype Columbia (Col-0) (Gene Universal, Newark, DE, USA). The candidate *SlbHLH$_{opt}$* sequence was then cloned into the Gateway binary vector pGWB415 (CaMV35S-3xHA-attR1-attR2-NOS terminator) using the Gateway LR Clonase™ II Enzyme Mix (Invitrogen, Carlsbad, CA, USA) (Nakagawa et al., 2007). An expression construct for subcellular local- ization studies was then created using pGWB406 (CaMV35S-3xHA-at- tR1-attR2-sGFP-NOS terminator) containing a C-terminal in-frame fusion of synthetic Green Fluorescent Protein (sGFP). Expression clones CaMV35S-3xHA-SlbHLH$_{opt}$ and CaMV35S-3xHA-SlbHLH$_{opt}$-sGFP were chemically transformed into NEB® 10-beta competent C3019H *Escherichia coli* cells (New England BioLabs, Ipswich, MA). Recombinant plasmids were extracted and verified by Sanger sequencing (GENEWIZ, South Plainfield, NJ, USA).

2.2.3 Transformation of *Arabidopsis* and identification of homozygous *SlbHLH$_{opt}$* overexpressing lines

The freeze-thaw method was used to introduce each final construct into *Agrobacterium tumefaciens* GV3101 cells (Wang, 2006). These constructs were then introduced into the *Arabidopsis* Col-0 WT plant genome via *Agrobacterium*-mediated transformation using the floral dip method (Zhang et al., 2006). Seedlings were grown on full-strength Murashige and Skoog (MS) modified basal medium pH = 5.7 with Gamborg's vitamins (M404; Phytotechnology Laboratories, USA), 3% sucrose (Caisson Laboratories, Inc., USA), and 8 g/L Tissue Culture Grade Agar (A111; Phytotechnology Laboratories, USA) in a growth chamber (MIR-254 Series, Panasonic Healthcare Co., Ltd., Japan) under a 16 h light/ 8 h dark cycle. Transgenic plants were selected using 50 µg/mL kanamycin (Caisson Laboratories, Inc., USA) in the growth medium described above. Kanamycin selection on putative transgenic seedlings was maintained to ensure transgene homozygosity. Four independent T_3-generation transgenic homozygous lines overexpressing the *SlbHLH$_{opt}$* gene (*OxSlbHLH$_{opt}$*-22, -26, -29, and -37) were selected based on detailed phenotypic characterization and quantitative real-time PCR (qRT-PCR) quantification of the transgene expression (Figure 2.4). The same four independent homozygous T_3 generation transgenic lines overexpressing the *SlbHLH$_{opt}$* gene were used throughout the study to explore the function of the *SlbHLH$_{opt}$* TF in water-use efficiency (WUE), abiotic stress responses, and plant growth and development.

2.2.4 Analysis of *SlbHLH$_{opt}$* gene expression

To identify four independent homozygous T_3 generation *SlbHLH$_{opt}$*-overexpressing transgenic lines, qRT-PCR was conducted on 14 different lines that were selected based on detailed phenotypic characterization. Total RNA was extracted from 100 mg of shoot tissues from each of

the 14 *SlbHLH$_{opt}$*-overexpressing lines and Col-0 WT using a Quick-RNA Plant Miniprep Kit (Zymo Research, Irvine, CA, USA) according to the manufacturer's instructions. Quantitative real-time PCR was performed using the Luna® Universal One-Step RT-qPCR Kit (New England Biolabs, Ipswich, MA, USA) following manufacturer's protocol with the Applied Biosystems QuantStudio 3 Real-Time PCR System (Thermo Fisher Scientific, Waltham, MA, USA). Relative changes in gene expression were calculated using the $2^{-\Delta\Delta CT}$ method (Livak and Schmittgen, 2001). *SlbHLH$_{opt}$* expression levels were normalized using the Actin gene from *A.thaliana* Col-0 WT as an internal control. All experiments were conducted in triplicate with three technical replicates. All of the primers used in gene expression analysis were synthesized by Integrated DNA Technologies, Inc. (Coralville, IA, USA). The following primer pairs were used: *SlbHLH$_{opt}$* (5'-CTG CTG GTG CTA CTG CTA AA-3' and 5'-GCA GGA GGA GGC TTA GAA ATC-3') and *Actin2* (5'-CTA CGA GCA GGA GAT GGA AAC-3' and 5'-TCT GAA TCT CTC AGC ACC AAT C-3') for these analyses.

2.2.5 Plant growth conditions and phenotypic characterization

Seeds were sterilized using the vapor-surface sterilization method (Lindsey et al., 2017) prior to germinating and growing them under *in vitro* conditions. For seed stratification, seeds were stored at least 3 d at 4°C in the dark before beginning experiments. Seedlings were first grown on full-strength MS modified basal medium pH = 5.7 with Gamborg's vitamins, 3% sucrose, and 8 g/L agar in a growth chamber (MIR-254 Series, Panasonic Healthcare Co., Ltd, Japan) at 23°C day/21°C night temperatures under a 16 h light/8 h dark cycle. *Arabidopsis* plants were grown in 89-mm-square pots (0.3 L rooting volume: Kord, Inc., Toronto, CA, USA) containing Miracle-Gro Moisture Control® Potting Mix (Scotts Miracle-Gro Company, Marysville, OH, USA) under controlled plant growth room conditions. Plant growth conditions were maintained at 23°C

day/21°C night temperatures, 16 h light/8 h dark long-day growth conditions, ambient humidity, and high-intensity full-spectrum fluorescent bulbs (6500 K) to ensure a minimum irradiance level of 80 mmol m^{-2} s^{-1}. Growth conditions that are specific to each experiment conducted are indicated below in the sections describing each of those experiments.

For plant phenotyping, two-week-old seedlings of the Col-0 WT control and the four *SlbHLH$_{opt}$*-overexpressing lines were transferred from MS plates to soilless potting mix, and plants were grown out for four weeks under controlled plant room conditions as described above. Plant height, rosette diameter, the number of siliques per primary inflorescence, and the number of leaves per mature rosette were scored on plants from the Col-0 WT control line and the four *SlbHLH$_{opt}$*-overexpressing lines.

2.2.6 Determination of subcellular localization of *SlbHLH$_{opt}$-sGFP* expression

The roots of two-week-old T_3-generation transgenic homozygous *35S-3xHA-SlbHLHopt-sGFP* seedlings were stained with 4',6-diamidino- 2-phenylindole (DAPI) solution (FluoroShield; with DAPI; Sigma- Aldrich, St. Louis, MO) for 15 min at room temperature (RT). To examine the localization of the *SlbHLH$_{opt}$-sGFP* fusion protein, root samples were observed using a confocal laser scanning microscope (Nikon A1 – Tokyo, Japan). DAPI and GFP were excited with a laser at 401 nm and 486 nm, respectively, and fluorescence emission was collected at 450/50 nm for DAPI and 525/50 nm for GFP.

2.2.7 Analysis of integrated water-use efficiency

The method described by Wituszynska and Karpinski (2014) was followed to evaluate the water-use efficiency (WUE) of *SlbHLH$_{opt}$*-overexpressing lines. Briefly, integrated WUE values of *SlbHLH$_{opt}$*-overexpressing lines and Col-0 WT controls were calculated by measuring biomass yield produced per volume of water consumed ($mgmL^{-1}$) in four-week-old plants under a 16 h

light/8 h dark cycle at 23°C in the light and 21°C in the dark (Wituszynska and Karpiński, 2014). Seeds of Col-0 WT and *SlbHLH*$_{opt}$-overexpressing lines were germinated and grown in 50 mL tubes filled with potting mix after adding 35 mL of water to the mix. After four weeks of growth, the rosettes of both the Col-0 WT and *SlbHLH*$_{opt}$-overexpressing lines were harvested and dried for 3 h at 105°C to determine the dry weight of each rosette. Each tube was weighed at the beginning of the experiment and after removal of the rosette at the end of the experiment to quantify water loss.

2.2.8 Assays of in vitro seed germination in *SlbHLH*$_{opt}$-overexpressing lines under abiotic stress conditions

To determine the effect of salt stress on seed germination in Col-0 WT and *SlbHLH*$_{opt}$-overexpressing lines, sterilized seeds of each line were sown on half-strength MS modified basal medium pH = 5.7 with Gamborg's vitamins, 3% sucrose, and 8 g/L agar plates supplemented with 100 mM, 150 mM, or 200 mM NaCl. Plates were placed at 4 °C for 2 d in the dark prior to placing them in a growth chamber at 23°C in the light and 21ºC in the dark under long-day conditions (16 h light/8 h dark). At 12 d after the NaCl treatments, the rates of seed germination and green cotyledon emergence were calculated.

To assay seed germination in Col-0 WT and *SlbHLH*$_{opt}$-overexpressing lines under in vitro water-deficit stress, sterilized seeds were sown on half-strength MS plates supplemented with 300 mM or 400 mM mannitol, and similar experimental steps were followed as those for assays of germination under NaCl stress. Seeds of Col-0 WT and *SlbHLH*$_{opt}$-overexpressing lines sown on half-strength MS modified basal medium pH = 5.7 with Gamborg's, 3% sucrose, and 8 g/L agar plates were used as controls in both the NaCl and water-deficit stress seed germination experiments.

2.2.9 Assay of in vitro NaCl stress in *SlbHLH$_{opt}$*-overexpressing lines

For the in vitro NaCl stress assay at the seedling stage, sterilized seeds of Col-0 WT and *SlbHLH$_{opt}$* overexpressing lines were stratified for 2 d at 4°C in the dark and germinated on MS medium for 6 d with plates held in a vertical position in a growth chamber at 23°C day/21°C night temperatures under a 16 h light/8 h dark cycle (Corrales et al., 2014). Six-day-old seedlings were transferred to plates containing MS medium supplemented with 150 mM NaCl or standard MS medium (control), and plates were placed in a vertical position in the growth chamber (Corrales et al., 2014). Plants were grown at 23°C day/ 21°C night temperatures under long-day conditions (16 h light/8 h dark) for 12 d, at which time primary root lengths and the number of lateral roots were measured using Image J software (https://imagej.nih.gov/ij/), and plant fresh and dry weights were determined.

2.2.10 Determination of total flavonoid content

The total flavonoid content of four-week-old *SlbHLH$_{opt}$*-overexpressing and Col-0 WT control lines were determined using the $AlCl_3$ method as described by Aryal et al. (2019) Click or tap here to enter text.with slight modifications. Aerial parts of plants from the Col-0 WT control and *SlbHLH$_{opt}$*-overexpressing lines were harvested after four weeks of growth and ground in liquid nitrogen. One-gram aliquots of ground powder from each sample were immersed in 30 mL of ethanol and incubated at RT for 7 d with frequent agitation. After 7 d, samples were filtered using vacuum filtration (Aryal et al., 2019). Final extracts were obtained by concentrating each filtrate to dryness in a rotary evaporator (R-200, Büchi Labortechnik, Germany) at 45°C and reduced pressure (Aryal et al., 2019).

To quantify total flavonoid content, the powdered extract obtained above was resuspended in ethanol to 200 µg/mL and a 1 mL aliquot of the 200 µg/mL extract solution was mixed with 0.2

mL of 10 % (w/v) $AlCl_3$ in ethanol (Sigma-Aldrich, USA), 0.2 mL (1 M) potassium acetate (Sigma-Aldrich, USA), and 5.6 mL distilled water (Aryal et al., 2019). Absorbances of samples were measured at 415 nm against blanks after incubating sample mixtures for 30 min at RT (Aryal et al., 2019). Total flavonoid contents of samples were estimated using a calibration curve (y = 0.0107x - 0.0383) prepared from quercetin solutions ranging in concentration from 0 to 100 µg/mL and total flavonoid contents were expressed as quercetin equivalents in milligrams per gram dry extract weight (mgQE/g) (Aryal et al., 2019).

2.3 Results

2.3.1 Phylogenetic analysis of the SlbHLH$_{opt}$ protein

To classify the *SlbHLH$_{opt}$* protein and identify the evolutionary relationships among the bHLH proteins from other plant species, an unrooted-tree was constructed using 60 amino acid sequences of various plant species that have the highest similarity to the *SlbHLH$_{opt}$* sequence (Figure 2.2). Phylogenetic analysis showed that the *SlbHLH$_{opt}$* protein is closely related to abiotic stress-responsive bHLH proteins of *VvCEB1*, *VvbHLH1*, *SlbHLH22, PebHLH35*, and *AtbHLH122*. Alignment of these bHLH proteins showed conserved motifs and a nuclear localization signal in the C-terminus (Figure 2.3). These results are indicative of the regulatory role of the *SlbHLH$_{opt}$* protein in abiotic stress responses.

2.3.2 *SlbHLH$_{opt}$* protein is localized to the nucleus

To determine the subcellular localization of *SlbHLH$_{opt}$*, a *SlbHLH$_{opt}$- sGFP* fusion protein was expressed in the roots of T_3-generation trangenic homozygous *SlbHLH$_{opt}$-sGFP* seedlings. Confocal imaging of protein fluorescence showed that fluorescence from the *SlbHLH$_{opt}$-sGFP* fusion was detected only in the nuclei of root cells from *SlbHLH$_{opt}$-sGFP*-expressing seedlings (Figure 2.5).

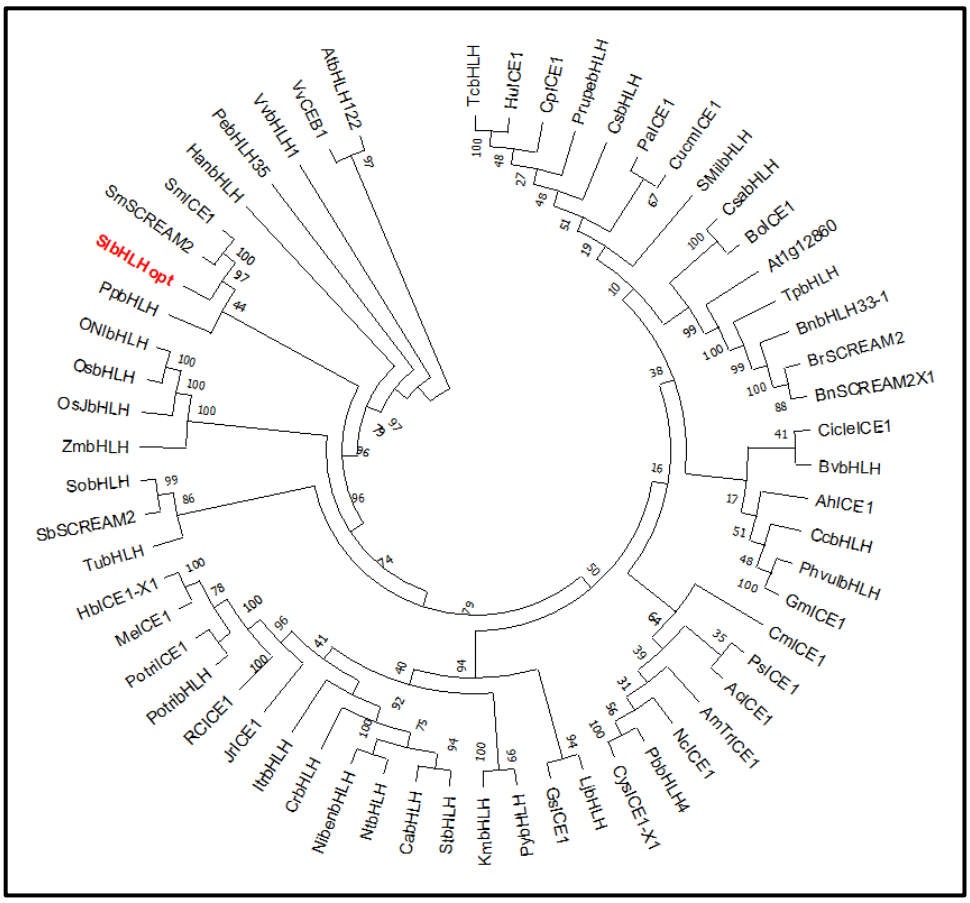

Figure 2.2- Phylogenetic analysis of the SlbHLH$_{opt}$ protein. (a) Phylogenetic tree showing evolutionary relationship of SlbHLH$_{opt}$ and other plant bHLH proteins. Phylogenetic tree was made by Neighbor Joining Method using MEGA X software (Kumar et al., 2018). [AtbHLH 122 – *Arabidopsis thaliana* bHLH122, VvCEB1 – *Vitis vinifera* bHLH, VvbHLH1 – *Vitis vinifera* bHLH1, PebHLH35 – *Populus euphratica* bHLH35, HanbHLH – *Helianthus annuus* bHLH, SmICE1 – *Selaginella moellendorffii* ICE1, SmSCREAM2 – *Selaginella moellendorffii* SCREAM2**, SlbHLHopt – *Selaginella lepidophylla* codon-optimized *bHLH***, PpbHLH – *Prunus persica* bHLH, ONIbHLH – *Oryza nivara* bHLH, OsbHLH – *Oryza sativa* subsp. *Indica* bHLH, OsJbHLH – *Oryza sativa* subsp. *Japonica* bHLH, ZmbHLH – *Zea mays* bHLH, SobHLH – *Saccharum officinarum* bHLH, SbSCREAM2 – *Sorghum bicolor* SCREAM2, TubHHLH – *Triticum urartu* bHLH, HbICE1-X1 – *Hevea brasiliensis* ICE1-like isoform X1, MeICE1 – *Manihot esculenta* ICE1, PotriICE1 – *Populus trichocarpa* ICE1, PotribHLH – *Populus trichocarpa* bHLH, RCICE1 – *Ricinus com- munis* ICE1, JrICE1 – *Juglans regia ICE1,* ItrbHLH – *Ipomoea trifida* bHLH, CrbHLH – *Catharanthus roseus* bHLH, NibenbHLH – *Nicotiana benthamiana* bHLH, NtbHLH – *Nicotiana tabacum*

bHLH, CabHLH – *Capsicum annuum* bHLH, StbHLH – *Solanum tuberosum* bHLH, KmbHLH – *Kalanchoe marnieriana* bHLH, PybHLH – *Prunus yedoensis* bHLH, GsICE1 – *Glycine soja* ICE1, LjbHLH – *Lotus japonicus* bHLH, CysICE1-X1 – *Cymbidium sinense* ICE1-like isoform X1, PbbHLH4 – *Phalaenopsis bellina* bHLH4, NcICE1 – *Nymphaea colorata* ICE1, AmTrICE1 – *Amborella trichopoda* ICE1, AcICE1 – *Ananas comosus* ICE1-like isoform X1, PsICE1 – *Papaver somniferum* ICE1, CmICE1 – *Cucurbita maxima* ICE1, GmICE1 – *Glycine max* ICE1, PhvulbHLH – *Phaseolus vulgaris* bHLH, CcbHLH – *Coffea canephora* bHLH, AhICE1 – *Arachis hypogaea* ICE1, BvbHLH – *Beta vulgaris* bHLH, CicleICE1 – *Citrus clementina* ICE1, BnSCREAM2 × 1 – *Brassica napus* SCREAM2-like isoform X1, BrSCRREAM2 – *Brassica rapa* SCREAM2, BnbHLH33-1 – *Brassica napus* bHLH 33-1, TpbHLH – *Thellungiella parvula* bHLH, At1g12860 – *Arabidopsis thaliana* 1g12860, BoICE1 – *Brassica oleracea* ICE1, CsabHLH – *Camelina sativa* bHLH, SMilbHLH – *Salvia miltiorrhiza* bHLH, CucmlCE1 – *Cucurbita maxima* ICE1, PaICE1 – *Prosopis alba* ICE1, CsbHLH – *Cannabis sativa* bHLH, Pru- pebHLH – *Prunus persica* bHLH, CpICE1 – *Carica papaya* ICE1, HuICE1 – *Herrania umbratical* ICE1, TcbHLH – *Theobroma cacao* bHLH DNA-binding superfamily protein, putative isoform 1].

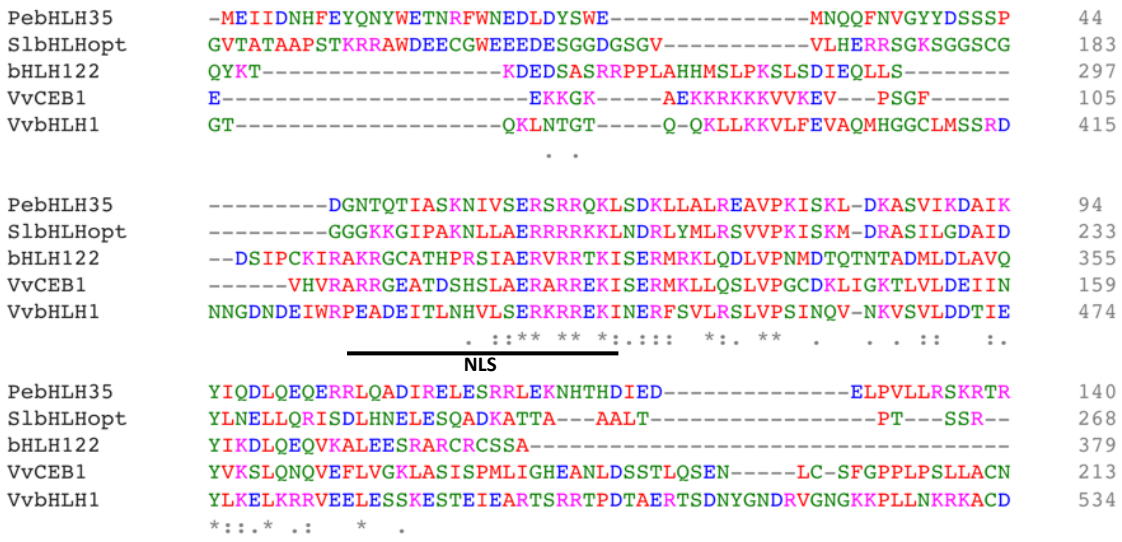

Figure 2.3 - Multiple sequence alignment showing conserved motifs and nuclear localization signal (NLS, black line) in the C-terminus of SlbHLH$_{opt}$ and several known abiotic stress-responsive bHLH proteins. * = highly conserved, : = moderately conserved, . = less conserved. The LOCALIZER web tool predicted the NLS of the bHLH protein as GGKKGIPAKNLLAERRRRKK.

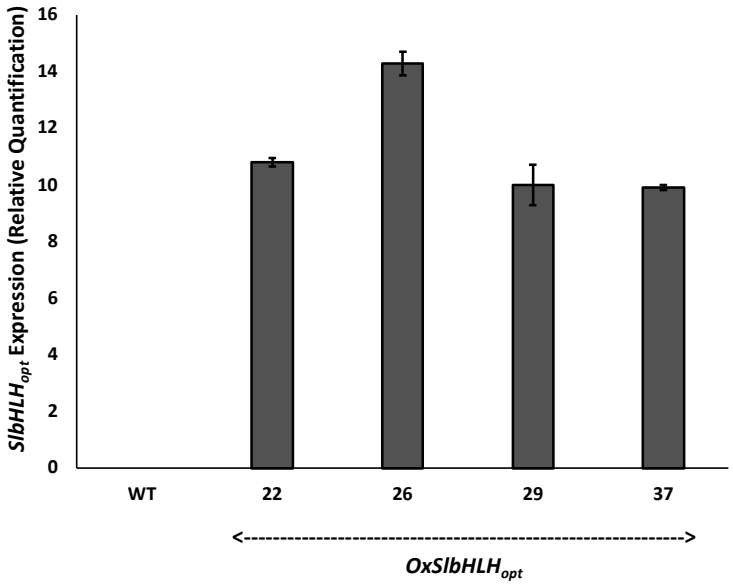

Figure 2.4 - Analysis of gene expression using Quantitative Real-Time PCR. *SlbHLH$_{opt}$* transcript abundance was determined in Col-0 WT and four different independent *SlbHLH$_{opt}$*-overexpressing lines (#22, #26, #29, and #37) that were used for all of the experiments throughout the present study (#22, #26, #29, and #37). Transcript abundances of *SlbHLH$_{opt}$* in each of these four *SlbHLH$_{opt}$*-overexpressing lines were quantified using an Actin-encoding gene from *A. thaliana* Col-0 WT as an internal control. Values represent means ± S.D. of three biological replicates.

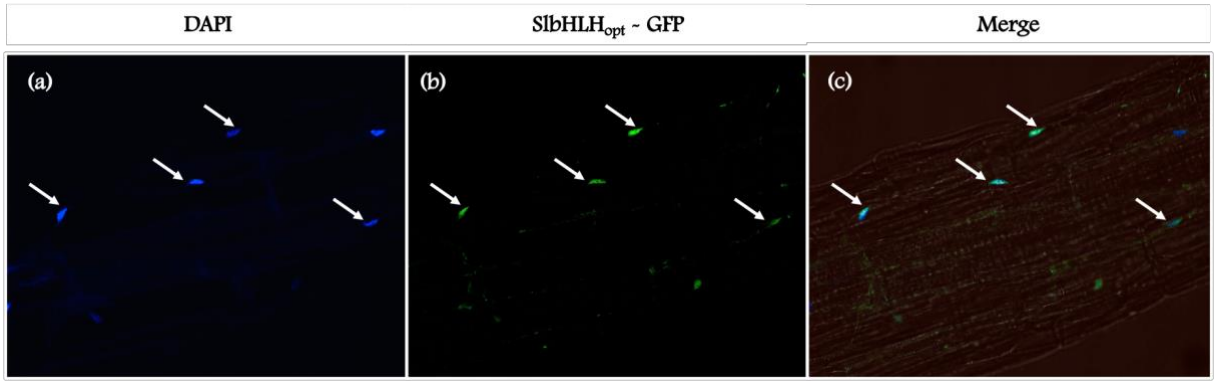

Figure 2.5 - Analysis of subcellular localization of *SlbHLH$_{opt}$-sGFP* fusion protein in *A. thaliana*. Nuclear localization of the *SlbHLH$_{opt}$-sGFP* fusion protein. Two-weeks-old roots of transgenic homozygous 35S-3xHA-*SlbHLH$_{opt}$-sGFP* T_3 seedlings were used to analyze the subcellular localization of overexpressed *SlbHLH$_{opt}$-sGFP* fusion protein . The images for a) of signals from DAPI, (b) *SlbHLH$_{opt}$-sGFP*,and (c) merged *SlbHLH$_{opt}$-sGFP* and DAPI were taken under a dark field at 60x magnification.

2.3.3 *SlbHLH$_{opt}$* overexpression enhances plant growth and development

The overexpression of *SlbHLH$_{opt}$* in six-week-old plants from T_3 homozygous transgenic *Arabidopsis* lines resulted in significantly greater rosette diameter (Figure 2.6a-c), taller plant height (Figure 2.6e-f), a larger number of leaves in the mature rosette (Figure 2.6b-d), and a larger number of siliques per primary inflorescence (Figure 2.6f-g) compared to Col-0 WT plants. Under controlled plant growth room conditions, soilless mixture-grown plants from *SlbHLH$_{opt}$*-overexpressing lines showed a 1.3- to 1.6- fold increase in rosette diameter (Figure 2.6a-c) and a 1.3- to 1.4-fold increase in plant height (Figure 2.6e-f) relative to Col-0 WT plants. Interestingly, plants from *SlbHLH$_{opt}$*-overexpressing lines also exhibited a 1.3- to 1.6-fold increase in the number of leaves per mature rosette (Figure 2.6b-d) and a 1.3- to 1.6-fold increase in the number of siliques per primary inflorescence (Figure 2.6f-g) compared to Col-0 WT plants, respectively. Altogether, these phenotyping results are suggestive of some possible roles of the *SlbHLH* TF in plant growth and development.

2.3.4 *SlbHLHopt* overexpression increases integrated water-use efficiency

SlbHLHopt overexpression resulted in enhanced integrated WUE (Figure 2.7a-b) in transgenic *Arabidopsis*. The increased integrated WUE observed in *SlbHLHopt*-overexpressing lines indicates greater biomass production per amount of water used. The *SlbHLHopt*-overexpressing lines exhibited 1.6- to 1.7-fold higher integrated WUE compared to Col-0 WT control lines (Figure 2.7a), representing an approximately 65% increase in WUE. These observations indicate that *SlbHLH* is a positive regulator of integrated WUE.

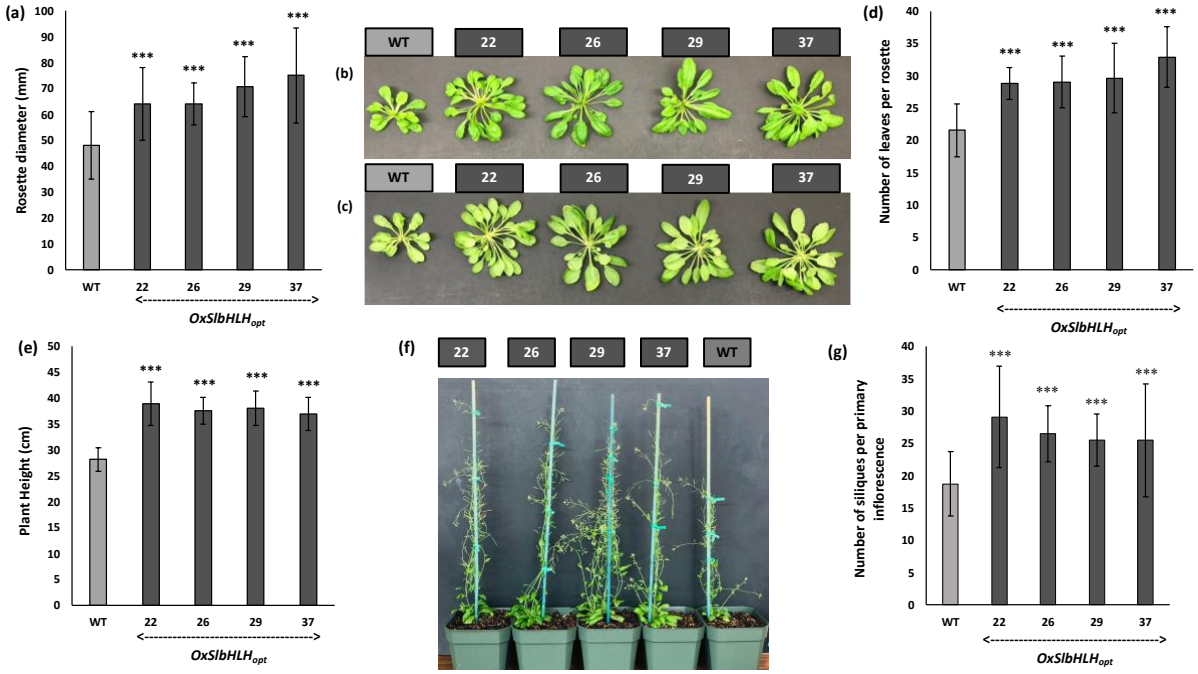

Figure 2.6 - Effect of *SlbHLH$_{opt}$* overexpression in *Arabidopsis* on plant growth and development. (a) Comparison of rosette diameters of four *SlbHLH$_{opt}$*-overexpressing lines (#22, #26, #29 and #37) and the Col-0 WT control line. (n = 25). (b) Representative image of abaxial surfaces of 6-week-old Col-0 WT and *SlbHLH$_{opt}$*-overexpressing T_3 *A. thaliana* rosettes (lines #22, #26, #29 and #37) (6-weeks-old). (c) Representative image of adaxial surface of 6-week-old Col-0 WT and *SlbHLH$_{opt}$*-overexpressing T_3 *A. thaliana* rosettes (lines #22, #26, #29 and #37) (6-weeks-old). (d) Comparison of the number of leaves per mature rosette in plants from four *SlbHLH$_{opt}$*-overexpressing lines (#22, #26, #29 and #37) and the Col-0 WT control line (n = 25). (e) Comparison of plant height in four *SlbHLH$_{opt}$*-overexpressing lines (#22, #26, #29 and #37) and the Col-0 WT control line (n = 25). (f) Representative image of 6-weeks-old *SlbHLH$_{opt}$*-overexpressing T_3 *A. thaliana* lines (#22, #26, #29 and #37) and Col-0 WT control plants. (g) Comparison of the number of siliques per primary inflorescence of plants from four *SlbHLH$_{opt}$*-overexpressing lines (#22, #26, #29 and #37) and the Col-0 WT control line (n = 25). Values represent means ± S.D., *** adjusted $p < 0.001$ compared to WT, one-way ANOVA with Tukey's multiple comparison test.

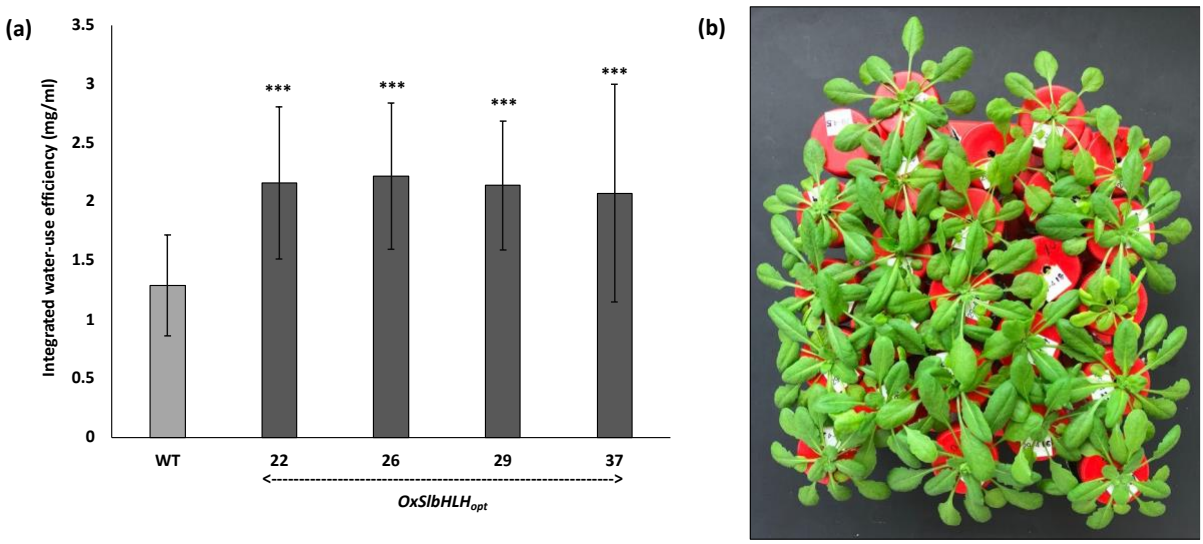

Figure 2.7 - Effect of *SlbHLH$_{opt}$* overexpression in *Arabidopsis* on integrated water-use efficiency. (a) Quantification of integrated WUE (n = 25) of four *SlbHLH$_{opt}$*-overexpressing lines (#22, #26, #29 and #37) and the Col-0 WT control line, Values represent means ± S.D., *** adjusted $p < 0.001$ compared to WT, one-way ANOVA with Tukey's multiple comparison test. (b) Representative image of WUE experimental arrangement of line *OxSlbHLH$_{opt}$ – 29*

2.3.5 *SlbHLH$_{opt}$* overexpression improves rates of seed germination and green cotyledon emergence under water-deficit stress and salinity stress

We tested the effect of *SlbHLH$_{opt}$* overexpression on the rates of seed germination and green cotyledon emergence under water-deficit stress conditions using mannitol as the osmoticum to impose water-deficit stress in seeds. Under normal growth conditions, there was no noticeable difference in the rates of seed germination or green cotyledon emergence between plants from *SlbHLH$_{opt}$*-overexpressing transgenic T_3 lines and Col-0 WT controls (Figure 2.8a-c). However, under both 300 mM and 400 mM mannitol stress conditions, the rates of seed germination and green cotyledon emergence in the *SlbHLH$_{opt}$*-overexpressing lines were much higher than those observed in Col-0 WT lines (Figure 2.8a-c). Under 300 mM mannitol stress conditions, *SlbHLH$_{opt}$*-

overexpressing lines showed a 2.0- to 2.2-fold increase in the rate of seed germination and a 6- to 7.6-fold increase in the rate of green cotyledon emergence relative to those in Col-0 WT controls (Figure 2.8a-c). Under 400 mM mannitol stress conditions, *SlbHLH*$_{opt}$ overexpression increased the rate of seed germination by 4.5- to 5.3-fold compared to Col-0 WT controls (Figure 2.8a-c). Interestingly, no green cotyledons emerged from Col-0 WT seeds under 400 mM mannitol stress conditions. However, *SlbHLH*$_{opt}$- overexpressing transgenic T_3 lines exhibited green cotyledon emergence rates of 12–21 % under 400 mM mannitol stress conditions (Figure 2.8b-c).

To investigate the ability of seeds from the *SlbHLH*$_{opt}$-overexpressing lines to germinate under salinity stress conditions, we tested the rates of germination and green cotyledon emergence in *SlbHLH*$_{opt}$-overexpressing lines under 100 mM and 150 mM NaCl stress conditions (Figure 2.8a-c). When grown on agar plates containing 100 mM or 150 mM NaCl, seeds from the *SlbHLH*$_{opt}$-overexpressing lines showed significantly higher rates of germination relative to Col-0 WT control seeds (Figure 2.8a-b). The *SlbHLH*$_{opt}$-overexpressing lines exhibited 1.6- to 1.8-fold and 5.9–6.5-fold increases in seed germination rates under 100 mM and 150 mM NaCl concentrations, respectively, relative to Col-0 WT lines (Figure 2.8a-b). Under 100 mM NaCl salinity stress conditions, the *SlbHLH*$_{opt}$- overexpressing lines also had significantly higher rates of green cotyledon emergence at 1.8- to 2.0-fold those of Col-0 WT (Figure 2.9b-c). However, green cotyledons did not emerge from seeds of either Col- 0 WT or *SlbHLH*$_{opt}$-overexpressing lines under 150 mM NaCl salinity stress conditions (Figure 2.9b-c). The increased rates of germination and green cotyledon emergence observed under water-deficit stress and salinity stress conditions suggest a potential role for *SlbHLH* TF in enhancing tolerance to those stress conditions at the germination stage.

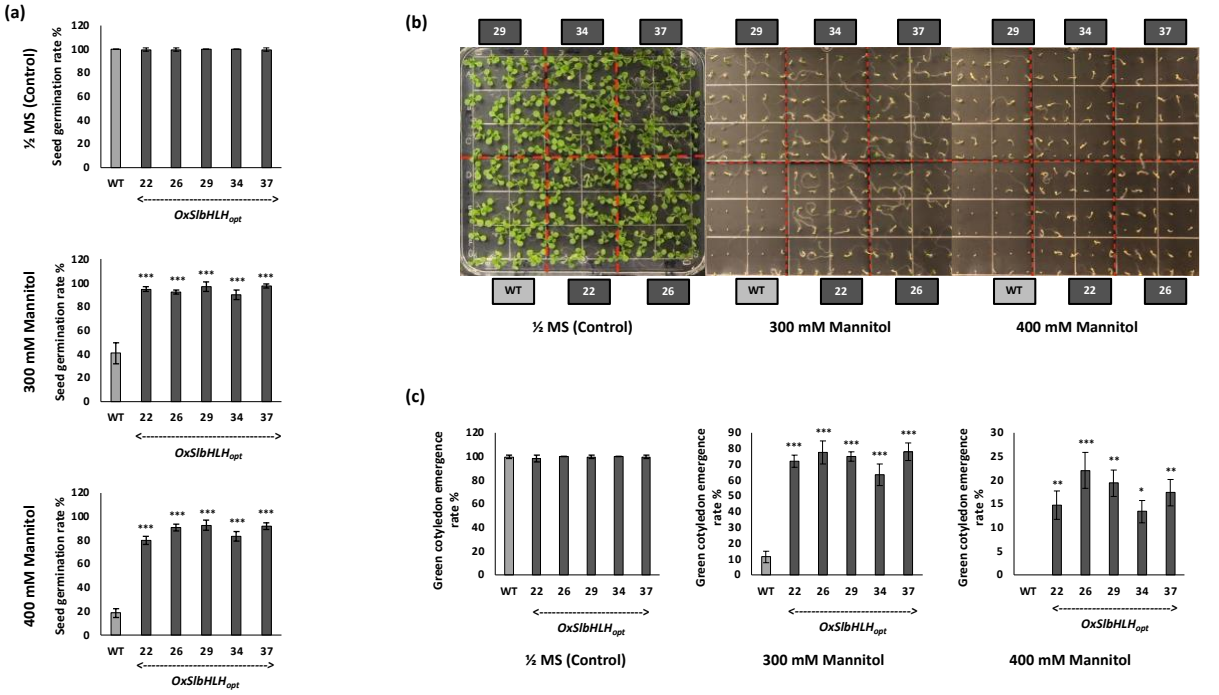

Figure 2.8 - ***Effect of SlbHLH$_{opt}$ overexpression in Arabidopsis on rates of seed germination and green cotyledon emergence under water-deficit stress conditions.*** *(a) Seed germination rates were quantified in four SlbHLH$_{opt}$-overexpressing lines (#22, #26, #29 and #37) and the Col-0 WT control line at 12 d after treatments with 0-, 300-, or 400-mM mannitol (n = 5 replicates with 30 seeds per replicate). (b) Representative image of the Col-0 WT and SlbHLH$_{opt}$-overexpressing lines ((#22, #26, #29 and #37) grown on half-strength MS medium supplemented with 0-, 300-, or 400-mM mannitol at 12 d after treatments. (c) Quantification of the rate of green cotyledon emergence in seeds of four SlbHLH$_{opt}$-overexpressing lines (#22, #26, #29 and #37) and the Col-0 WTCol-0 control line at 12 d after treatments with 0-, 300-, or 400-mM mannitol (n = 5 replicates with 30 seeds per replicate). Values represent means ± S.D., *p < 0.1, **p < 0.01, and ***p < 0.001 compared to WT, one-way ANOVA with Tukey's multiple comparison test.*

2.3.6 *SlbHLHopt* overexpression results in enhanced tolerance to salinity stress conditions at the seedling stage

Under *in vitro* 150 mM NaCl salinity stress conditions, *SlbHLHopt*-overexpressing lines showed increased primary root length, number of lateral roots, and fresh and dry biomass

compared to those of Col-0 WT lines (Figure 2.10a-e). *SlbHLH$_{opt}$* overexpression resulted in a 1.7- to 2.4-fold increase in primary root length and a 1.3- to 1.5-fold increase in the number of lateral roots compared to Col-0 WT lines after growth for 12 d under *in vitro* 150 mM NaCl stress conditions (Figure 2.10a-c). Furthermore, fresh weights and dry weights of plants from *SlbHLH$_{opt}$*-overexpressing lines were 1.3- to 1.5-fold higher and 1.4 to 1.7-fold higher, respectively, than those of Col-0 WT lines after 12 d *in vitro* salinity stress treatments (Figure 2.10d-e). These results demonstrate that plants from *SlbHLH$_{opt}$*-overexpressing lines have a greater ability to tolerate salinity stress than do Col-0 WT plants under in vitro salinity stress conditions.

2.3.7 *SlbHLH$_{opt}$* overexpression enhances flavonoid accumulation

Total flavonoid contents were assessed in plants from Col-0 WT and *SlbHLH$_{opt}$*-overexpressing lines that were grown under normal controlled plant growth room conditions. The total flavonoid content of plants from *SlbHLH$_{opt}$*-overexpressing lines was significantly higher than that Col-0 WT plants (Figure 2.11). The total flavonoid content of *SlbHLH$_{opt}$*- overexpressing lines ranged from 45.62 to 48.53 mg QE/g, representing a 1.3- to 1.4-fold increase compared with control Col-0 WT lines (Figure 2.11). These results suggest that *SlbHLH* expression affects flavonoid accumulation.

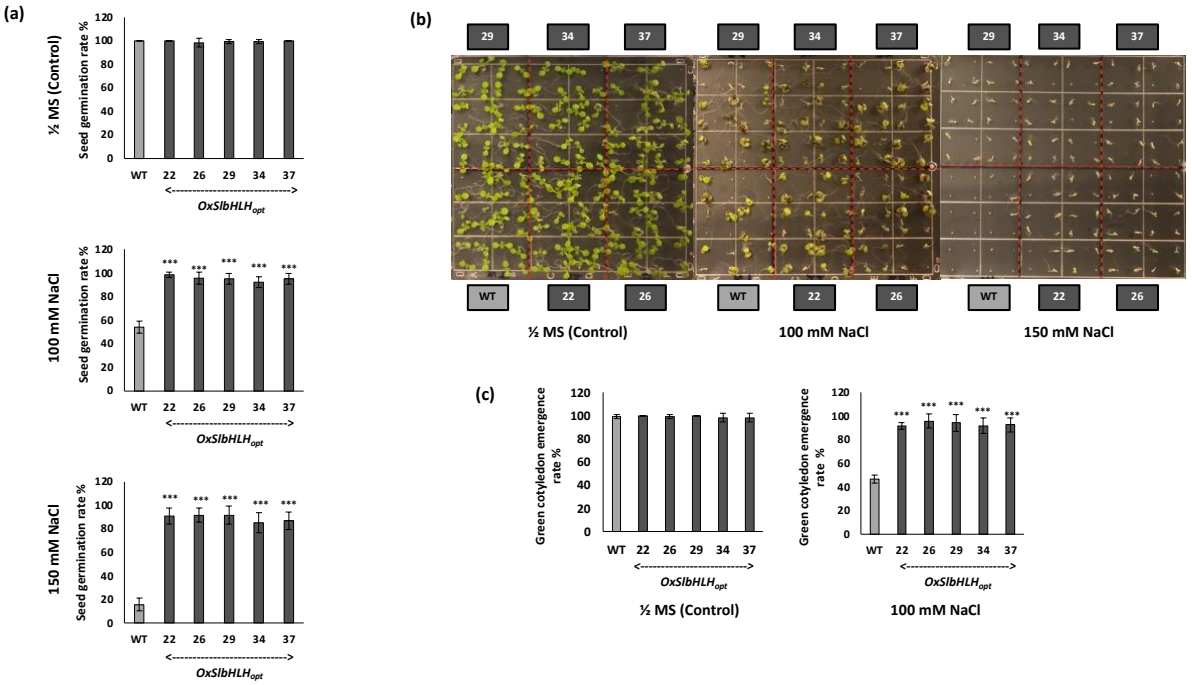

Figure 2.9 - Effect of *SlbHLH$_{opt}$* overexpression in *Arabidopsis* on rates of seed germination and green cotyledon emergence under salinity stress conditions. (a) Seed germination rates were quantified in four *SlbHLH$_{opt}$*-overexpressing lines (#22, #26, #29 and #37) and the Col-0 WT control line at 12 d after NaCl salinity treatments (n = 5 replicates with 24 seeds per replicate). (b) Representative image of the Col-0 WT and *SlbHLH$_{opt}$* overexpressing lines ((#22, #26, #29 and #37) grown on half-strength MS medium supplemented with 0, 100, or 150 mM NaCl at 12 d after treatments. (c) Quantification of the rate of green cotyledon emergence in four *SlbHLH$_{opt}$*-overexpressing lines (#22, #26, #29 and #37) and the Col-0 WT control line at 12 d after NaCl salinity treatments (n = 5 replicates with 24 seeds per replicate). Values represent means ± S.D., adjusted ***$p < 0.001$ compared to WT, one-way ANOVA with Tukey's multiple comparison test.

2.4. Discussion

To our knowledge, this study is the first to describe the potential role of an overexpressed *S. lepidophylla* transcription factor in enhancing plant abiotic stress tolerance, WUE, and plant growth and development. The observed 1.6- to 1.7-fold improvement in integrated WUE compared to Col-0 WT control lines is one significant benefit of *SlbHLH$_{opt}$* overexpression (Figure 2.7a-b).

This improvement in integrated WUE was correlated with the degree of *SlbHLH*$_{opt}$ overexpression (Figure 2.4). Several studies have shown that reduction of stomatal aperture and modulation of stomatal density corresponds to improvements in WUE (Aryal et al., 2019; Franks et al., 2015; Lim et al., 2020; Meng and Yao, 2015; Yoo et al., 2011). Lim et al. (2020) showed that the significant reduction in stomatal apertures in a codon-optimized wine grape bHLH transcription factor (*VvCEB1*$_{opt}$)-overexpressing lines resulted in increased integrated WUE. We assume that the improved WUE observed in *SlbHLH*$_{opt}$-overexpressing lines might be due to reductions of stomatal apertures and stomatal density. However, because various factors such as auxin levels, leaf water status, and abscisic acid (ABA) concentrations (Lim et al., 2020) contribute to the regulation of stomatal behavior, studying how stomatal number and morphology are involved in regulating WUE is complex. In addition to stomata, other important structures on the plant epidermis such as trichomes, the cuticle, and cuticular waxes (Bertolino et al., 2019) can also reduce water loss. For example, plants with the highest ratio of trichomes to stomata have increased WUE (Bertolino et al., 2019). Thus, more detailed studies are needed to explore the contribution of stomata and other epidermal structures to the regulation of WUE in *SlbHLH*$_{opt}$-overexpressing plants.

According to Lim et al., (2020) both reduced stomatal densities and apertures resulted in increased integrated WUE with reduced CO_2 assimilation without any negative impacts on plant growth and development. Similarly, our *SlbHLH*$_{opt}$-overexpressing lines showed enhanced plant growth and development compared to Col-0 WT control lines with increased rosette diameter (Figure 2.6a-c), plant height (Figure 2.6e-f), number of leaves in the mature rosette (Figure 2.6b-d), and number of siliques per primary inflorescence (Figure 2.6f-g). If the observed increased integrated WUE in *SlbHLHopt*-overexpressing lines corresponds to reductions of stomatal

apertures and modulation of stomatal densities, further studies would be required to determine how such reductions result in enhanced plant growth and development.

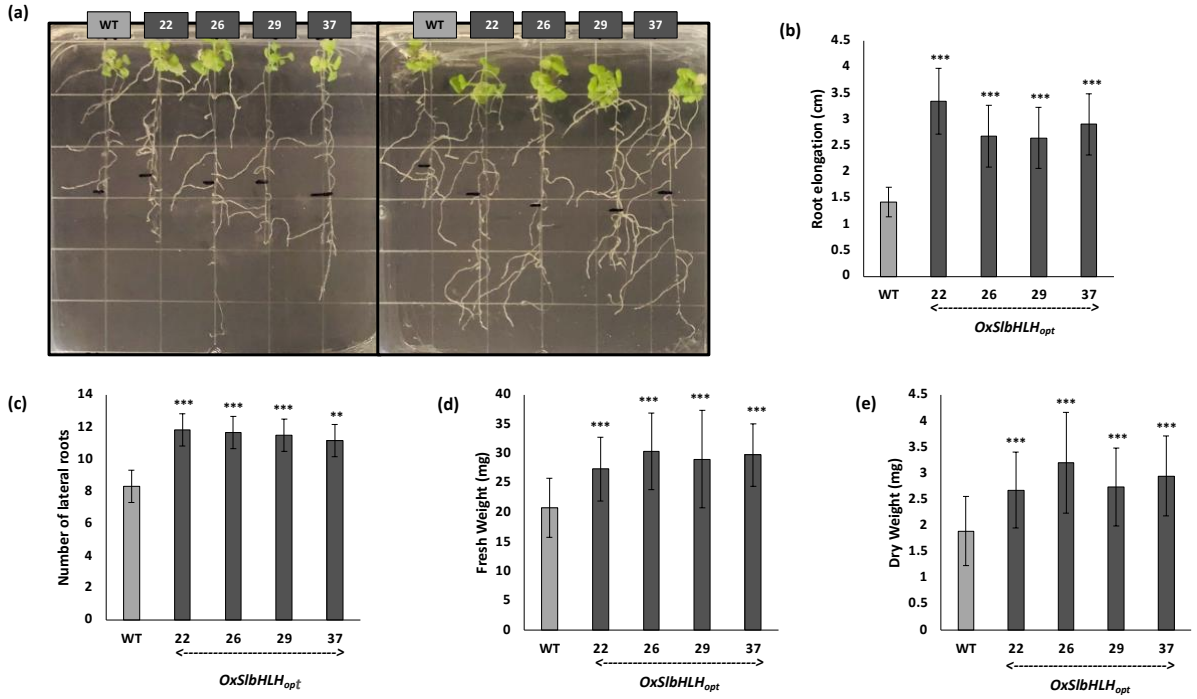

Figure 2.10 - Effect of SlbHLH$_{opt}$ overexpression in Arabidopsis on seedling response to salinity stress conditions. (a) Representative images at 12 d of plants from the Col-0 WT and *SlbHLH$_{opt}$*-overexpressing lines ((#22, #26, #29 and #37) grown on vertically on half-strength MS medium supplemented with 150 mM NaCl in vertically oriented plates. (b) Quantification of root elongation (= root length on the 12th day minus initial root length) in plants from four *SlbHLH$_{opt}$*-overexpressing lines (#22, #26, #29 and #37) and the Col-0 WT control line at 12 d after treatments (n = 30). (c) Quantification of the number of lateral roots on plants from four *SlbHLH$_{opt}$*-overexpressing lines (#22, #26, #29 and #37) and the Col-0 WT control line at 12 d after NaCl salinity treatments (n = 30). (d) Quantification of fresh weights of plants from four *SlbHLH$_{opt}$*-overexpressing lines (#22, #26, #29 and #37) and the Col-0 WT control line at 12 d after NaCl salinity treatments (n = 30). (e) Quantification of dry weights of plants from four *SlbHLH$_{opt}$*-overexpressing lines (#22, #26, #29 and #37) and the Col-0 WT control line at 12 d after NaCl salinity treatments (n = 30). Values represent means ± S.D., **p < 0.01, and ***p < 0.001 compared to WT, one-way ANOVA with Tukey's multiple comparison test.

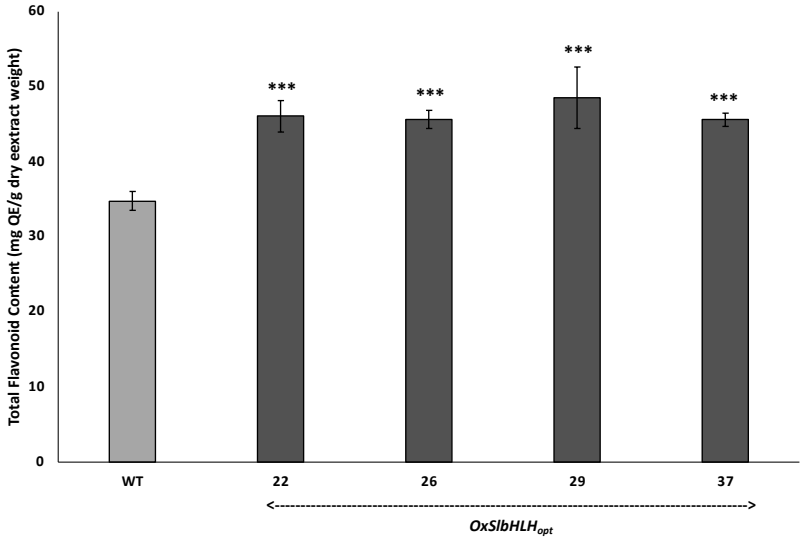

Figure 2.11 - Effect of *SlbHLH$_{opt}$* overexpression in *Arabidopsis* on flavonoid accumulation. Comparison of total flavonoid content of one month old four *SlbHLH$_{opt}$*-overexpressing lines (#22, #26, #29 and #37) and the Col-0 WT control line. Three biological replicates from each *SlbHLH$_{opt}$*-overexpressing line and Col-0 WT line and three technical replicates from each biological replicate. Values represent means ± S.D., **p < 0.01, and ***p < 0.001 compared to WT, one-way ANOVA with Tukey's multiple comparison test.

Flavonoids are a widespread class of secondary metabolites found in all land plants (Weng and Noel, 2013). Many flavonoids serve as screeners of damaging short-wave solar radiation and also as color cues in flowering plants for pollinators and seed dispersers (Weng and Noel, 2013). Other than those functions, flavonoids are also capable of a wide range of functional roles in stressed plants, including reactive oxygen species (ROS) scavenging and inhibition of the activity of auxin efflux facilitator proteins, and can also function as phytoalexins and antifeedants in plant defenses against pathogens and herbivores, respectively (Di Ferdinando et al., 2012; Weng and Noel, 2013). However, not all flavonoids are capable of multiple functions (Di Ferdinando et al., 2012). The bHLH proteins have been identified as one of the main transcriptional regulators of flavonoid biosynthetic pathway genes (Hichri et al., 2011). The bHLH TFs regulating the flavonoid pathway were first identified in maize (Chandler et al., 1989). Several recent studies

have shown that bHLH-family TFs are involved in increased flavonoid accumulation. For instance, a grape bHLH TF gene, codon-optimized *VvbHLH1*, increases the accumulation of flavonoids (Wang et al., 2016), and the *Solanum lycopersicum* L. bHLH TF gene *SlbHLH22* induces total flavonoid accumulation in *SlbHLH22*-overexpressing lines (Waseem et al., 2019). Most flavonoids have some potential to enhance water-deficit and salinity stress tolerances because of their ability to act as antioxidants to counter superoxide, peroxides, and free radicals produced during stress (Di Ferdinando et al., 2012). For example, *Vitis vinifera VvbHLH1*-overexpressing *Arabidopsis* lines with increased flavonoid accumulation exhibited increased resistance to drought and salinity (Wang et al., 2016). In both of our assays of seed germination and green cotyledon emergence under water-deficit and salt stress conditions, *SlbHLH* acts as a positive regulator in response to water-deficit and salt stress at the germination stage (Figure 2.8 a-c and 2.9 a-c). Further, $SlbHLH_{opt}$ overexpression results in enhanced tolerance to salinity stress conditions at the seedling stage (Figure 2.10a-e). Therefore, we hypothesize that higher total flavonoid contents of plants from the transgenic $SlbHLH_{opt}$-overexpressing lines might increase their antioxidant capabilities and result in increased tolerance to water-deficit stress at the germination stage and salinity stress at both germination and seedling stages. However, additional studies would be required to explore this possibility further. Flavonoid production is modulated by jasmonic acid (JA) in plants (Dombrecht et al., 2007; Goossens et al., 2016; Premathilake et al., 2020). Importantly, the *bHLH* TF family plays an essential and conserved role in JA-modulated processes in the plant kingdom (Goossens et al., 2016), such as plant growth, development, and defense, including plant abiotic stress tolerance (Goossens et al., 2016). In addition to the genes involved in the jasmonic signaling pathway as possible key genes behind the water-deficit and salt stress responses, the collective results of the study also suggest the up-regulation of genes involved in

flavonoid biosynthesis, abscisic acid (ABA) signaling pathway, and ROS scavenging in our transgenic *Arabidopsis* with the $SlbHLH_{opt}$ gene. Such up-regulation of key abiotic stress responsive-genes would be consistent with the published reports on *bHLH* overexpression of other plant species in *Arabidopsis* in regulating drought and salt stress responses (Guo et al., 2021; Wang et al., 2016).

2.5 Conclusions

Our study is the first to functionally characterize a TF from the spike moss, *S. lepidophylla*, a distant relative of the flowering plants. The study suggests that abiotic stress-responsive bHLH proteins are highly conserved. Altogether, our results demonstrated that *SlbHLH* TF functions as an important regulator of plant growth, development, abiotic stress tolerance, and improved WUE.

The desiccation tolerance of *S. lepidophylla* is among the most remarkable and successful adaptations of lycophytes that allows them to survive in extremely dry regions of the world. Thus, a better understanding of this desiccation tolerance adaptation could offer practical solutions for improving crop abiotic stress tolerance and WUE. Further exploration of *S. lepidophylla* TFs will help to provide a better understanding of this desiccation tolerance trait with broad relevance to gene regulation in plants and might help generate new hypotheses about the evolution of abiotic stress tolerance.

2.6 Funding

The work was supported by South Dakota Board of Regents Competitive Research Grant #A18-0015-001 to B.W.M. Wone. This study was also partially funded by the University of South

Dakota Graduate Research and Creative Scholarship Grant, and Department of Biology Cable/Nelson Research Assistantships to M.A. Ariyarathne.

2.7 Acknowledgements

The authors gratefully acknowledge Beate Wone, Nisitha Wijewantha, Averi Devish, David Melanson, Owen Alvine, and Shannon Fanning for helping with the study. We also thank Kelly Graber for assisting with confocal microscopy imaging. Special thanks to John C. Cushman and Won C. Yim for providing the *SlbHLH* sequence.

Chapter 3 : Developing a Genetic transformation System for the *Selaginella moellendorffii* using nanohydroxyapatite rods

Abstract

The genus *Selaginella* is in a pivotal phylogenetic position for being a sister species to all vascular plants and containing desiccation-tolerant species. Some *Selaginella* species can survive extreme dry conditions by losing almost all their water and then resurrecting when rehydrated. The plant's vegetative and reproductive desiccation responses make *Selaginella* species an emerging model system in plant science. The genus *Selaginella* also has key characteristics related to reproduction and root development. To better understand the desiccation tolerance mechanism of *Selaginella* species and the evolution and development of their vascular systems, we need to have an efficient genetic transformation system. However, the lack of an efficient genetic transformation system has hindered research progress. To address this limitation, a nanoparticle-mediated transformation tool was developed using arginine-functionalized nanohydroxyapatites, which successfully delivered reporter genes into *Selaginella moellendorffii*. Developing a genetic transformation technique for *S. moellendofii* holds the potential to be applicable to other *Selaginella* species, including *S. lepidophylla.* This tool might help identify genetic resources for crop improvement and develop a better understand of genome-level regulatory mechanisms underlying desiccation tolerance in *Selaginella*. Additionally, the tool may enable the identification of key regulatory genes of desiccation tolerance, which could be used to improve drought-sensitive crops and ensure sustainable food production.

3.1 Introduction

The genus *Selaginella* belongs in the spike moss family (*Selaginellaceae*) of lycophytes that occupies a key phylogenetic position as a sister species to all vascular plants (Banks, 2009). Approximately 700 species are found in the genus *Selaginella* and are distributed over tropical, arctic, temperate, and desert regions (Banks, 2009). The genus *Selaginella* contains both desiccation tolerant and desiccation sensitive species (Yobi et al., 2012). At least 15 members within the genus have been identified as desiccation tolerant (Alejo-Jacuinde et al., 2020), such as *S. lepidophylla* (Iturriaga et al., 2006; VanBuren et al., 2018; Yobi et al., 2013), *S. tamariscina* (Wang et al., 2010), *S. sellowii* (Alejo-Jacuinde et al., 2020), and *S. bryopteris* (Deeba et al., 2016). These species are ideal models for studying the genetic basis of plant vegetative desiccation tolerance because of their vegetative and reproductive desiccation responses and key position in the early evolution of plant vascular system (Banks, 2009; VanBuren et al., 2018; Xu et al., 2018).

The genus *Selaginella* is an emerging model system to better understand the desiccation tolerance trait and the evolution and development of plant vascular systems. An efficient genetic transformation method is essential to dissect the genetic basis of this complex trait. To our knowledge, a genetic transformation protocol is not available not only for the genus *Selaginella* but also not for any lycophytes, which greatly limits its usefulness as a model organism. Therefore, we've developed a genetic transformation protocol for *Selaginella moellendofii* species using a nanoparticle-mediated approach as Objective 2. Developing a genetic transformation technique for *S. moellendorffii* is likely to be applicable to other *Selaginella* species, such as *S. lepidophylla*.

The presence of a rigid and multilayered cell wall makes genetic material delivery uniquely challenging to accomplish in plants. The most used methods for biomolecule (i.e., DNA) delivery

in plants are *Agrobacterium*-mediated transformation, biolistic delivery, electroporation, and polyethylene glycol (PEG)-mediated delivery (Demirer and Landry, 2017). *Agrobacterium* is the most frequently used method in plant genome engineering because of higher transformation efficiencies. However, *Agrobacterium*-mediated genetic transformation is limited only to a narrow range of plant species and results in random DNA integration (Baltes et al., 2017). Even though gene delivery via biolistic particles can deliver genetic materials into a wider range of plant species, it has considerable limitations, such as plant tissue damage and random transgene integration (Altpeter et al., 2016). Despite being a fast and cost-effective method, electroporation has various drawbacks when used on plant cells. It is only effective on a limited number of plant species, and high intensity of electric field pulses used in electroporation affect the delivered gene and may even be harmful to the cells (Barampuram and Zhang, 2011; Rakoczy-Trojanowska, 2002). While PEG-mediated delivery allows for efficient transformation of protoplasts, in most plant species, it is not possible to regenerate protoplasts into fertile and whole plants. As a result, the use of PEG-mediated delivery is not practical for mature plant transformations (Barampuram and Zhang, 2011).

Nanoparticles are ideal for delivering biomolecules across the plant cell wall without external forces (Cunningham et al., 2018). At the same time, they will be an efficient tool to deliver genetic material for the high-throughput implementation of plant genetic modification without transgene integration (Demirer et al., 2019; Wang et al., 2019). Recently, nanohydroxyapatite particles (nHA) have attracted considerable attention as a new potential candidate for gene delivery in plants because of their excellent properties, namely biodegradability, biocompatibility, noncytotoxicity, nonecotoxicity, protection of DNA from nuclease degradation, ease of synthesis and surface modification to enhance gene delivery efficiency, and they are readily broken down

and used by plants as nutrients ((Izuegbunam et al., 2021; Nair et al., 2010; Priyam et al., 2019; Wang et al., 2015). In a study by Izuegbunam et al. (2021), hydroxyapatite nano rods were used to successfully deliver plasmid DNA of reporter genes into leaves of *Arabidopsis*, ice plant, tobacco, and into seed tissues of barley, wheat, and field mustard highlighting the effectiveness of nanohydroxyapatite-based gene delivery systems in plants and offering new possibilities for genetic manipulation and crop plant improvements. Here I report the use of arginine-functionalized rod-shaped nanohydroxyapatites (R-nHAs) as biocompatible nanocarriers of genes to deliver DNA into *S. moellendofii* plant cells. Such an approach will not damage plant tissues or have toxic effects to plant growth and development as with most of the conventional gene delivery methods.

3.2 Materials and methods

3.2.1 Synthesis of arginine-functionalized nanohydroxyapatite particles

Nanohydroxyapatite particles were synthesized following the method of Izuegbunam et al (2021). Briefly, a 1.5% (w/w) aqueous solution of PEG was prepared. The prepared PEG solution was mixed with $CaCl_2$ to obtain a 0.05 M, 100 ml solution. The solution was left to equilibrate overnight at room temperature (RT) and then added dropwise at a rate of 1.6 ml/min into 100 ml of a 0.03 M aqueous Na_2HPO_4 solution with constant mechanical stirring at 1000 rpm. The resulting solution was transferred to a sealed glass vial and incubated for 48 hours at RT. After 48 hours, the solution was centrifuged at 11 000 rpm for 10 minutes to separate the white precipitate. The precipitate was washed three times with deionized water, followed by three washes with absolute ethanol, and finally dried at 60 °C overnight. The resulting dried powder was then calcined at 500 °C for 2 h to obtain the nHA product.

Nanohydroxyapatite rods were arginine functionalized by mixing them with a solution 0.1 wt% arginine (100 ml). The mixture was stirred at 600 rpm for 1 hr. The functionalized particles were then separated and washed three times with deionized water. Subsequently, centrifugation at 8000 rpm for 10 min was performed to isolate the washed particles. Finally, the washed particles were dried at room temperature overnight to obtain R-nHA.

3.2.2 Plant growth

Selaginella moellendorffii plants were purchased from Plants Delight Nursery Inc. (http://www.plantdelights.com) and were grown in Miracle-Gro® Moisture Control® Potting Mix (The Scotts Company LLC, Marysville, OH, USA) under a 16 h day : 8 h night photoperiod at 22 °C in an environmentally-controlled room.

3.2.3 Arginine-functionalized nanohydroxyapatite particle–mediated delivery of GFP and GUS reporter genes in *S. moellendofii* sporophylls

3.2.3.1 Cloning and plasmid isolation of the G3GFP-GUS fusion construct

The β-glucuronidase (GUS) gene with flanking Att sites needed for LR cloning were synthesized by Gene Universal (Gene Universal Inc., Newark DE). A LR cloning reaction (Gateway^{TM} LR Clonase^{TM} II Enzyme Mix, Invitrogen, Carlsbad, CA) with the gateway binary vector pGWB452 (35S-G3GFP-R1-R2-Tnos) (Nakagawa et al., 2007) and the GUS gene were performed to generate a G3GFP-GUS fusion construct (pGWB452::GUS), where both reporter genes can be expressed in the transformed plant. The resulting pGWB452::GUS construct were transformed into NEB® 10-beta competent C3019H competent *E. coli* cells for amplification and/or storage (New England BioLabs, Ipswich, MA). Plasmid DNA were extracted from the *E.*

coli cells using the Qiagen Plasmid Mini Kit (Qiagen, Hilden, Germany). The 11,833 bp pGWB452::GUS vector is referred to as pDNA in sections 3.2.3.2 – 3.2.3.3.

3.2.3.2 Preparation of pDNA|R-nHA conjugate solution

The method described by lzuegbunam et al. (2021) was used to prepare pDNA|R-nHA conjugates with slight modifications. Briefly, an aqueous suspension of R-nHA (1 mg ml−1) was prepared by sonicating in an ice bath for 10 min to enhance dispersion. Three μg of pDNA and 600 μg of R-nHA was used to make a 1:200 pDNA|R-nHA, w/w ratio conjugate mixture. The 1:200 pDNA|R-nHA mixture was thoroughly mixed for 30 s without vertexing. The mixture was then incubated at 37 °C with shaking at 200 rpm for 90 min and mixing thoroughly every 30 mins. Exactly 10 ml of 0.5% low-viscosity Carboxymethylcellulose (CMC) was added and stirred for 15 min at room temperature to keep the pDNA|R-nHA conjugates in suspension (Liu and Lal, 2014). The formation of pDNA|R-nHA conjugates was visualized on 1% agarose gel.

3.2.3.3 Transient transformation of pDNA|R-nHA conjugates in S. moellendofii

Healthy intact *S. moellendorffii* plantlets were incubated in small beakers containing pDNA|R-nHA conjugates in a 0.5% CMC solution, R-nHAs suspended 0.5% CMC solution (control) and water only (control). The solutions were vacuum infiltrated at -0.01 MPa for 1 min following the procedure of lzuegbunam et al. (2021), and the process was repeated twice before transferring the beakers containing the infiltrated plantlets to an environmentally controlled room. The infiltrated *S. moellendorffii* plantlets were kept in the pDNA|R-nHA solution for 3 d prior to assaying for GFP and GUS expression.

3.2.3.4 Determination of GFP and GUS reporter gene expression

For GFP expression analysis, *S. moellendorffii* sporophyll slides were prepared, and GFP activity was imaged with a fluorescence microscope with a Leica DFC3000 G camera (Leica Microsystems Inc., Buffalo Grove, IL). A histochemical assay for GUS activity was performed according to Lim et al. (2018) with minor modifications. Briefly, *S. moellendorffii* plantlets were vacuum infiltrated at - 0.07 MPa for 10 min with GUS staining solution [0.5 mg/ml of X-Gluc (5-bromo-4- chloro-3-indolyl glucuronide) in 1 ml dimethylformamide, 50 mM sodium phosphate buffer (pH 7.0), 0.1 mM $K_4Fe(CN)_6$; 0.1 mM $K_3Fe(CN)_6$; and 4 mM EDTA] and were incubated at 37 °C overnight (Lim et al., 2018). To enhance the contrast for GUS staining, the treated samples were cleared with 70% EtOH to remove chlorophyll before examination with the Leica DM500 Binocular Microscope and Leica EZ24 HD Stereo Microscope (Leica Microsystems Inc., Buffalo Grove, IL).

3.2.4 Arginine-functionalized nanohydroxyapatite particle – mediated delivery of eYGFPuv reporter gene in *S. moellendofii* sporophylls

3.2.4.1 Plasmid isolation of the pAXY001 expression clone that contain the eYGFPuv gene

The pAXY0001 plasmid containing the *eYGFPuv* gene described by Yuan et al. (2021) was purchased from Addgene (Addgene plasmid #179834 - http://n2t.net/addgene:179834; RRID: Addgene_179834). The pAXY001 plasmid was in a bacterial stab, it was streaked on an agar plate with the appropriate antibiotic to obtain a single colony. Plasmid DNA was then extracted from a single colony using the Qiagen Plasmid Mini Kit (Qiagen, Hilden, Germany). The 14,360 bp pAXY001 vector is referred to as pDNA in sections 3.2.4.2 – 3.2.4.3.

3.2.4.2 Preparation of pDNA|R-nHA conjugate solution and transient transformation of pDNA|R-nHA conjugates into S. moellendorffii

The method described in section 3.2.3.2 was followed to prepare pDNA|R-nHA conjugate solution with a slight modification. Instead of using CMC, 10 ml of 0.1% w/v Trimethyl chitosan (TMC) was used to suspend the pDNA|R-nHA conjugates (Zhang and Wang, 2009).

Healthy intact *S. moellendorffii* plantlets were used for pDNA|R-nHA transient transformation. For *eYGFPuv* gene transient transformation assay 10 ml of conjugate solution with 0.02% Silwet was loaded into a 15 ml spray atomizer (Hu et al., 2020; Thagun et al., 2022) . The conjugate solution was sprayed until the spray mist covered entire plantlet. Then intact *S. moellendorffii* plantlets were incubated in small beakers containing the pDNA|R-nHA conjugate solution in an environmentally controlled room. The infiltrated *S. moellendorffii* plantlets were kept in the pDNA|R-nHA solution for 3 d prior to assaying for *eYGFPuv* gene expression. Healthy intact *S. moellendorffii* plantlets sprayed with R-nHA suspended 0.1% TMC solution were kept in the R-nHA solution for 3 d to use as control.

3.2.4.3 Determination of eYGFPuv gene expression

Fluorescence of *eYGFPuv* gene expression was observed by naked eyes under UV light uvBeast UVB-V3-365 (365 nm) (Yuan et al., 2021).

3.2.5 Characterization of Conjugates and sample preparation

The pDNA|R-nHA conjugates suspended in water, pDNA|R-nHA conjugates coated with CMC (pDNA|R-nHA-CMC), and conjugates coated with TMC (pDNA|R-nHA-TMC) were freeze dried for 24 h (0.05 mbar, -890C) for characterization using TEM and zeta potential measurements.

Transmission Electron Microscopy (TEM) was utilized to analyze changes in the prepared conjugate morphology, size, shape, and agglomeration. Zeta potential measurements were obtained to confirm CMC and TMC binding to the pDNA|R-nHA conjugates.

3.2.5.1 Transmission electron microscopy imaging

Conjugate morphologies were observed via FEI Tecnai G2 TWIN Transmission electron microscope (TEM) with an accelerating voltage of 200 kV (Field Electron and Ion Company, Hillsboro, OR, USA). Monodispersed solution from conjugates (1mg/ml) was diluted 20 times with Nanopure water. A drop of the resultant solution was deposited on copper-coated TEM grids and air-dried for 2 d in a vacuum desiccator.

3.2.5.2 Zeta potential measurements

A Malvern Zetasizer Nano ZS was used to conduct zeta potential measurements for conjugates (Malvern Panalytical Ltd., Malvern, UK). The conjugates (1mg) were dispersed in 10 ml of Phosphate-buffered saline (PBS) solution (pH=7.4, 0.1M) by sonicating for 10 minutes using an ultrasonication probe. The suspension (0.1mg/ml in PBS, pH 7.4) was transferred to a disposable capillary zeta cell to measure zeta potential. Zeta potentials were measured 5 times for each sample, and each measurement consisted of 10 runs. The presented zeta potentials values are the averages of those measurements. The conductivity of the measured suspension was always above 0.8 mS/cm for PBS.

3.2.6 *Agarobacterium* mediated delivery of GUS reporter gene

The β-glucuronidase (*GUS*) gene with flanking Att sites needed for LR cloning were synthesized by Gene Universal (Gene Universal Inc., Newark DE). The GUS gene was cloned into the gateway binary vector pGWB402 (Nakagawa et al., 2007) using the Gateway^{TM} LR Clonase^{TM} II Enzyme Mix (Invitrogen, Carlsbad, CA) to generate the pGWB402::GUS construct. Recombinant plasmid was then chemically transformed into 10-beta competent *E. coli* cells (New England Biolabs, Ipswich, MA, USA). The plasmids were extracted from the *E. coli* cells using the Qiagen Plasmid Mini Kit (Qiagen, Hilden, Germany). The vector pGWB402::GUS was transformed into *Agrobacterium* strain GV3101 using the freeze–thaw method (Wang, 2006). The day before transformation, a single *Agrobacterium* colony was grown in liquid Luria–Bertani (LB) medium containing the appropriate antibiotics. This feeder culture was incubated at 28 °C, 250 rpm for 2 d. Then the feeder culture was centrifuged at 3000 rpm for 10 min at RT and the supernatant discarded. The pellet was resuspended in infiltration buffer (10 mM MES, 10 mM $MgCl_2$, pH = 5.6). Centrifugation and resuspension steps were repeated three times to remove any remaining LB to stop *Agrobacterium* growth. The bacterial pellet was resuspended in the infiltration buffer to obtain a 1:10 dilution (OD600 = 0.5) and acetosyringone was added to the infiltrate to a final concentration of 200 M.

Healthy intact *S. moellendorffii* plantlets were incubated in small beakers containing infiltrate. The solution was vacuum infiltrated at -0.01 MPa for 1 min following the procedure of lzuegbunam et al. (2021), and the process was repeated twice before transferring the beakers containing the infiltrated plantlets to an environmentally controlled room. *S. moellendorffii* plantlets were then kept in the infiltrate for 3 d prior to assaying GUS expression.

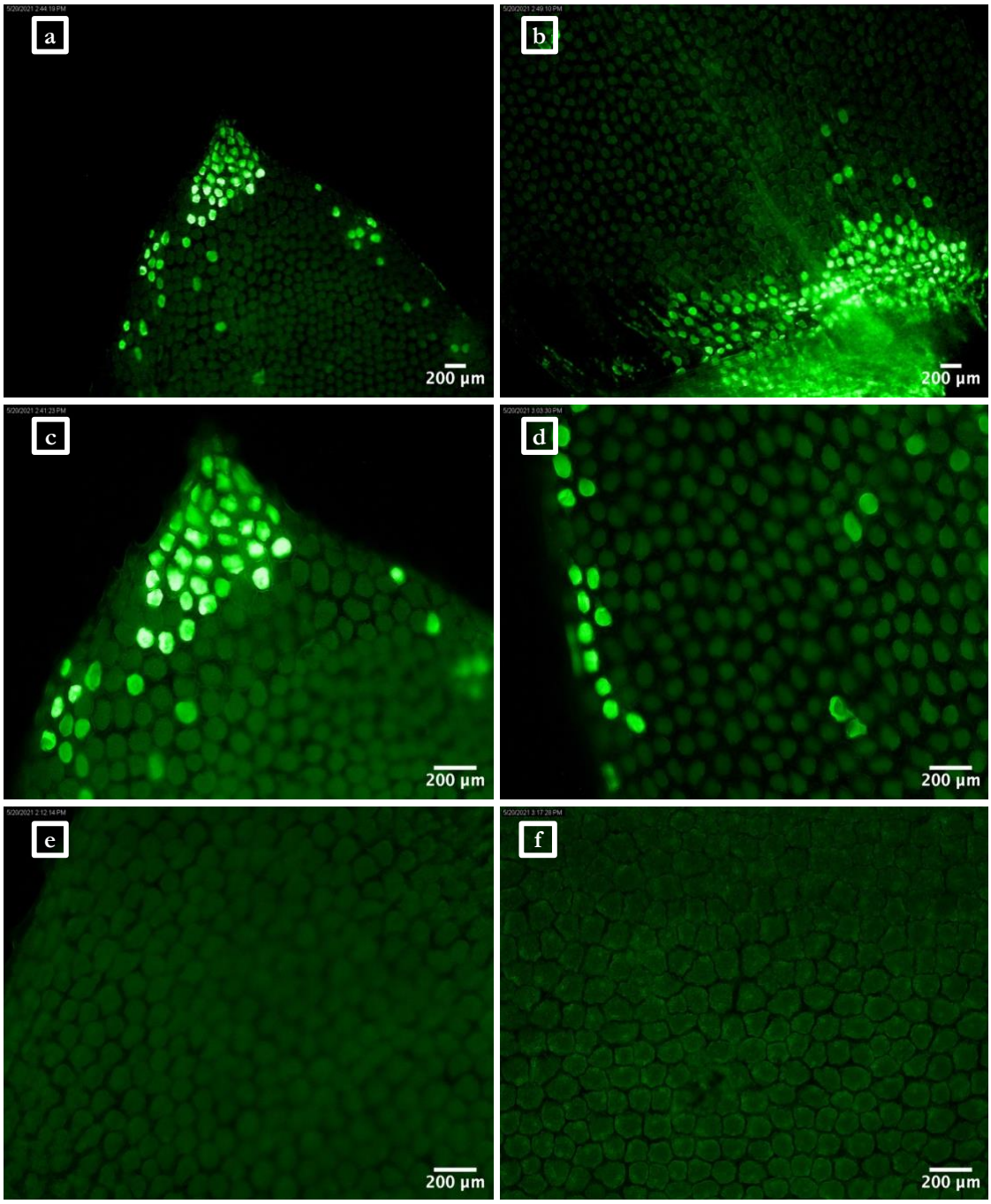

Figure 3.1 - Arginine-functionalized nano-hydroxyapatites (R-nHAs)- mediated transient expression of GFP in *S. meollendorfffii* sporophylls. GFP fluorescence was visualized using a Leica DMRA2 fluorescence microscope with a Leica DFC3000 G camera (a-d) Transient GFP expression in *S. meollendorffii* sporophyll 3d after in planta R-nHAs- mediated transformation. (e) *Selaginella meollendorffii* sporophyll 3d after incubating plantlets in R-nHAs

suspended 0.5% low-viscosity carboxymethylcellulose (CMC) solution (Control) (f) Control (untreated – incubated in water) [(a-b) Images are at 100x magnification. (c-f) Images are at 200x magnification.]

3.3 Results

3.3.1 Arginine-functionalized nanohydroxyapatite particle – mediated expression of GFP and GUS reporter genes in *S. moellendorffii* sporophylls

GFP protein expression was observed using a Leica DMRA2 fluorescence microscope with a Leica DFC3000 G camera (Leica Microsystems Inc., Buffalo Grove, IL) in the cytoplasm as green patches within the R-nHA mediated pGWB452::GUS pDNA infiltered *S. moellendorffii* sporophylls (Figure 3.1).

Arginine-functionalized nanohydroxyapatite particle-mediated pGWB452::GUS pDNA infiltered *S. moellendorffii* plantlets were subjected to histochemical GUS assay, 3 d after infiltration. The staining was followed by a destaining step using ethanol to remove chlorophyll, which can interfere with the visualization of the staining. The results showed that the GUS gene was expressed transiently in the infiltered *S. moellendorffii* plant tissues, as evidenced by the appearance of blue spots or patches (Figure 3.2).

3.3.2 Arginine-functionalized nanohydroxyapatite particle-mediated expression of *eYGFPuv* reporter gene in *S. moellendorffii* sporophylls

The *eYGFPuv*, a variant of GFP, is a recently discovered *in planta* reporter gene. It has been specifically optimized to emit the maximal fluorescence to be observed by naked eyes when exposed to ultraviolet (UV) light, eliminating the need of a fluorescence or confocal microscope (Yuan et al., 2021).

As expected, green fluorescence was observed by naked eyes under UV light on *S. moellendorffii* sporophylls 3 d post infiltration with R-nHA-mediated pAXY001 pDNA, while untransformed tissues showed red autofluorescence (Figure 3.3). Interestingly, the green fluorescence of eYGFPuv expression with the presence of red autofluorescence resulted in a brownish coloration. This combination of red auto fluorescence and green fluorescence contributed to the observed brownish hue. In contrast, the control *S. moellendorffi* showed distinctively red autofluorescence only under UV light (Figure 3.3).

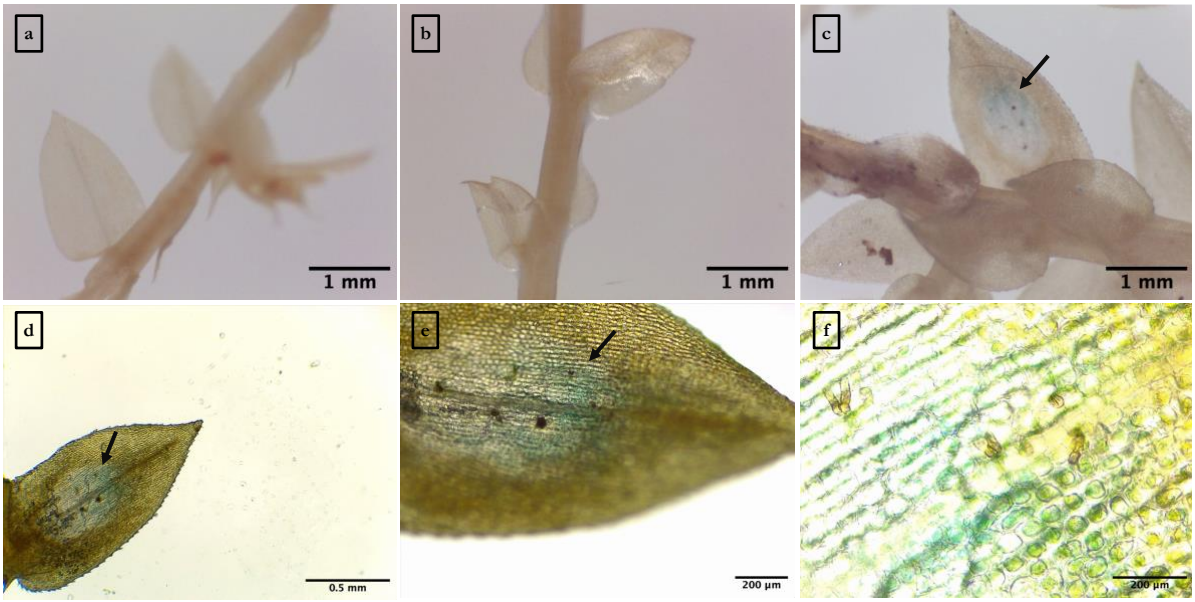

Figure 3.2- Arginine-functionalized nano-hydroxyapatites (R-nHAs)-mediated transient expression of GUS in *S. meollendorffii* sporophylls. (a-c) Images were captured using a Leica EZ24 HD Stereo Microscope and (d-f) images were captured using a Leica DM500 Binocular Microscope. (a) Control (untreated – incubated in water) (b) *Selaginella meollendorffii* sporophyll 3d after incubating plantlets in R-nHA suspended 0.5% low-viscosity carboxymethylcellulose (CMC) solution (Control) (c-f) Transient GUS expression in *S. meollendorffii* sporophyll 3d after in planta R-nHAs-mediated transformation. [(a-c) Images are at 35x magnification. (d) Image is at 40x magnification. (e) Image is at 100x magnification. (f) Image is at 400x magnification.

3.3.3 *Agrobacterium*-mediated transient expression of GUS in *S. meollendorffii* sporophylls

Agrobacterium-mediated transient expression of GUS in *S. meollendorffii* sporophylls were observed using a Leica EZ24 HD Stereo Microscope and Leica DM500 Binocular Microscope. *S. meollendorffii* sporophylls were assayed by histochemical staining for GUS followed by clearing of chlorophyll using ethanol 3 d after infiltrations. Transient GUS expression was observed in the sporophylls as characteristic blue spots or patches within *S. meollendorffii* sporophylls tissues (Figure 3.4).

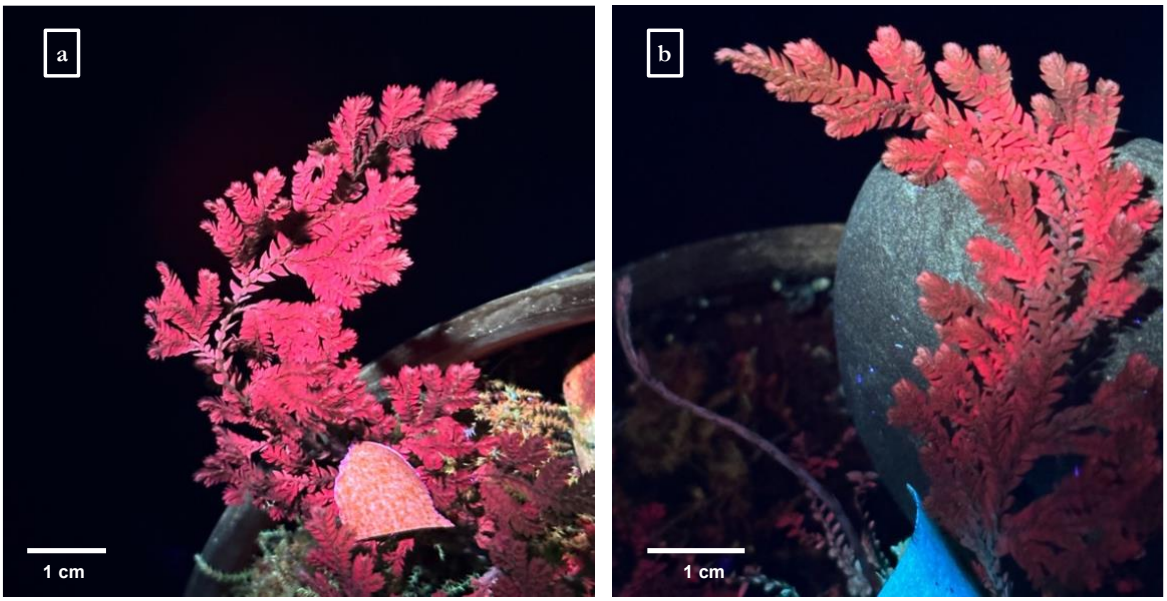

Figure 3.3 - Arginine-functionalized nano-hydroxyapatites (R-nHAs)-mediated transient expression of *eYGFPuv* in *S. meollendorffii* sporophylls. (a) Visualization of *S. meollendorffii* sporophyll under UV light 3 d after incubating plants in R-nHA suspended in 0.1% trimethyl chitosan (TMC) solution (Control). (b) Visualization of *eYGFPuv* expression in *S. meollendorffii* sporophylls under UV light 3d after *in planta* R-nHAs-mediated foliar transformation. eYGFPuv-expressing sporophylls is brownish due the combination of red autofluorescence and green fluorescence compared to non-transformed sporophylls, which show distinctively red autofluorescence.

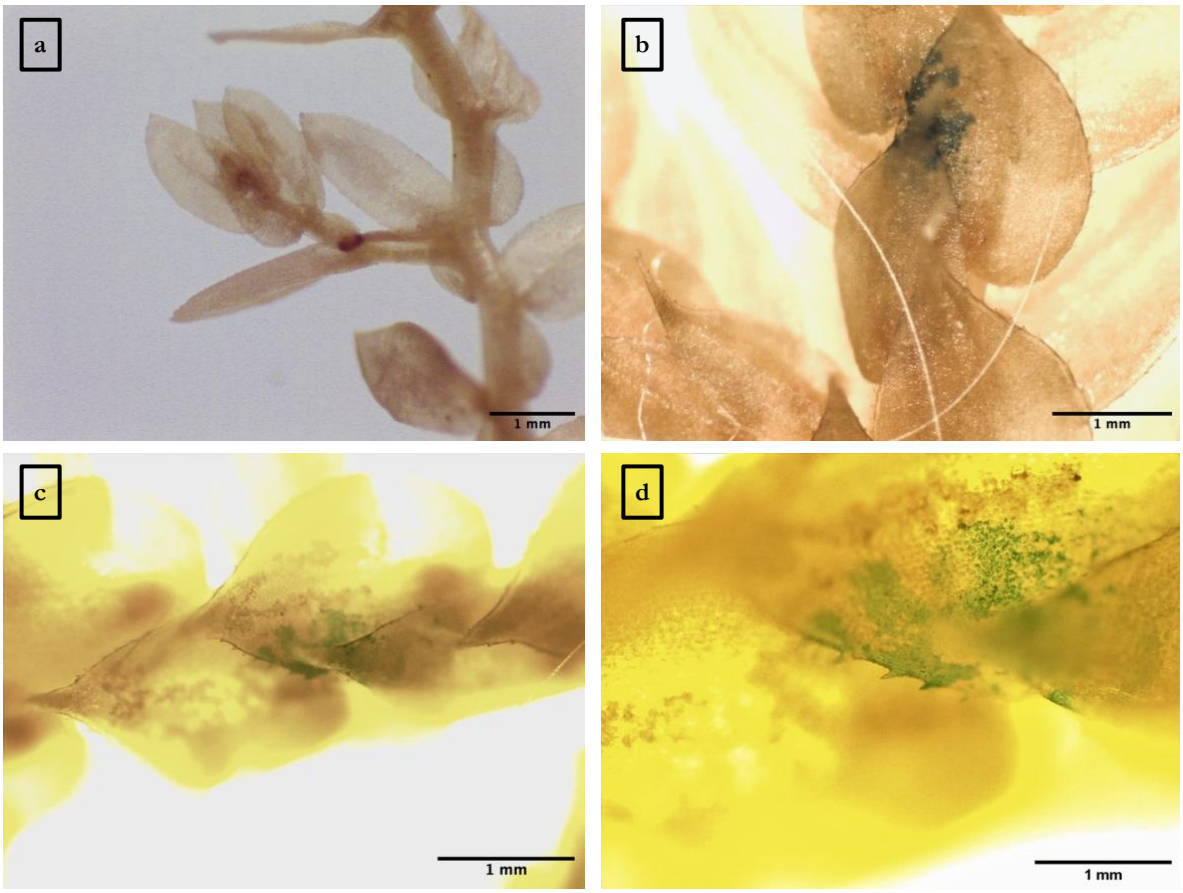

Figure 3.4 - *Agrobacterium*-mediated transient expression of GUS in *S. meollendorffii* sporophylls. (a-b) Images were captured using a Leica EZ24 HD Stereo Microscope and (c-d) images were captured using a Leica DM500 Binocular Microscope. [(a) Image is at 25x magnification. (b) Image is at 35x magnification (c) Image is at 40x magnification. (d) Image is at 100x magnification. (f) Image is at 400x magnification.]

3.3.4 Characterization of conjugates

Transmission electron microscopy images showed a significant reduction in agglomeration when the conjugates were coated with CMC or TMC, indicating that the stabilizing agents mitigated particle aggregation (Figure 3.5). The size and shape of the pDNA|R-nHA conjugates didn't change much after coating with CMC or TMC (Figure 3.5).

Zeta potential measurements were employed to assess the surface charge changes of conjugates (Figure 3.6). The initial nHA nanoparticles exhibited a slight negative charge (-19.2

mV), which was slightly reduced upon functionalization with arginine, resulting in a zeta potential of -14.33 mV for R-nHA nanoparticles (Figure 3.6). The attachment of pDNA to the R-nHA surface increased the negative charge, as indicated by a zeta potential of -24.533 mV for pDNA-R-nHA conjugates (Figure 3.6). The pDNA|R-nHA conjugates coated with CMC further enhanced the negative charge, yielding a zeta potential of -29.89 mV (Figure 3.6). Conversely, coating with TMC led to a positive zeta potential of 9.266 mV (Figure 3.6).

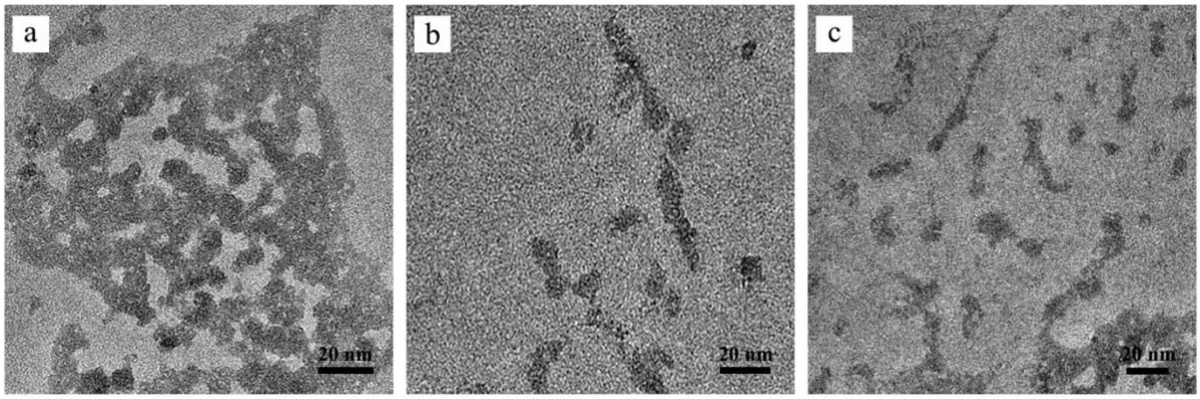

Figure 3.5 - Morphological characterization of conjugates. Transmission electron microscopy images of (a) pDNA|R-nHA (b) pDNA|R-nHA-CMC and (c) pDNA|R-nHA-TMC. Conjugate morphologies were observed via FEI Tecnai G2 TWIN TEM with an accelerating voltage of 200 kV.

3.4 Discussion

Here we report the development of simple, fast, reproducible methods for transiently introducing genes of interest into *S. meollendorfffii* through R-nHA particles. *Selaginella* species are excellent model species for studying desiccation tolerance and plant survival strategies. Evolutionary significance, desiccation tolerance and experimental accessibility make *Selaginella* species ideal model organisms in plant biology. *Selaginella* species diverged from the main lineage, flowering plants over 400 million years ago (Banks, 2009). They have unique

characteristics and survival mechanisms that have been conserved throughout their evolutionary history (Dinakar and Bartels, 2013). Studying *Selaginella* species can provide insights into the early evolution of land plants and the adaptations that allowed them to colonize terrestrial environments. Moreover, *Selaginella* species are relatively small, have a short life cycle, and can be easily propagated in the laboratory (Schulz et al., 2010). Therefore, having a genetic transformation tool will make them practical and efficient model organisms for studying desiccation tolerance and other aspects of plant biology.

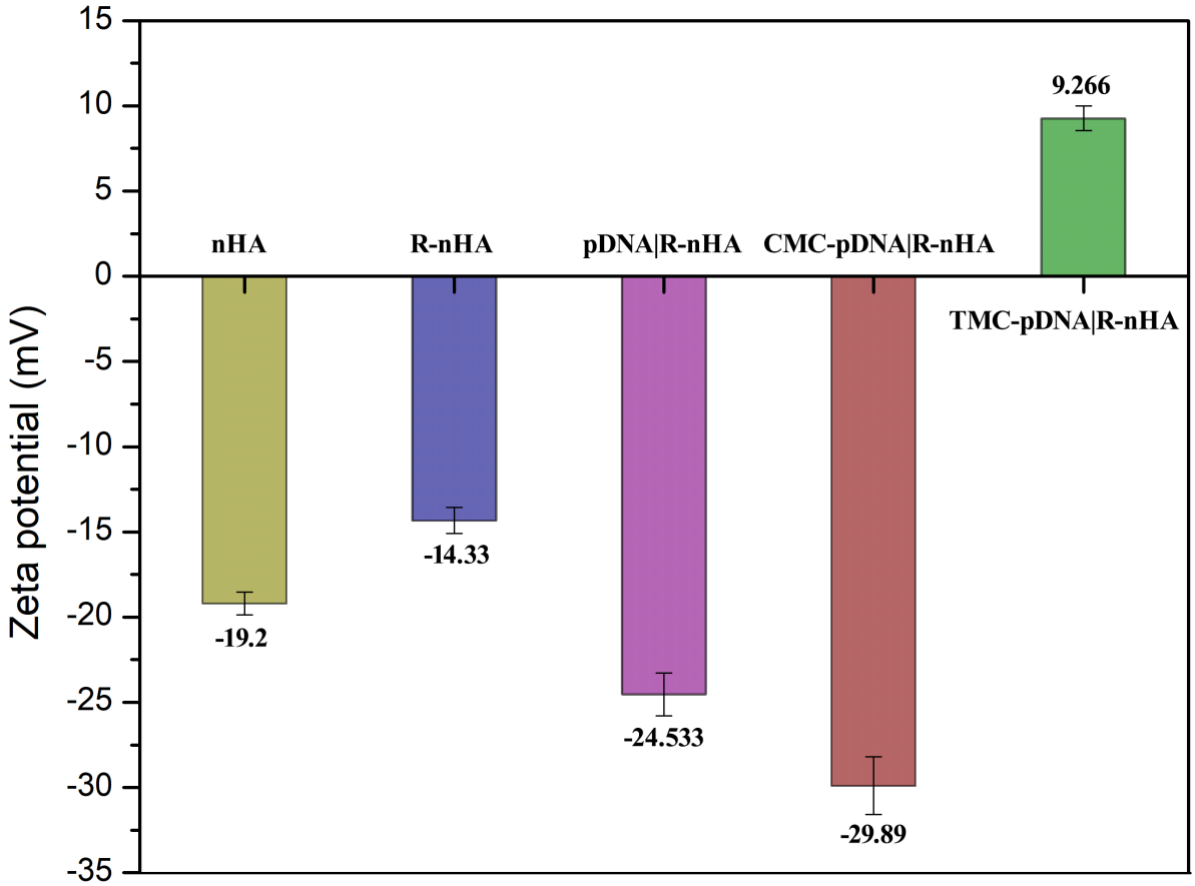

Figure 3.6 - Zeta potential measurements for nHA, R-nHA, pDNA|R-nHA, pDNA|R-nHA-CMC, and pDNA|R-nHA-TMC particles at pH 7.4. A Malvern Zetasizer Nano ZS was used to conduct zeta potential measurements.

Nanohydroxyapatite-mediated plant gene delivery has gained attention as an effective method for introducing exogenous genes into plant cells. Hydroxyapatite nanoparticles, composed of calcium and phosphate ions, resembles the composition of calcium phosphate found in the bones and teeth of mammals (Cai et al., 2007). Nanohydroxyapatite-mediated plant gene delivery tool is a cost-effective, easy, fast, species-independent, and scalable method that does not cause damage to the target organisms (Izuegbunam et al., 2021; Wang et al., 2015). Importantly, this system avoids the undesired integration of vector sequences into the genome of the target organism, ensuring the integrity of the native genetic material (Demirer et al., 2019; Izuegbunam et al., 2021). Furthermore, these nanocarriers are non-toxic, easy biodegradable, biocompatible, and a reduce the likelihood of horizontal transfer of the delivered genetic cargo (Izuegbunam et al., 2021; Wang et al., 2015). These excellent properties of nHA-mediated plant gene delivery make it a valuable tool for precise and effective genetic manipulation in plants to advance plant biotechnology and genetic engineering applications.

To enhance gene delivery efficiency, we utilized R-nHAs. The positive charge of arginine promotes electrostatic interactions with negatively charged nucleic acids (Deshmukh et al., 2019; Wang et al., 2015). When arginine is attached to the surface of nHA, it can facilitate the binding of nucleic acids, increasing the cellular uptake of gene-loaded nanoparticles (Deshmukh et al., 2019; Wang et al., 2015). Arginine is a naturally occurring cationic amino acid and the use of arginine for functionalizing nHA does not pose significant toxicity concerns (Deshmukh et al., 2019).

The zeta potential values obtained in this study provided insights into the surface charge changes of conjugates (Figure 3.6). The initial nHA nanoparticles exhibited a slight negative charge, which can be attributed to the presence of hydroxyl groups on the surface (Figure 3.6).

Upon functionalization with arginine, the zeta potential of R-nHA particles became less negative, indicating the successful attachment of arginine molecules to the nanoparticle surface (Figure 3.6). Subsequently, binding pDNA to the R-nHA surface further increased the negative charge of pDNA|R-nHA conjugates (Figure 3.6). This increase in negative charge suggests the binding of pDNA molecules onto the nanoparticle surface through electrostatic interactions (Figure 3.6).

To enhance gene delivery efficiency pDNA|R-nHA conjugates were coated with stabilizing agents, CMC and TMC. The conjugates coated with the negatively charged polymer CMC (Arumughan et al., 2021) resulted in a highly negative zeta potential, indicating effective incorporation of CMC molecules onto the particle surface (Figure 3.6). In contrast, coating with as a positively charged polymer TMC (Mourya and Inamdar, 2009) led to a positive zeta potential reading, indicating incorporation of TMC onto the conjugate surface (Figure 3.6). The positively charged TMC layer likely contributed to enhanced electrostatic stabilization, improving the dispersibility and stability of the particles, resulting in efficient gene delivery (Mi et al., 2008; Zhang and Wang, 2009). The zeta potential measurements provided further confirmation of coated conjugates, as well as the impact of stabilizing agents on the surface charge of pDNA|R-nHA conjugates.

Transmission electron microscopy images of the pDNA|R-nHA conjugates (Figure 3.5) revealed their size, shape, and aggregation state. Aggregates were observed in the non-coated conjugates (pDNA|R-nHA), indicating the presence of electrostatic interactions and van der Waals forces between the conjugates (Figure 3.5 a). These aggregates can hinder proper dispersion and subsequent gene delivery. However, when the pDNA|R-nHA particles were coated with CMC or TMC, TEM images showed a notable reduction in agglomeration (Figure 3.5 b-c). This suggests that the stabilizing agents mitigated particle aggregation. Carboxymethylcellulose, being a

negatively charged polymer (Arumughan et al., 2021), likely created a repulsive barrier between conjugates, preventing their proximity and subsequent agglomeration (Ibrahim et al., 2020). Trimethyl chitosan, on the other hand, as a positively charged polymer (Mourya and Inamdar, 2009), may have enhanced electrostatic stabilization, thereby reducing aggregation (Mi et al., 2008; Zhang and Wang, 2009). Further, Trimethyl chitosan (TMC) is a modified form of chitosan, a biocompatible and biodegradable polysaccharide derived from chitin (Zhang and Wang, 2009). TMC has gained significant attention in the biomedical field of gene delivery due to its unique properties and advantages (Zhang and Wang, 2009). As TMC is positively charged, it might enhance the cellular uptake of the gene-loaded nanoparticles, leading to a more efficient delivery of genetic material (Zhang and Wang, 2009). Importantly, the coating process did not significantly alter the size and shape of the pDNA|R-nHA conjugates (Figure 3.5 b-c). This is advantageous as the original size and shape are critical for efficient cellular uptake and gene delivery (Izuegbunam et al., 2021). The coated conjugates exhibited stable and well-dispersed characteristics, potentially enhancing their interaction with plant cell wall and membranes, and thus improving transformation efficiency. Altogether R-nHA gene delivery tool transiently transformed *GFP,* and *GUS* and *eYGFPuv* reporter genes into *S. meollendorfffii.*

3.5 Conclusions

The *in-planta* nano-biomimetic plant transformation method I have developed for *S. meollendorfffii* could be optimized as a stable transformation system to deliver a Cas9 and guide RNAs (gRNAs) plasmid into the reproductive tissues (strobili). Genetic transformation of *Selaginella* species may provide a powerful tool for studying the molecular mechanisms underlying desiccation tolerance. By introducing or silencing specific genes, researchers can examine their roles in conferring the desiccation tolerance trait and unravel the complex pathways

involved. This knowledge is crucial for understanding the fundamental processes of desiccation tolerance and can aid in the development of strategies to enhance drought resistance in other plant species.

3.6 Funding

The authors thank the University of South Dakota Graduate Research and Creative Scholarship Grant, and Department of Biology Graduate Travel Award to MA Ariyarathne, as well as partial support from Bayer Crop Science 4Ag Grant to BWM Wone and C Izuegnunam.

3.7 Acknowledgements

The authors gratefully acknowledge Beate Wone, and all Wone Lab members and Nisitha Wijewantha and Sereda Lab for their help with the study.

Chapter 4 : Identification of Dehydration Responsive Genes from the Transcriptome of *Selaginella lepidophylla* during dehydration time course

Abstract

Selaginella lepidophylla, a desiccation tolerant lycophyte species, possesses the unique ability to survive extreme arid conditions. This remarkable adaptation involves the regulation of numerous genes that play vital roles in desiccation tolerance. To uncover the genes associated with this desiccation tolerance phenomenon, we conducted a comprehensive transcriptomic analysis of *S. lepidophylla* during the dehydration process. Through high-throughput sequencing, we generated a vast dataset comprising 126,655 transcripts. Among these transcripts, 4,750 were identified as differentially expressed at 25% relative water content (RWC) compared to 100% RWC. Notably, 2,409 transcripts displayed an increased relative abundance, while 2,340 transcripts exhibited a decreased relative abundance. Among the highly abundant genes at 25% RWC were those known to function in stress response, including early light-inducible proteins (ELIPs), pentatricopeptide repeat-containing proteins (PPRs), antioxidant enzymes (Catalase, Peroxidase, Glutathione reductase), antioxidant compounds (Peroxiredoxin, thioredoxin), drought-responsive protein kinases, stress-responsive proteins, and ABC transporter B family members (ABCB). Intriguingly, three transcription factor (TF) families, namely trihelix TF, transcription factor AS1, and WRKY TF, exhibited increased transcript abundance under dehydration stress. This transcriptomic analysis identified dehydration responsive genes involved in the desiccation mechanism of *S. lepidophylla*. The findings of this study provide valuable information and serve as a resource for future functional analyses, aimed at improving the drought tolerance of crop plants. To gain a deeper understanding of the regulatory mechanisms underlying desiccation tolerance, further gene

co-expression analysis is recommended. Such analyses can shed light on the presence of constitutively expressed genes associated with the desiccation tolerance response. Moreover, the application of the time-delay correlation (TDCor) gene regulatory network approach holds promise in identifying master regulatory genes that initiate the genetic cascade involved in the desiccation stress tolerance pathway. The identification of these master regulatory genes will greatly contribute to future research on desiccation stress response regulation and the bioengineering of master regulatory genes into drought-sensitive crop species.

4.1 Introduction

Plant vegetative desiccation tolerance refers to the ability of certain plant species to withstand extreme water loss in their non-reproductive tissues, such as leaves, stems, and roots. While desiccation tolerance is commonly observed in seeds of angiosperm plants, only a limited number of plants (approximately 330) plants have evolved the capacity to survive severe dehydration in their vegetative organs (Costa et al., 2016; Leprince and Buitink, 2015). These plants, often referred to as resurrection plants, can endure water contents as low as 1% to 5% without suffering irreversible damage (Giarola et al., 2017; Oliver, 1996). The development of desiccation tolerance in vegetative tissues is thought to have originated early in the evolution of land plants as they colonized terrestrial habitats (Gaff and Oliver, 2013). However, during plant evolution, desiccation tolerance in vegetative organs was gradually lost in favor of other traits like enhanced growth rate and structural complexity (Farrant and Moore, 2011). Nevertheless, in response to prolonged drought stress, some plants have reactivated or reacquired the ability to tolerate desiccation in their vegetative tissues, possibly by rewiring ancestral desiccation tolerance mechanisms (Hilhorst et al., 2018). Understanding the mechanisms underlying vegetative desiccation tolerance in plants can shed light on the fundamental processes involved in stress

adaptation and may have implications for crop improvement and the development of strategies to mitigate the impacts of drought on agriculture.

Selaginella lepidophylla is a desiccation-tolerant plant, exhibits the extraordinary ability to survive extreme dehydration and revive upon rehydration. During periods of drought, *S. lepidophylla* undergoes desiccation-induced dormancy, curling up its leaves and appearing lifeless. This state, known as anhydrobiosis, allows the plant to withstand near-complete dehydration, with its water content dropping to less than 5% (Giarola et al., 2017). After years of desiccation, when water is reintroduced, the plant can fully recover and resume normal metabolic activities (Yobi et al., 2013). *Selaginella lepidophylla* possesses a relatively small genome, 109 Mb in size. Whole-genome duplication is a significant evolutionary process observed in many vascular land plants. Interestingly, the *Selaginellaceae* family, to which *S. lepidophylla* belongs, has been suggested to be the only group of vascular plants that did not undergo a whole-genome duplication event (Jiao et al., 2011).

Through metabolic profiling of *S. lepidophylla*, it has been observed that this plant maintains higher levels of various sugars, amino acids, sucrose, monosaccharides, polysaccharides, sugar alcohols, betaine (an osmoprotectant), flavonoids, g-glutamyl amino acids, and lipoxygenase (Yobi et al., 2013, 2012). These compounds are believed to play a role in detoxifying reactive oxygen species (ROS) and contributing to desiccation tolerance (Yobi et al., 2012). The sequencing of the *S. lepidophylla* genome by VanBuren et al. (2018) has furnished the research community with valuable assets that facilitate the study of the molecular foundations of desiccation tolerance. This milestone equips scientists with essential resources and information to delve into the genetic basis and mechanisms underlying the desiccation tolerance trait. (VanBuren

et al., 2018). However, the precise molecular mechanisms that distinguish desiccation-sensitive species from desiccation-tolerant species are still not well understood (Yobi et al., 2012).

Selaginella lepidophylla is an ideal model organism for studying desiccation tolerance in plants as it represents the earliest-diverging lineage of vascular plants and can withstand extremely dry conditions in its natural habitats (Banks, 2009; VanBuren et al., 2018). By unraveling the mechanisms underlying the remarkable resilience of *S.lepidophylla*, we will be able gain a deeper understanding of how plants can adapt to water scarcity and develop strategies to enhance crop plant resilience in drought-prone areas.

Some bryophytes, such as *Tortula ruralis*, are fully desiccation-tolerant mosses that can endure the complete loss of free protoplasmic water regardless of the rate of water loss (Liu et al., 2008; Oliver, 1996; Oliver et al., 2000). These bryophytes exhibit desiccation tolerance by employing constitutive cellular protection and rehydration-induced cellular repair mechanisms, making them tolerant to desiccation irrespective of the rate of water loss (Oliver, 1996). In contrast, desiccation-tolerant angiosperms that are described as modified desiccation-tolerant plants rely on induced cellular protection and repair processes to survive desiccation but only when the rate of water loss is slow (Ingram and Bartels, 1996; Oliver, 1996). *Selaginella lepidophylla*, a member of the lycophyte group, holds an intermediate phylogenetic position between bryophytes and angiosperms (Banks, 2009). The objective of this chapter is to gain an understanding of the remarkable desiccation tolerance trait in *S. lepidophylla*, exploring the genes responsible for the desiccation tolerance. Here we report our study on identification of dehydration responsive genes of *S. lepidophylla* through transcriptomic analysis.

4.2 Materials and methods

4.2.1 Plant material maintenance and water-deficit stress treatments

Selaginella lepidophylla plants were purchased in the dried state and were maintained the dry state until the plants were put through a rehydration cycle to remove non-viable tissue. Before sample collection for RNA extraction, the method described by Yobi et al. 2013 with slight modifications was followed to determine the RWC loss during the dehydration process (Figure 4.1). Briefly, to determine the rate of RWC loss during the dehydration process, five desiccated *S. lepidophylla* plants were submerged in distilled water under controlled plant growth room conditions (constant 100 μmol m^{-2} s^{-1} cool-white fluorescent and incandescent light at 28°C and 33% relative humidity) (Yobi et al., 2013). After 24 h of rehydration, fully hydrated plants, were then removed from the water and weighed (time zero – T_0) (Yobi et al., 2013). After the initial weighing, the plants were blotted dry and placed in dry trays and weighed at regular intervals over a 24-h period (Yobi et al., 2013). Then dry weights were obtained by incubating plants at 65 °C for 2 d. The morphologies of the rehydrated *S. lepidophylla* plants and plant during dehydration process were observed.

To construct the dehydration curve for *S. lepidophylla,* the RWC were calculated using the following formula described by Yobi et al. (2013), where F_{wt} is the fresh weight at specific time points during the dehydration cycle, D_{wt} is the weight after incubation at 65°C for 2 d, and FT_{wt} is the weight after 24 h of rehydration (Equation 4.1).

Equation 4.1- Calculation of RWC

$$RWC\ (\%) = (F_{wt} - D_{wt})/(FT_{wt} - D_{wt}) \times 100$$

4.2.2 Sample collection and RNA extraction from *S. lepidophylla* tissues

Plant leaf samples representing five RWCs (100% RWC, 85% RWC, 75% RWC, 50% RWC and 25% RWC) were collected for RNA extraction (Figure 4.2). Leaf tissues harvested from each RWC were placed immediately in liquid nitrogen for total RNA isolation. The *Selaginella lepidophylla* dehydration curve that was constructed as described in 4.2.1 was used to determine the RWC for sample collection. Sampling was done in triplicate for each time point. Total RNA was extracted from collected *S. lepidophylla* plant samples using a Quick-RNA Plant Miniprep Kit (Zymo Research, Irvine, CA, USA) according to the manufacturer's instructions.

4.2.3 Library construction and sequencing

Extracted and purified RNA samples were sent to Novogene (Sacramento, CA, USA) for RNA-Seq analysis. Library preparation and sequencing was performed by Novogene (Sacramento, CA, USA). cDNA libraries were sequenced using the 2x150 paired end on the NextSeq platform (Illumina, San Diego, CA).

4.2.4 RNA-Seq data analysis

4.2.4.1 Mapping sequence reads to the reference genome

Sequence reads were trimmed to remove adapter sequences and nucleotides with poor quality using bcl2fastq (v.1.8.4; Illumina). The trimmed reads were mapped to the *S. lepidophylla* reference genome by VanBuren et al., (2018) using the HISAT2 (Galaxy Version 2.2.1+galaxy1), splice-aware aligner (Kim et al., 2015). All transcriptome versions ar available on request from the authors.

4.2.4.2 Transcript assembly and merging transcript assemblies

Transcripts were assembled and quantified using StringTie (Galaxy Version 2.2.1+galaxy1) (Pertea et al., 2015). Reference transcript was used to guide the assembly. StringTie's merge function (Galaxy Version 2.2.1+galaxy1) was employed to merge the transcripts from each time point separately (Tuba et al., 1998). Assembled transcripts for each RWC from three biological replicates were merged to create the merged transcripts. StringTie provides read-count data for each transcript, which is required by differential expression analysis. Count matrices for transcripts were generated using output files obtained from StringTie. The expression value for each transcript was calculated with the fragments per kilobase of transcript per million mapped reads (FPKM) method. The hierarchical clustering and Principal component analysis (PCA) of RNA-Seq data were performed using IDEP. 96 (Ge et al., 2018).

4.2.4.3 Differential expression analysis

The DESeq2 software, version 1.26.0 (Love et al., 2014) was utilized for differential expression analysis. The transcripts based on experimental conditions were grouped to determine which genes are differentially expressed between conditions. To control the false discovery rate, the resulting p-values were then adjusted using the Benjamini and Hochberg (1995) approach. According to the results of the DESeq2 analysis, a gene whose FDR, P_{adj}-value was < 0.01 and log2fold-change ≥ 2 or log2fold-change ≤ -2 was categorized as a differentially expressed gene (DEG).

4.2.4.4 Functional annotation of DEGs

To gain insights into the potential functions of these differentially expressed transcripts, a functional annotation was employed using BLASTN (RRID:SCR_001598). Transcripts with a

significant difference in DESeq2 analysis (FDR, P_{adj}-value < 0.01) at 25% RWC compared to the 100% RWC were functionally annotated using BLASTN (bit score ≥90) against *Selaginella moellendorffii* and *Arabidopsis thaliana* NCBI RefSeq databases.

4.2.4.5 Visualization of results of the differential expression analysis

DESeq2 includes plotting tools as part of the R/Bioconductor package. Those tools and IDEP.96 (Ge et al., 2018) were utilized to visualize the results of the differential expression analysis.

4.2.4.6 Gene Ontology (GO) analysis

Gene ontology enrichment was performed to identify enriched biological processes (BP), molecular functions (MF), and cellular components (CC) for the DEGs that showed statistical significance (P_{adj}-value < 0.01) and were annotated with *A. thaliana* RefSeq database. The Database for Annotation, Visualization, and Integrated Discovery (DAVID) tool was used for the analysis (Huang et al., 2009; Sherman et al., 2022). Only hits with a Benjamini-Hochberg False Discovery Rate below 0.01 were accepted as significant.

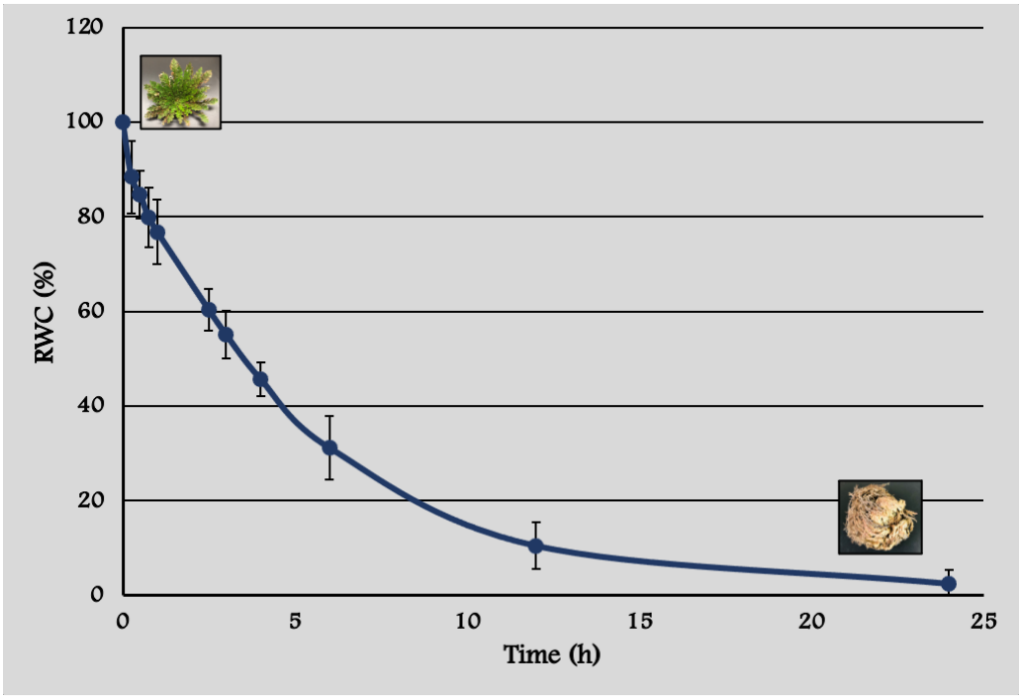

Figure 4.1 - *Selaginella lepidophylla* dehydration curve. The dehydration process was assessed by tracking the percentage of relative water content (RWC) lost over 24 h period. The data presented in the graph represent the average values from six replicates (n = 6). Values represent means ± S.D.

4.3 Results

4.3.1 Dehydration rates in *S. lepidophylla*

Selaginella lepidophylla RWCs was monitored over a 24 h period to determine dehydration rates. First plants were allowed to hydrate, then dehydrate over 24 h period. Upon hydration, *S. lepidophylla* plants exhibited expanded green microphylls. Notably, chlorophyll was observed to be present, at least partially, on the inner surface of the microphylls, indicating that *S. lepidophylla* retain chlorophyll when dehydrated. This characteristic suggests that *S. lepidophylla* is homiochlorophyllous (Tuba et al., 1998). Dehydration occurred in *S. lepidophylla*, with 75% of water loss taking approximately 7.5 hours (Figure 4.1). As the plants dehydrated, the microphylls curled tightly into a protective ball (Figure 4.1). This response is considered adaptive, projecting against damage from high levels of irradiance and/or temperatures.

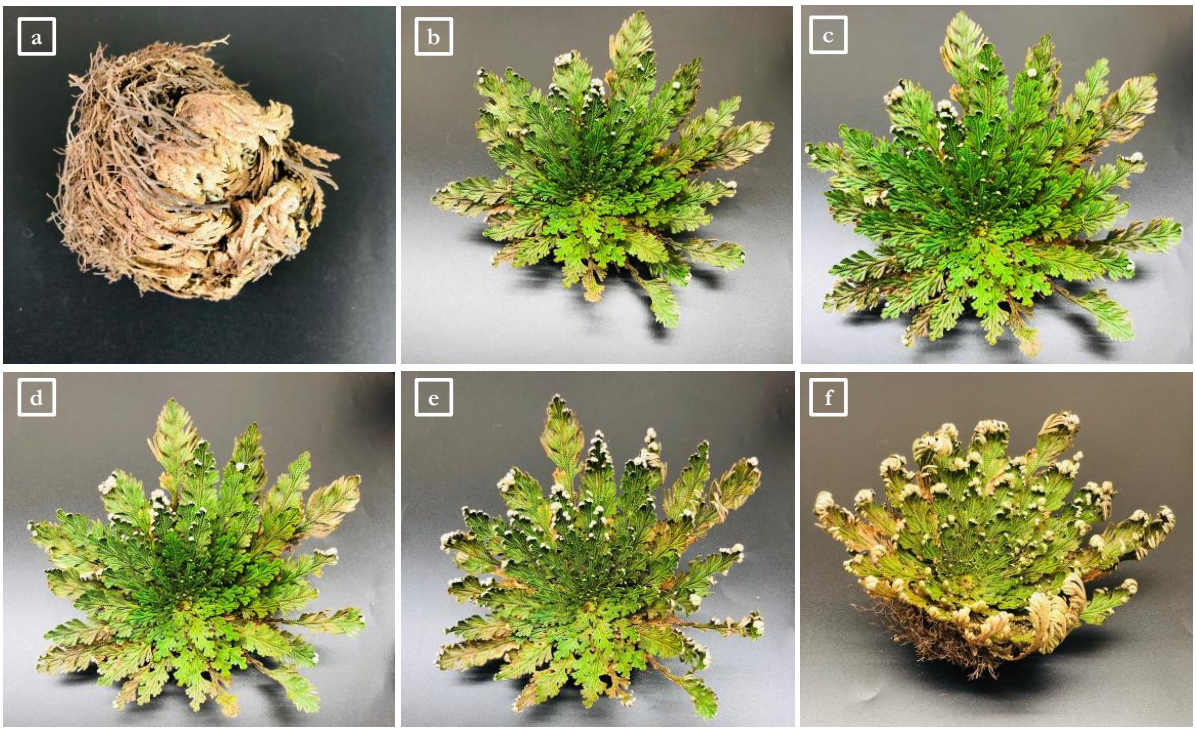

Figure 4.2 - Overview time course sampling of *S. lepidophylla* during dehydration process. (a) Initial dry stage of desiccated *S. lepidophylla*. Samples were collected from **(b)** at at time 0 - fully hydrated (fully recovered) – 100% RWC, 0.0T **(c)** after 0.5h of the dehydration process – 85% RWC, 0.5T, **(d)** after 1h of the dehydration process – 75% RWC, 1.0T, **(e)** after 3.5h of the dehydration process – 50% RWC, 3.5T, and **(f)** after 7.5h of the dehydration process – 25% RWC, 7.5T of *S. lepidophylla.*

4.3.2 Read alignment with HISAT and Transcript assembly and quantification with StringTie

We extracted RNA from *S. lepidophylla* leave tissues at different RWCs to obtain a global overview of changes in transcript abundance during the dehydration process. After sequencing, a large amount of clean data was obtained, confirming the reliability of the sequencing results. The detailed transcriptional pattern information is summarized in Table S1. Over 93% of the clean reads from each sample were mapped to the *S. lepidophylla* reference genome sequence (Table S1 and Figure S1). Transcripts were assembled and quantified using StringTie. After assembling all

the samples, the gene and transcript models were merged using the StringTie merge operation. Merged transcripts were obtained corresponding to each RWC level.

(a)

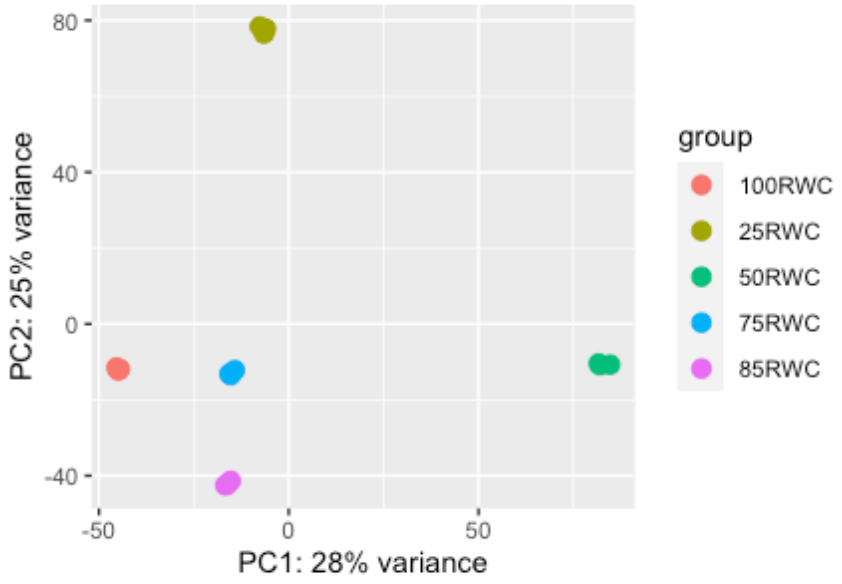

(b)

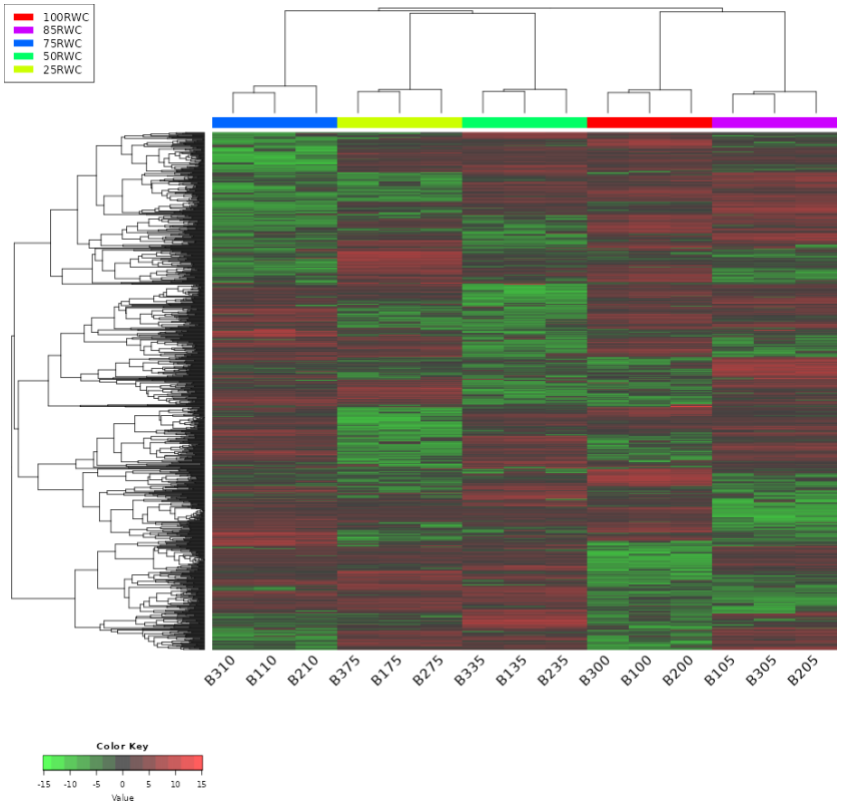

Figure 4.3 – Relative transcripts abundance changes of different samples in response to dehydration. (a) Hierarchical clustering of the top 1000 genes reveals patterns of relative transcript abundance. IDEP.96 (Ge et al., 2018) was utilized to visualize the results. (b) Principal component analysis (PCA) plot of transcriptomic data at different RWC. Hierarchical clustering and PCA analyses indicate the substantial difference in thousands of genes induced by dehydration.

The PCA analysis demonstrated that the global gene expression profiles exhibited distinct patterns across different RWCs (Figure 4.3a). Notably, the PCA plot clearly exhibited a noticeable distinction and separation between different RWCs, emphasizing the influence of dehydration levels on gene expression. We performed hierarchical clustering using the top 1000 genes. The resulting hierarchical clustering plot, as depicted in Figure 4.3b, revealed dehydration stress led to a significant alteration in the expression of hundreds of genes. Moreover, we observed very minimal variations among replicates, indicating the reliability of our results.

4.3.3 Screening of differentially expressed genes (DEGs)

Differentially gene expression analysis was conducted to gain a comprehensive overview of the *S. lepidophylla* transcriptome during dehydration process. Differentially expressed genes (DEGs) under dehydration stress were identified based on the three biological replicates. A total of 126, 655 transcripts were generated from the sequencing and 36 141, 35 992, 36 328, 35 139 and 35 143 were expressed at 100% RWC, 85% RWC, 75% RWC, 50% RWC and 25% RWC respectively. The number of dehydration stress responsive genes that increased in relative abundance (log2fold-change $\geq$ 2) was 2 409 in 25% RWC compared to 100% RWC (Figure 4.4). The number of dehydration stress responsive genes that decreased in relative abundance (log2fold-change $\leq$ -2) was 2340 at 25% RWC compared to 100% RWC respectively (Figure 4.4).

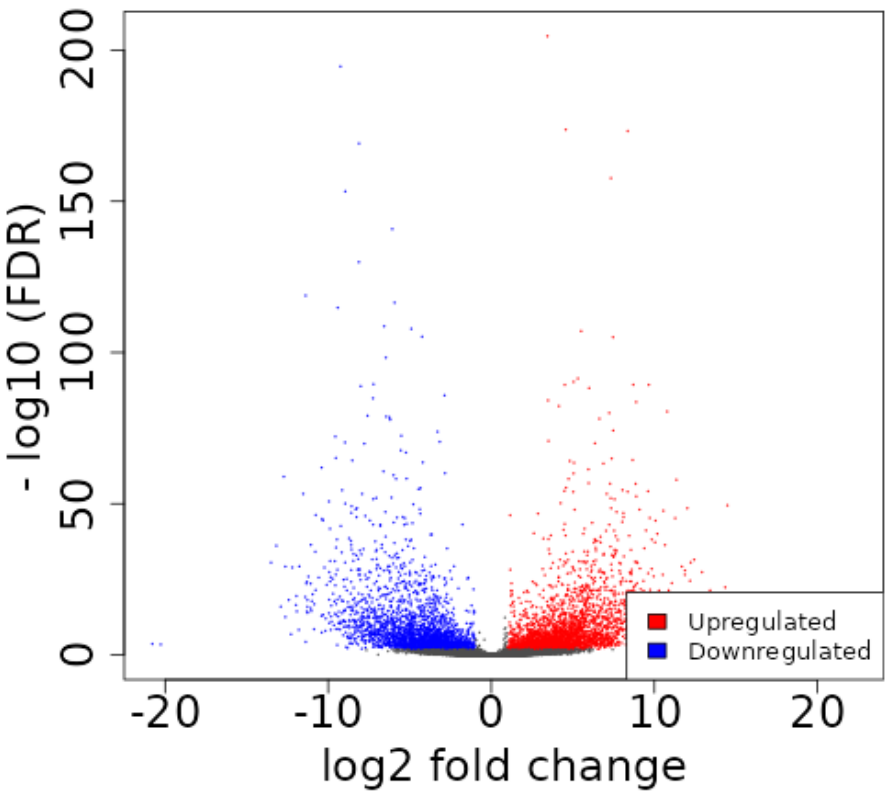

Figure 4.4 - Volcano plot of DEGs. Red dots are the genes that increased in relative abundance (log2fold-change > 2), and blue dots are the genes that decreased in relative abundance (log2fold-change ≤ -2) in 25% RWC compared to 100% RWC. IDEP.96 (Ge et al., 2018) was utilized to visualize the results.

4.4.4 Identification of dehydration responsive genes

Differentially expressed transcripts under dehydration stress were identified using the combined criteria multiple False Discovery Rate corrected Students' t-tests ($P_{adj} < 0.01$) with logFC ≥ 2 or ≤ -2 based on three biological replicates. A total of 4 750 transcripts were identified as differentially expressed transcripts in 25% RWC compared to 100% RWC. Those 4 750 transcripts were annotated using BLASTN (RRID:SCR_001598) and we identified a total of 637 annotations for differentially expressed transcripts by searching against *S. moellendorffii* and *Arabidopsis thaliana* NCBI RefSeq databases. A deeper investigation into the functional annotations of the dehydration responsive DEGs was conducted to clarify specific molecular

mechanisms of dehydration response in *S. lepidophylla.* Early light inducible proteins (ELIPs) transcript, pentatricopeptide repeat-containing proteins (PPRs) transcripts, antioxidant enzymes (Catalase, Peroxidase, Glutathione reductase) transcripts, antioxidant compounds (Peroxiredoxin, thioredoxin) transcripts, drought-responsive gene encoding protein kinases transcripts, stress responsive proteins and ABC transporter B family member (ABCB) transcripts were highly abundant during the dehydration process (Table 4.1). In addition, three transcription factor (TF) families were annotated including trihelix TF (1 gene), transcription factor AS1 (2 gene), and WRKY (2 gene) TFs under dehydration stress (Table 4.1). Interestingly Heat shock proteins (HSP) showed decreased relative abundance at extreme dehydration (Table 4.1).

4.3.5 Gene ontology (GO) analysis of DEGs

Gene ontology enrichment was performed to determine the association of DEGs involved in the desiccation tolerance response. Specifically, the 178 DEGs in 25% RWC compared to 100% RWC with with *A. thaliana* annotations were used for the GO analysis. Those DEGs were annotated in 45 GO subcategories, including 16 in biological process (BP), 11 in cellular component (CC), and 18 in molecular function (MF). Notably, we identified some interesting terms, such as cellular protein metabolic process (GO:0019538), cellular component organization (GO:0016043), primary metabolic process (GO:0044238), response to high light intensity (GO:0009644), protein metabolic process (GO:0019538), generation of precursor metabolites and energy (GO:0006091), cellular protein modification process (GO:0036211), and enzyme activator activity (GO:0008047), among the DEGs.

Table 4.1 - Selected differentially expressed genes (DEGs) under dehydration stress with known stress responsive functions. Gene ID - *Selaginella moellendorffii* and *Arabidopsis thaliana* annotations for differentially expressed genes resulted from the BLASTN.

Classification	Gene ID	Gene description	No. of Genes
ELIP	NM_116012.5	Arabidopsis thaliana photosystem I light harvesting complex protein (LHCA2)	1
PPR	XP_024516890.1_3931	pentatricopeptide repeat-containing protein At2g13600-like	1
	XP_024516890.1_3932	pentatricopeptide repeat-containing protein At2g33680-like	4
	XP_024516890.1_3933	pentatricopeptide repeat-containing protein At2g35030, mitochondrial-like	1
	XP_024516890.1_3934	pentatricopeptide repeat-containing protein At3g02330, mitochondrial-like isoform X2	1
	XP_024516890.1_3935	pentatricopeptide repeat-containing protein At3g12770	2
	XP_024516890.1_3936	pentatricopeptide repeat-containing protein At3g28660-like	1
	XP_024516890.1_3937	pentatricopeptide repeat-containing protein At3g46790, chloroplastic-like	1
	XP_024516890.1_3938	pentatricopeptide repeat-containing protein At3g53360, mitochondrial-like	1
	XP_024516890.1_3939	pentatricopeptide repeat-containing protein At3g62890-like	1
	XP_024516890.1_3940	pentatricopeptide repeat-containing protein At4g02750	8
	XP_024516890.1_3941	pentatricopeptide repeat-containing protein At5g04780, mitochondrial	2
	XP_024516890.1_3942	pentatricopeptide repeat-containing protein At5g16860-like	1
	XP_024516890.1_3943	pentatricopeptide repeat-containing protein At5g27110-like isoform X2	1
	XP_024516890.1_3944	pentatricopeptide repeat-containing protein At1g69350, mitochondrial	1
Antioxidant enzymes	XP_024516890.1_3945	catalase-3	1
	XP_024516890.1_3946	peroxidase 46	1
	NC_003074.8	Glutathione_reductase	1
Antioxidant compounds	NC_003070.9	1-cys_peroxiredoxin	2
	XP_002964841.1_6559	thioredoxin-like protein YLS8	1
Protein kinases	XP_024514808.1_33267	leucine-rich repeat receptor-like serine/threonine-protein kinase BAM2	3
	XP_002991210.2_41015	LRR receptor-like serine/threonine-protein kinase At1g12460	1
	XP_024522575.1_43540	serine/threonine-protein kinase PBS1 isoform X2	1
	XP_024544291.1_31123	serine/threonine-protein kinase RUNKEL	1
	XP_002988575.2_37601	serine/threonine-protein kinase SRPK	1
	XP_002979177.2_25550	LRR receptor-like serine/threonine-protein kinase FLS2	1
	XP_002961155.2_1259	mitogen-activated protein kinase 15	1
	XP_024527172.1_8416	inactive leucine-rich repeat receptor kinase XIAO	1
	XP_024525645.1_6618	receptor-like protein kinase At1g80640 isoform X2	1
	XP_002960796.2_237	pyruvate kinase, cytosolic isozyme isoform X2	2
	XP_024527827.1_9036	receptor-like protein kinase HSL1	1
	XP_002991645.1_41657	shaggy-related protein kinase epsilon	1
	XP_002993638.2_44048	uridine-cytidine kinase C	1
ABCB	XP_024534012.1_17472	ABC transporter B family member 10 isoform X3	1
	XP_024526524.1_7808	ABC transporter B family member 19	1
	XP_024535008.1_18896	ABC transporter B family member 25, mitochondrial	1
	XP_024542487.1_28793	ABC transporter B family member 4	1
Stress responsive protein	NM_115842.4	Arabidopsis thaliana stress response protein (AT3G59800)	1
HSP	XP_024534668.1_18529	heat shock 70 kDa protein 15	1
	XP_002976367.1_21620	heat shock cognate 70 kDa protein	2
	XP_002964394.1_5413	heat shock protein 17.3 kDa class II	1
	XP_002973159.1_17591	heat shock protein 81-1	2
	XP_002981406.1_28211	heat shock protein 90-2	1
TF	XP_002967719.2_10554	WRKY transcription factor 39	1
	XP_024536119.1_20489	WRKY transcription factor 4	1
	XP_002965233.1_6693	transcription factor AS1	2
	XP_024542990.1_29113	trihelix transcription factor GT-2-like	1

4.4 Discussion

The transition from an aquatic environment to land presented distinctive obstacles for the ancestors of land plants. One of the primary challenges they encountered was the need to cope

with periodic drying and low atmospheric water potential, which were not prevalent concerns in aquatic habitats. To overcome these challenges, early land plants had to evolve mechanisms that would protect them from desiccation, or extreme dehydration, which could occur when exposed to air or during dry periods (Oliver et al., 2000). Recognizing the significance of *S. lepidophylla* in evolution and its remarkable desiccation tolerance, our study aimed to identify dehydration responsive genes by surveying gene expression changes during the dehydration process in this species. By conducting a comparative transcriptional pattern analysis across different relative water contents (RWCs) of *S. lepidophylla*, we sought to pinpoint specific genes associated with desiccation responses.

We analyzed the DEGs in 25% RWC (dehydrated) compared to 100% RWC (hydrated) and we identified the expression of the genes involved in desiccation tolerance. Early light-induced proteins (ELIPs), late embryogenesis abundant (LEA) proteins, and heat shock proteins (HSPs) are known to play important role in desiccation tolerance (Dinakar and Bartels, 2013; Silva Artur et al., 2019). Early Light-Induced Proteins play a crucial role in protecting the photosynthetic apparatus from photo-oxidative damage caused by high light and various abiotic stresses (Hutin et al., 2003; Silva Artur et al., 2019). Late embryogenesis abundant proteins play a vital role in desiccation tolerance by protecting cellular components, stabilizing membranes, scavenging ROS, and macromolecular protection. Moreover, HSPs exhibit properties similar to LEA proteins, and research has demonstrated their ability to safeguard membranes from desiccation, or extreme drying conditions (Moore et al., 2009; Silva Artur et al., 2019). However, we identified only one differentially expressed ELIPs transcript (photosystem I light harvesting complex protein (LHCA2)) and haven't identified any differentially expressed LEA protein transcripts at 25% RWC compared to 100% RWC (Table 4.1). We found eight different HSP transcripts that showed

decreased relative abundance at extreme dehydration conditions (Table 4.1). There could be several reasons for this observation. It is possible that ELIP, LEA and HSP proteins that are important for desiccation tolerance are highly expressed in both well-hydrated and dehydrated tissues, indicating their involvement in constitutive protection mechanisms. Alternatively, there might be desiccation responsive ELIP, LEA and HSP proteins that are not annotated by BLASTN against *S. moellendorffii* and *A. thaliana* NCBI RefSeq databases we used for our analysis. To gain a more comprehensive understanding of the exact involvement of ELIP, LEA and HSP proteins in *S. lepidophylla* desiccation tolerance, further studies are needed. One approach could involve conducting gene-co-expression analyses using RNA-seq time course data across hydration and subsequent dehydration stages. This would help identify whether there are constitutively expressed ELIP, LEA and HSP proteins that may contribute to desiccation tolerance. Moreover, considering the limitations of the annotation, it would be beneficial to search the transcriptomes for matching sequences in other NCBI databases beyond *S. moellendorffii* and *A. thaliana* NCBI RefSeq. This can be achieved using BLASTN, allowing for a more comprehensive identification of ELIP, LEA and HSP proteins in *S. lepidophylla*.

Pentatricopeptide repeat-containing proteins (PPRs) are a gene family with diverse functions in plants, including involvement in ABA signaling and playing crucial roles in desiccation tolerance, as well as tolerance to cold and salinity stresses (Jiang et al., 2015). They are also essential for plant growth and development (Xu et al., 2018). In particular, PPRs have been found to be highly expressed during rehydration and dehydration in desiccation tolerant *S. tamariscina*, where they contribute to chloroplast development (Kwon et al., 2021). In *Arabidopsis*, the high expression of PPR genes has been shown to enhance the plant's defense mechanisms against abiotic stress (Jiang et al., 2015; Yuan and Liu, 2012). Additionally,

overexpression of PPR genes in *Arabidopsis* significantly increases drought tolerance (Jiang et al., 2015; Yuan and Liu, 2012). In our study, we identified 26 different PPRs with increased relative abundance under dehydration conditions, suggesting their potential role in desiccation tolerance through the maintenance and development of chloroplasts (Table 4.1).

Plants produce reactive oxygen species (ROS) as a result of different stresses or as natural byproducts of oxygen metabolism. ROS can have both harmful and beneficial effects, depending on their levels, leading to either cell signaling or cell death (Mittler et al., 2004). Maintaining a balance in ROS accumulation is crucial for plants to defend themselves, as both biotic and abiotic stresses can increase ROS levels (Mittler et al., 2004). Excessive ROS can severely harm normal plant cells. An increase in antioxidant enzymatic activities as tissues lose water has been reported in desiccation tolerant *S. tamariscina* (Gu et al., 2019) . Our differential gene expression analysis showed that transcripts of antioxidant enzymes such as Catalase, Peroxidase and Glutathione reductase (Yobi et al., 2013, 2012), antioxidant compounds such as Peroxiredoxin, thioredoxin (Yobi et al., 2013, 2012) were highly abundant at dehydrated conditions, indicating *S. lepidophylla* has evolved defense mechanisms to counteract ROS-induced damage (Table 4.1).

A total of 36 DEGs encoding protein kinases were identified at 25% RWC. Among those genes, the serine/threonine kinase (STKs) genes were the most prevalent, with eight genes showing increased relative abundance (Table 4.1). Additionally, two receptor-like protein kinase (RLKs), four leucine-rich repeat receptor-like protein kinase (LRR-RLK), and one mitogen-activated protein kinase (MAPK) genes were detected, all of which exhibited increased relative abundance in *S. lepidophylla* during extreme dehydration at 25% RWC (Table 4.1). Receptor kinases play significant roles in sensing external stimuli and initiating downstream signaling responses. LRR-containing protein genes are typically essential for plant responses to both biotic and abiotic

stresses (Dong et al., 2005; Liu et al., 2008, 2017). LRR domain-containing proteins are involved in defense mechanisms and various developmental processes in plants (Becraft, 2002) . The LRR domain is believed to facilitate ligand recognition and interactions with other proteins or subdomains within LRR-containing proteins (Becraft, 2002). MAPKs, as integral components of the MAPK cascade, often play pivotal roles in plant responses to stress (Ning et al., 2010; Ye et al., 2017). Noticeably increased relative abundance of genes encoding protein kinases suggest their potential role in desiccation resistance of *S. lepidophylla.*

ABC transporters, which are among the most extensive and ancient protein families found in both prokaryotes and eukaryotes, fulfill crucial roles in transporting various molecules essential for the survival of plants (Hwang et al., 2016). Notably, the overexpression of the ABC transporter G family member (ABCG25) gene in *A. thaliana* has been demonstrated to decrease the rate of water loss (Kuromori et al., 2010). Further, Kwon et al., (2021) reported increased abundance of ABC transporter G family members during the resurrection process of *S. tamariscina.* In our research, we observed an increased abundance of four ABCB genes under dehydration conditions, suggesting that those ABCB proteins likely plays a significant role in the process of resurrection.

Altogether findings of this study demonstrate that *S. lepidophylla* exhibits a significant inducible response to dehydration stress, akin to the more advanced tolerance mechanisms observed in angiosperms. However, a metabolomics study conducted by Yobi et al. in 2012 revealed that most metabolomic compounds, including the highly abundant trehalose, sucrose, and glucose, were produced constitutively in *S. lepidophylla*. To identify potential constitutively expressed dehydration responsive genes, gene co-expression analysis can be conducted. Furthermore, we found many unnamed DEGs in 25% RWC compared to 100% RWC, which might play adaptive roles in the acquisition of desiccation tolerance. To gain a more comprehensive

understanding of their functions, we can perform BLASTN searches against an expanded range of NCBI RefSeq databases, beyond *S. moellendorffii* and *A. thaliana*.

4.5 Conclusions and future directions

Through transcriptomic analysis, we identified dehydration responsive genes in *S. lepidophylla*. Our findings provide valuable information and candidate dehydration responsive genes for future functional analysis aimed at improving the drought tolerance of crop plants. To gain a deeper understanding of the regulatory mechanisms involved, it would be beneficial to conduct gene-co-expression analysis. These analyses can help determine whether there are constitutively expressed genes associated with the desiccation tolerance response. Moreover, the time-delay correlation (TDCor) gene regulatory network approach can be used to identify master regulatory genes that start the entire genetic cascade of the desiccation stress tolerance pathway (Lavenus et al., 2015). By leveraging the nanohydroxyapatite gene delivery tool developed for *Selaginella moellendorffii*, we can employ both loss-of-function and gain-of-function approaches to validate those master regulatory genes in *S. lepidophylla*. The identification and validation of the master regulatory genes will aid future studies on desiccation stress response regulation and bioengineering master regulatory genes into drought-sensitive crop species. Application of those candidate master regulatory genes of desiccation tolerance might not only be beneficial for improving drought stress tolerance but also might improve other abiotic stress responses because these master regulatory genes might have the capability to activate entire genetic cascades leading to multiple stress responses (Balderas-Hernandez et al., 2013).

4.6 Funding

The authors thank the University of South Dakota Graduate Research and Creative Scholarship Grant, John W. Carlson research grant and Department of Biology Nelson Fellowship to MA Ariyarathne and Nolop Research Funds.

4.7 Acknowledgements

The authors gratefully acknowledge Dr. Miyuraj Harishchandra, Beate Wone, Dr. Pasan Fernando, Kara Wilkens-Reiman, and all Wone Lab members and help with the study.

Chapter 5 : Conclusions and future directions

This dissertation has made notable strides in unraveling the genetic basis of desiccation tolerance in a spike moss, *Selaginella lepidophylla* known for its remarkable ability to survive extreme desiccation. Our comprehensive studies on *S. lepidophylla* have yielded significant findings and potential applications for improving crop plant abiotic stress tolerance. Firstly, Objective 1 revealed the functional characterization of the *SlbHLH* transcription factor, demonstrating its crucial role in regulating plant growth, development, abiotic stress tolerance, and water use efficiency. Finding of our study highlights the potential of abiotic stress-responsive TF as highly conserved regulators across plant species.

The development of a nano-biomimetic plant transformation method for *Selaginella moellendorffii* presents an opportunity to establish a stable transformation system for the species and other *Selaginella* spp. This system enables researchers to explore the molecular mechanisms underlying desiccation tolerance by editing or silencing specific genes. The knowledge gained from these studies is crucial for understanding the fundamental processes of desiccation tolerance and can contribute to the development of strategies for enhancing abiotic stress tolerance in other plant species.

The desiccation tolerance mechanism observed in *S. lepidophylla* represents an extraordinary adaptation and will offer valuable insights for improving crop abiotic stress tolerance and WUE. The identification of dehydration responsive genes through transcriptomic analysis provides a foundation for future functional investigations and genetic engineering approaches aimed at enhancing abiotic stress tolerance in crop plants.

Further exploration, such as gene-co-expression analysis of collected time course RNA-seq data, will help elucidate more on the regulatory mechanisms involved in the desiccation tolerance response, particularly constitutive desiccation tolerance mechanisms. Moreover, the application of the time-delay correlation gene regulatory network approach to time course RNA-seq data can aid in identifying master regulatory genes that initiate the genetic cascade leading to desiccation stress tolerance. These master regulatory genes have the potential to activate multiple stress responses, thus enhancing not only drought stress tolerance but also other abiotic stress responses in crop plants.

Future directions should focus on expanding the understanding of desiccation tolerance by exploring additional transcription factors and regulatory genes in *S. lepidophylla*. Investigating the gene regulatory networks involved in the desiccation stress response will provide comprehensive insights into the underlying mechanisms. Furthermore, comprehensive functional analysis of the candidate dehydration responsive genes identified through transcriptomic analysis will contribute to the development of novel strategies for improving drought tolerance in crop plants. The integration of identified master regulatory genes of desiccation stress tolerance may pave the way for bioengineering drought-tolerant crops that can withstand a range of abiotic stresses. Overall, the findings from this dissertation lay the foundation for future advancements in crop improvement, sustainable agriculture, and the understanding of desiccation tolerance mechanisms in plants. By harnessing the unique adaptations of desiccation-tolerant species like *S. lepidophylla*, we can develop innovative solutions to mitigate the challenges posed by abiotic stresses in a changing climate.

References

Alejo-Jacuinde, G., González-Morales, S.I., Oropeza-Aburto, A., Simpson, J., Herrera-Estrella, L., 2020. Comparative transcriptome analysis suggests convergent evolution of desiccation tolerance in Selaginella species. BMC Plant Biol 20. https://doi.org/10.1186/s12870-020-02638-3

Altpeter, F., Springer, N.M., Bartley, L.E., Blechl, A., Brutnell, T.P., Citovsky, V., Conrad, L., Gelvin, S.B., Jackson, D., Kausch, A.P., Lemaux, P.G., Medford, J.I., Orozo-Cardenas, M., Tricoli, D., VanEck, J., Voytas, D.F., Walbot, V., Wang, K., Zhang, Z.J., Stewart, , C. Neal, 2016. Advancing Crop Transformation in the Era of Genome Editing. Plant Cell tpc.00196.2016. https://doi.org/10.1105/tpc.16.00196

Amin, A.B., Rathnayake, K.N., Yim, W.C., Garcia, T.M., Wone, B., Cushman, J.C., Wone, B.W.M., 2019. Crassulacean Acid Metabolism Abiotic Stress-Responsive Transcription Factors: a Potential Genetic Engineering Approach for Improving Crop Tolerance to Abiotic Stress. Front Plant Sci 10. https://doi.org/10.3389/fpls.2019.00129

Arumughan, V., Nypelö, T., Hasani, M., Brelid, H., Albertsson, S., Wågberg, L., Larsson, A., 2021. Specific ion effects in the adsorption of carboxymethyl cellulose on cellulose: The influence of industrially relevant divalent cations. Colloids Surf A Physicochem Eng Asp 626, 127006. https://doi.org/10.1016/j.colsurfa.2021.127006

Aryal, S., Baniya, M.K., Danekhu, K., Kunwar, P., Gurung, R., Koirala, N., 2019. Total Phenolic Content, Flavonoid Content and Antioxidant Potential of Wild Vegetables from Western Nepal. Plants 8. https://doi.org/10.3390/plants8040096

Balderas-Hernandez, V.E., Alvarado-Rodriguez, M., Fraire-Velazquez, S., 2013. Conserved versatile master regulators in signalling pathways in response to stress in plants. AoB Plants 5. https://doi.org/10.1093/aobpla/plt033

Baltes, N.J., Gil-Humanes, J., Voytas, D.F., 2017. Genome Engineering and Agriculture: Opportunities and Challenges. pp. 1–26. https://doi.org/10.1016/bs.pmbts.2017.03.011

Banks, J.A., 2009. Selaginella and 400 Million Years of Separation. Annu Rev Plant Biol 60. https://doi.org/10.1146/annurev.arplant.59.032607.092851

Barampuram, S., Zhang, Z.J., 2011. Recent Advances in Plant Transformation. pp. 1–35. https://doi.org/10.1007/978-1-61737-957-4_1

Becraft, P.W., 2002. Receptor Kinase Signaling in Plant Development. Annu Rev Cell Dev Biol 18, 163–192. https://doi.org/10.1146/annurev.cellbio.18.012502.083431

Bertolino, L.T., Caine, R.S., Gray, J.E., 2019. Impact of Stomatal Density and Morphology on Water-Use Efficiency in a Changing World. Front Plant Sci 10. https://doi.org/10.3389/fpls.2019.00225

Cai, Y., Liu, Y., Yan, W., Hu, Q., Tao, J., Zhang, M., Shi, Z., Tang, R., 2007. Role of hydroxyapatite nanoparticle size in bone cell proliferation. J Mater Chem 17, 3780. https://doi.org/10.1039/b705129h

Castilhos, G., Lazzarotto, F., Spagnolo-Fonini, L., Bodanese-Zanettini, M.H., Margis-Pinheiro, M., 2014. Possible roles of basic helix-loop-helix transcription factors in adaptation to drought. Plant Science 223. https://doi.org/10.1016/j.plantsci.2014.02.010

Chandler, V.L., Radicella, J.P., Robbins, T.P., Chen, J., Turks, D., 1989. Two regulatory genes of the maize anthocyanin pathway are homologous: isolation of B utilizing R genomic sequences. Plant Cell 1. https://doi.org/10.1105/tpc.1.12.1175

Condon, A.G., 2004. Breeding for high water-use efficiency. J Exp Bot 55. https://doi.org/10.1093/jxb/erh277

Corrales, A., Carrillo, L., Nebauer, S., Renau-Morata, B., Sánchez-Perales, M., Fernández-Nohales, P., Marqués, J., Granell, A., Pollmann, S., Vicente-Carbajosa, J., Molina, R., Medina, J., 2014. Salinity Assay in Arabidopsis. Bio Protoc 4. https://doi.org/10.21769/BioProtoc.1216

Costa, M.C.D., Farrant, J.M., Oliver, M.J., Ligterink, W., Buitink, J., Hilhorst, H.M.W., 2016. Key genes involved in desiccation tolerance and dormancy across life forms. Plant Science 251, 162–168. https://doi.org/10.1016/j.plantsci.2016.02.001

Cunningham, F.J., Goh, N.S., Demirer, G.S., Matos, J.L., Landry, M.P., 2018. Nanoparticle-Mediated Delivery towards Advancing Plant Genetic Engineering. Trends Biotechnol 36, 882–897. https://doi.org/10.1016/j.tibtech.2018.03.009

Deeba, F., Pandey, A.K., Pandey, V., 2016. Organ Specific Proteomic Dissection of Selaginella bryopteris Undergoing Dehydration and Rehydration. Front Plant Sci 7. https://doi.org/10.3389/fpls.2016.00425

Demirer, G.S., Landry, M.P., 2017. Delivering Genes to Plants. Chem Eng Prog 113, 40–45.

Demirer, G.S., Zhang, H., Matos, J.L., Goh, N.S., Cunningham, F.J., Sung, Y., Chang, R., Aditham, A.J., Chio, L., Cho, M.-J., Staskawicz, B., Landry, M.P., 2019. High aspect ratio

nanomaterials enable delivery of functional genetic material without DNA integration in mature plants. Nat Nanotechnol 14, 456–464. https://doi.org/10.1038/s41565-019-0382-5

Deshmukh, K., Ramanan, S.R., Kowshik, M., 2019. Novel one step transformation method for Escherichia coli and Staphylococcus aureus using arginine-glucose functionalized hydroxyapatite nanoparticles. Materials Science and Engineering: C 96, 58–65. https://doi.org/10.1016/j.msec.2018.10.088

Di Ferdinando, M., Brunetti, C., Fini, A., Tattini, M., 2012. Flavonoids as Antioxidants in Plants Under Abiotic Stresses, in: Abiotic Stress Responses in Plants. Springer New York, New York, NY. https://doi.org/10.1007/978-1-4614-0634-1_9

Dinakar, C., Bartels, D., 2013. Desiccation tolerance in resurrection plants: new insights from transcriptome, proteome and metabolome analysis. Front Plant Sci 4. https://doi.org/10.3389/fpls.2013.00482

Dombrecht, B., Xue, G.P., Sprague, S.J., Kirkegaard, J.A., Ross, J.J., Reid, J.B., Fitt, G.P., Sewelam, N., Schenk, P.M., Manners, J.M., Kazan, K., 2007. MYC2 Differentially Modulates Diverse Jasmonate-Dependent Functions in *Arabidopsis*. Plant Cell 19. https://doi.org/10.1105/tpc.106.048017

Dong, H.-P., Yu, H., Bao, Z., Guo, X., Peng, J., Yao, Z., Chen, G., Qu, S., Dong, H., 2005. The ABI2-dependent abscisic acid signalling controls HrpN-induced drought tolerance in Arabidopsis. Planta 221, 313–327. https://doi.org/10.1007/s00425-004-1444-x

Dong, Y., Wang, C., Han, X., Tang, S., Liu, S., Xia, X., Yin, W., 2014. A novel bHLH transcription factor PebHLH35 from Populus euphratica confers drought tolerance through regulating

stomatal development, photosynthesis and growth in Arabidopsis. Biochem Biophys Res Commun 450. https://doi.org/10.1016/j.bbrc.2014.05.139

Farrant, J.M., Moore, J.P., 2011. Programming desiccation-tolerance: from plants to seeds to resurrection plants. Curr Opin Plant Biol 14, 340–345. https://doi.org/10.1016/j.pbi.2011.03.018

Franks, P.J., W. Doheny-Adams, T., Britton-Harper, Z.J., Gray, J.E., 2015. Increasing water-use efficiency directly through genetic manipulation of stomatal density. New Phytologist 207. https://doi.org/10.1111/nph.13347

Gaff, D.F., Oliver, M., 2013. The evolution of desiccation tolerance in angiosperm plants: a rare yet common phenomenon. Functional Plant Biology 40, 315. https://doi.org/10.1071/FP12321

Ge, S.X., Son, E.W., Yao, R., 2018. iDEP: an integrated web application for differential expression and pathway analysis of RNA-Seq data. BMC Bioinformatics 19, 534. https://doi.org/10.1186/s12859-018-2486-6

Giarola, V., Hou, Q., Bartels, D., 2017. Angiosperm Plant Desiccation Tolerance: Hints from Transcriptomics and Genome Sequencing. Trends Plant Sci 22. https://doi.org/10.1016/j.tplants.2017.05.007

Goossens, J., Mertens, J., Goossens, A., 2016. Role and functioning of bHLH transcription factors in jasmonate signalling. J Exp Bot. https://doi.org/10.1093/jxb/erw440

Gu, W., Zhang, A., Sun, H., Gu, Y., Chao, J., Tian, R., Duan, J.-A., 2019. Identifying resurrection genes through the differentially expressed genes between Selaginella tamariscina (Beauv.)

spring and Selaginella moellendorffii Hieron under drought stress. PLoS One 14, e0224765. https://doi.org/10.1371/journal.pone.0224765

Guo, J., Sun, B., He, H., Zhang, Y., Tian, H., Wang, B., 2021. Current Understanding of bHLH Transcription Factors in Plant Abiotic Stress Tolerance. Int J Mol Sci 22, 4921. https://doi.org/10.3390/ijms22094921

Hichri, I., Barrieu, F., Bogs, J., Kappel, C., Delrot, S., Lauvergeat, V., 2011. Recent advances in the transcriptional regulation of the flavonoid biosynthetic pathway. J Exp Bot 62. https://doi.org/10.1093/jxb/erq442

Hilhorst, H.W.M., Costa, M.-C.D., Farrant, J.M., 2018. A Footprint of Plant Desiccation Tolerance. Does It Exist? Mol Plant 11, 1003–1005. https://doi.org/10.1016/j.molp.2018.07.001

Hu, P., An, J., Faulkner, M.M., Wu, H., Li, Z., Tian, X., Giraldo, J.P., 2020. Nanoparticle Charge and Size Control Foliar Delivery Efficiency to Plant Cells and Organelles. ACS Nano 14, 7970–7986. https://doi.org/10.1021/acsnano.9b09178

Huang, D.W., Sherman, B.T., Lempicki, R.A., 2009. Systematic and integrative analysis of large gene lists using DAVID bioinformatics resources. Nat Protoc 4, 44–57. https://doi.org/10.1038/nprot.2008.211

Hutin, C., Nussaume, L., Moise, N., Moya, I., Kloppstech, K., Havaux, M., 2003. Early light-induced proteins protect *Arabidopsis* from photooxidative stress. Proceedings of the National Academy of Sciences 100, 4921–4926. https://doi.org/10.1073/pnas.0736939100

Hwang, J.-U., Song, W.-Y., Hong, D., Ko, D., Yamaoka, Y., Jang, S., Yim, S., Lee, E., Khare, D., Kim, K., Palmgren, M., Yoon, H.S., Martinoia, E., Lee, Y., 2016. Plant ABC Transporters Enable Many Unique Aspects of a Terrestrial Plant's Lifestyle. Mol Plant 9, 338–355. https://doi.org/10.1016/j.molp.2016.02.003

Ibrahim, H.M., Awad, M., Al-Farraj, A.S., Al-Turki, A.M., 2020. Stability and Dynamic Aggregation of Bare and Stabilized Zero-Valent Iron Nanoparticles under Variable Solution Chemistry. Nanomaterials 10, 192. https://doi.org/10.3390/nano10020192

Ingram, J., Bartels, D., 1996. THE MOLECULAR BASIS OF DEHYDRATION TOLERANCE IN PLANTS. Annu Rev Plant Physiol Plant Mol Biol 47, 377–403. https://doi.org/10.1146/annurev.arplant.47.1.377

Iturriaga, G., Cushman, M.A.F., Cushman, J.C., 2006. An EST catalogue from the resurrection plant Selaginella lepidophylla reveals abiotic stress-adaptive genes. Plant Science 170, 1173–1184. https://doi.org/10.1016/j.plantsci.2006.02.004

Izuegbunam, C.L., Wijewantha, N., Wone, B., Ariyarathne, M.A., Sereda, G., Wone, B.W.M., 2021. A nano-biomimetic transformation system enables *in planta* expression of a reporter gene in mature plants and seeds. Nanoscale Adv 3. https://doi.org/10.1039/D1NA00107H

Jiang, S.-C., Mei, C., Liang, S., Yu, Y.-T., Lu, K., Wu, Z., Wang, X.-F., Zhang, D.-P., 2015. Crucial roles of the pentatricopeptide repeat protein SOAR1 in Arabidopsis response to drought, salt and cold stresses. Plant Mol Biol 88, 369–385. https://doi.org/10.1007/s11103-015-0327-9

Jiao, Y., Wickett, N.J., Ayyampalayam, S., Chanderbali, A.S., Landherr, L., Ralph, P.E., Tomsho, L.P., Hu, Y., Liang, H., Soltis, P.S., Soltis, D.E., Clifton, S.W., Schlarbaum, S.E., Schuster,

S.C., Ma, H., Leebens-Mack, J., dePamphilis, C.W., 2011. Ancestral polyploidy in seed plants and angiosperms. Nature 473, 97–100. https://doi.org/10.1038/nature09916

Joshi, R., Wani, S.H., Singh, B., Bohra, A., Dar, Z.A., Lone, A.A., Pareek, A., Singla-Pareek, S.L., 2016. Transcription Factors and Plants Response to Drought Stress: Current Understanding and Future Directions. Front Plant Sci 7. https://doi.org/10.3389/fpls.2016.01029

Kim, D., Langmead, B., Salzberg, S.L., 2015. HISAT: a fast spliced aligner with low memory requirements. Nat Methods 12, 357–360. https://doi.org/10.1038/nmeth.3317

Kumar, S., Stecher, G., Li, M., Knyaz, C., Tamura, K., 2018. MEGA X: Molecular Evolutionary Genetics Analysis across Computing Platforms. Mol Biol Evol 35. https://doi.org/10.1093/molbev/msy096

Kuromori, T., Miyaji, T., Yabuuchi, H., Shimizu, H., Sugimoto, E., Kamiya, A., Moriyama, Y., Shinozaki, K., 2010. ABC transporter AtABCG25 is involved in abscisic acid transport and responses. Proceedings of the National Academy of Sciences 107, 2361–2366. https://doi.org/10.1073/pnas.0912516107

Kwon, E., Basnet, P., Roy, N.S., Kim, J.-H., Heo, K., Park, K.-C., Um, T., Kim, N.-S., Choi, I.-Y., 2021. Identification of resurrection genes from the transcriptome of dehydrated and rehydrated *Selaginella tamariscina*. Plant Signal Behav 16. https://doi.org/10.1080/15592324.2021.1973703

Lavenus, J., Goh, T., Guyomarc'h, S., Hill, K., Lucas, M., Voß, U., Kenobi, K., Wilson, M.H., Farcot, E., Hagen, G., Guilfoyle, T.J., Fukaki, H., Laplaze, L., Bennett, M.J., 2015. Inference of the Arabidopsis Lateral Root Gene Regulatory Network Suggests a Bifurcation Mechanism

That Defines Primordia Flanking and Central Zones. Plant Cell 27, 1368–1388. https://doi.org/10.1105/tpc.114.132993

Leprince, O., Buitink, J., 2015. Introduction to desiccation biology: from old borders to new frontiers. Planta 242, 369–378. https://doi.org/10.1007/s00425-015-2357-6

Lim, S.D., Mayer, J.A., Yim, W.C., Cushman, J.C., 2020. Plant tissue succulence engineering improves water-use efficiency, water-deficit stress attenuation and salinity tolerance in Arabidopsis. The Plant Journal 103. https://doi.org/10.1111/tpj.14783

Lim, S.D., Yim, W.C., Liu, D., Hu, R., Yang, X., Cushman, J.C., 2018. A Vitis vinifera basic helix-loop-helix transcription factor enhances plant cell size, vegetative biomass and reproductive yield. Plant Biotechnol J 16. https://doi.org/10.1111/pbi.12898

Lindsey, B.E., Rivero, L., Calhoun, C.S., Grotewold, E., Brkljacic, J., 2017. Standardized Method for High-throughput Sterilization of Arabidopsis Seeds. Journal of Visualized Experiments. https://doi.org/10.3791/56587

Liu, M.-S., Chien, C.-T., Lin, T.-P., 2008. Constitutive Components and Induced Gene Expression are Involved in the Desiccation Tolerance of Selaginella tamariscina. Plant Cell Physiol 49, 653–663. https://doi.org/10.1093/pcp/pcn040

Liu, P.-L., Du, L., Huang, Y., Gao, S.-M., Yu, M., 2017. Origin and diversification of leucine-rich repeat receptor-like protein kinase (LRR-RLK) genes in plants. BMC Evol Biol 17, 47. https://doi.org/10.1186/s12862-017-0891-5

Liu, R., Lal, R., 2014. Synthetic apatite nanoparticles as a phosphorus fertilizer for soybean (Glycine max). Sci Rep 4, 5686. https://doi.org/10.1038/srep05686

Liu, W., Tai, H., Li, S., Gao, W., Zhao, M., Xie, C., Li, W., 2014. bHLH122 is important for drought and osmotic stress resistance in Arabidopsis and in the repression of ABA catabolism. New Phytologist 201. https://doi.org/10.1111/nph.12607

Livak, K.J., Schmittgen, T.D., 2001. Analysis of Relative Gene Expression Data Using Real-Time Quantitative PCR and the 2−ΔΔCT Method. Methods 25. https://doi.org/10.1006/meth.2001.1262

Long, S.P., Marshall-Colon, A., Zhu, X.-G., 2015. Meeting the Global Food Demand of the Future by Engineering Crop Photosynthesis and Yield Potential. Cell 161. https://doi.org/10.1016/j.cell.2015.03.019

Love, M.I., Huber, W., Anders, S., 2014. Moderated estimation of fold change and dispersion for RNA-seq data with DESeq2. Genome Biol 15, 550. https://doi.org/10.1186/s13059-014-0550-8

Meng, L.-S., Yao, S.-Q., 2015. Transcription co-activator Arabidopsis ANGUSTIFOLIA3 (AN3) regulates water-use efficiency and drought tolerance by modulating stomatal density and improving root architecture by the transrepression of YODA (YDA). Plant Biotechnol J 13. https://doi.org/10.1111/pbi.12324

Mi, F.-L., Wu, Y.-Y., Lin, Y.-H., Sonaje, K., Ho, Y.-C., Chen, C.-T., Juang, J.-H., Sung, H.-W., 2008. Oral Delivery of Peptide Drugs Using Nanoparticles Self-Assembled by Poly(γ-glutamic acid) and a Chitosan Derivative Functionalized by Trimethylation. Bioconjug Chem 19, 1248–1255. https://doi.org/10.1021/bc800076n

Mittler, R., Vanderauwera, S., Gollery, M., Van Breusegem, F., 2004. Reactive oxygen gene network of plants. Trends Plant Sci 9, 490–498. https://doi.org/10.1016/j.tplants.2004.08.009

Moore, J.P., Le, N.T., Brandt, W.F., Driouich, A., Farrant, J.M., 2009. Towards a systems-based understanding of plant desiccation tolerance. Trends Plant Sci 14, 110–117. https://doi.org/10.1016/j.tplants.2008.11.007

Mourya, V.K., Inamdar, N.N., 2009. Trimethyl chitosan and its applications in drug delivery. J Mater Sci Mater Med 20, 1057–1079. https://doi.org/10.1007/s10856-008-3659-z

Nair, R., Varghese, S.H., Nair, B.G., Maekawa, T., Yoshida, Y., Kumar, D.S., 2010. Nanoparticulate material delivery to plants. Plant Science 179, 154–163. https://doi.org/10.1016/j.plantsci.2010.04.012

Nakagawa, T., Kurose, T., Hino, T., Tanaka, K., Kawamukai, M., Niwa, Y., Toyooka, K., Matsuoka, K., Jinbo, T., Kimura, T., 2007. Development of series of gateway binary vectors, pGWBs, for realizing efficient construction of fusion genes for plant transformation. J Biosci Bioeng 104. https://doi.org/10.1263/jbb.104.34

Ning, J., Li, X., Hicks, L.M., Xiong, L., 2010. A Raf-Like MAPKKK Gene *DSM1* Mediates Drought Resistance through Reactive Oxygen Species Scavenging in Rice . Plant Physiol 152, 876–890. https://doi.org/10.1104/pp.109.149856

Oliver, M.J., 1996. Desiccation tolerance in vegetative plant cells. Physiol Plant 97, 779–787. https://doi.org/10.1111/j.1399-3054.1996.tb00544.x

Oliver, M.J., Tuba Zoltán, Mishler Brent D., 2000. The Evolution of Vegetative Desiccation Tolerance in Land Plants. Plant Ecol 151, 85–100.

Pertea, M., Pertea, G.M., Antonescu, C.M., Chang, T.-C., Mendell, J.T., Salzberg, S.L., 2015. StringTie enables improved reconstruction of a transcriptome from RNA-seq reads. Nat Biotechnol 33, 290–295. https://doi.org/10.1038/nbt.3122

Premathilake, A.T., Ni, J., Shen, J., Bai, S., Teng, Y., 2020. Transcriptome analysis provides new insights into the transcriptional regulation of methyl jasmonate-induced flavonoid biosynthesis in pear calli. BMC Plant Biol 20. https://doi.org/10.1186/s12870-020-02606-x

Priyam, A., Das, R.K., Schultz, A., Singh, P.P., 2019. A new method for biological synthesis of agriculturally relevant nanohydroxyapatite with elucidated effects on soil bacteria. Sci Rep 9, 15083. https://doi.org/10.1038/s41598-019-51514-0

Rakoczy-Trojanowska, M., 2002. Alternative methods of plant transformation--a short review. Cell Mol Biol Lett 7, 849–58.

Schulz, C., Little, D.P., Stevenson, D.W., Bauer, D., Moloney, C., Stützel, T., 2010. An Overview of the Morphology, Anatomy, and Life Cycle of a New Model Species: The Lycophyte *Selaginella apoda* (L.) Spring. Int J Plant Sci 171, 693–712. https://doi.org/10.1086/654902

Sherman, B.T., Hao, M., Qiu, J., Jiao, X., Baseler, M.W., Lane, H.C., Imamichi, T., Chang, W., 2022. DAVID: a web server for functional enrichment analysis and functional annotation of gene lists (2021 update). Nucleic Acids Res 50, W216–W221. https://doi.org/10.1093/nar/gkac194

Silva Artur, M.A., Costa, M.-C.D., Farrant, J.M., Hilhorst, H.W.M., 2019. Genome-level responses to the environment: plant desiccation tolerance. Emerg Top Life Sci 3, 153–163. https://doi.org/10.1042/ETLS20180139

Sperschneider, J., Catanzariti, A.-M., DeBoer, K., Petre, B., Gardiner, D.M., Singh, K.B., Dodds, P.N., Taylor, J.M., 2017. LOCALIZER: subcellular localization prediction of both plant and effector proteins in the plant cell. Sci Rep 7. https://doi.org/10.1038/srep44598

Thagun, C., Horii, Y., Mori, M., Fujita, S., Ohtani, M., Tsuchiya, K., Kodama, Y., Odahara, M., Numata, K., 2022. Non-transgenic Gene Modulation *via* Spray Delivery of Nucleic Acid/Peptide Complexes into Plant Nuclei and Chloroplasts. ACS Nano 16, 3506–3521. https://doi.org/10.1021/acsnano.1c07723

Tuba, Z., Protor, C.F., Csintalan, Z., 1998. Ecophysiological responses of homoiochlorophyllous and poikilochlorophyllous desiccation tolerant plants: a comparison and an ecological perspective. Plant Growth Regul 24, 211–217. https://doi.org/10.1023/A:1005951908229

VanBuren, R., Wai, C.M., Ou, S., Pardo, J., Bryant, D., Jiang, N., Mockler, T.C., Edger, P., Michael, T.P., 2018. Extreme haplotype variation in the desiccation-tolerant clubmoss Selaginella lepidophylla. Nat Commun 9. https://doi.org/10.1038/s41467-017-02546-5

Wang, F., Zhu, H., Chen, D., Li, Z., Peng, R., Yao, Q., 2016. A grape bHLH transcription factor gene, VvbHLH1, increases the accumulation of flavonoids and enhances salt and drought tolerance in transgenic Arabidopsis thaliana. Plant Cell, Tissue and Organ Culture (PCTOC) 125. https://doi.org/10.1007/s11240-016-0953-1

Wang, G., ZHAO, Y., TAN, J., ZHU, S., ZHOU, K., 2015. Arginine functionalized hydroxyapatite nanoparticles and its bioactivity for gene delivery. Transactions of Nonferrous Metals Society of China 25, 490–496. https://doi.org/10.1016/S1003-6326(15)63629-9

Wang, K., 2006. Agrobacterium Protocols, 2nd ed. Humana Press Inc.

Wang, P., Zhao, F.-J., Kopittke, P.M., 2019. Engineering Crops without Genome Integration Using Nanotechnology. Trends Plant Sci 24, 574–577. https://doi.org/10.1016/j.tplants.2019.05.004

Wang, X., Chen, S., Zhang, H., Shi, L., Cao, F., Guo, L., Xie, Y., Wang, T., Yan, X., Dai, S., 2010. Desiccation Tolerance Mechanism in Resurrection Fern-Ally *Selaginella tamariscina* Revealed by Physiological and Proteomic Analysis. J Proteome Res 9. https://doi.org/10.1021/pr100767k

Waseem, M., Rong, X., Li, Z., 2019. Dissecting the Role of a Basic Helix-Loop-Helix Transcription Factor, SlbHLH22, Under Salt and Drought Stresses in Transgenic Solanum lycopersicum L. Front Plant Sci 10. https://doi.org/10.3389/fpls.2019.00734

Weng, J.-K., Noel, J.P., 2013. Chemodiversity in Selaginella: a reference system for parallel and convergent metabolic evolution in terrestrial plants. Front Plant Sci 4. https://doi.org/10.3389/fpls.2013.00119

Wituszynska, W., Karpiński, S., 2014. Determination of Water Use Efficiency for Arabidopsis thaliana. Bio Protoc. https://doi.org/10.21769/BioProtoc.1041

Xu, Z., Xin, T., Bartels, D., Li, Y., Gu, W., Yao, H., Liu, S., Yu, H., Pu, X., Zhou, J., Xu, J., Xi, C., Lei, H., Song, J., Chen, S., 2018. Genome Analysis of the Ancient Tracheophyte Selaginella tamariscina Reveals Evolutionary Features Relevant to the Acquisition of Desiccation Tolerance. Mol Plant 11, 983–994. https://doi.org/10.1016/j.molp.2018.05.003

Ye, J., Yang, H., Shi, H., Wei, Y., Tie, W., Ding, Z., Yan, Y., Luo, Y., Xia, Z., Wang, W., Peng, M., Li, K., Zhang, H., Hu, W., 2017. The MAPKKK gene family in cassava: Genome-wide identification and expression analysis against drought stress. Sci Rep 7, 14939. https://doi.org/10.1038/s41598-017-13988-8

Yobi, A., Wone, B.W.M., Xu, W., Alexander, D.C., Guo, L., Ryals, J.A., Oliver, M.J., Cushman, J.C., 2013. Metabolomic Profiling in Selaginella lepidophylla at Various Hydration States Provides New Insights into the Mechanistic Basis of Desiccation Tolerance. Mol Plant 6. https://doi.org/10.1093/mp/sss155

Yobi, A., Wone, B.W.M., Xu, W., Alexander, D.C., Guo, L., Ryals, J.A., Oliver, M.J., Cushman, J.C., 2012. Comparative metabolic profiling between desiccation-sensitive and desiccation-tolerant species of *Selaginella* reveals insights into the resurrection trait. The Plant Journal 72. https://doi.org/10.1111/tpj.12008

Yoo, C.Y., Pence, H.E., Jin, J.B., Miura, K., Gosney, M.J., Hasegawa, P.M., Mickelbart, M. V., 2011. The Arabidopsis GTL1 Transcription Factor Regulates Water Use Efficiency and Drought Tolerance by Modulating Stomatal Density via Transrepression of SDD1. Plant Cell 22. https://doi.org/10.1105/tpc.110.078691

Yuan, G., Lu, H., Tang, D., Hassan, M.M., Li, Y., Chen, J.-G., Tuskan, G.A., Yang, X., 2021. Expanding the application of a UV-visible reporter for transient gene expression and stable transformation in plants. Hortic Res 8, 234. https://doi.org/10.1038/s41438-021-00663-3

Yuan, H., Liu, D., 2012. Functional disruption of the pentatricopeptide protein SLG1 affects mitochondrial RNA editing, plant development, and responses to abiotic stresses in Arabidopsis. The Plant Journal 70, 432–444. https://doi.org/10.1111/j.1365-313X.2011.04883.x

Zhang, J., Wang, S., 2009. Topical use of Coenzyme Q10-loaded liposomes coated with trimethyl chitosan: Tolerance, precorneal retention and anti-cataract effect. Int J Pharm 372, 66–75. https://doi.org/10.1016/j.ijpharm.2009.01.001

Zhang, X., Henriques, R., Lin, S.-S., Niu, Q.-W., Chua, N.-H., 2006. Agrobacterium-mediated transformation of Arabidopsis thaliana using the floral dip method. Nat Protoc 1. https://doi.org/10.1038/nprot.2006.97

Appendix: Supporting materials for Chapter 4

Table S1 - A table summarizing the sequencing data quality of *S. lepidophylla* dehydration time course samples. **Sample** - sample name, **Raw reads**: Total amount of reads of raw data, **Raw data**: (Raw reads) * (sequence length), calculating in G, **Effective**: (Clean reads/Raw reads) *100%, **Error**: base error rate, **Q20, Q30**: (Base count of Phred value > 20 or 30) / (Total base count), **GC**: (G & C base count) / (Total base count)[2]

Sample	Raw reads	Raw data	Effective(%)	Error(%)	Q20(%)	Q30(%)	GC(%)
B1-100	63252252	9.5	98.08	0.03	97.56	93.28	52.43
B2-100	51853340	7.8	97.96	0.03	96.80	91.49	52.37
B3-100	40195300	6.0	98.08	0.03	97.67	93.44	52.29
B1-85	50132774	7.5	97.70	0.03	97.54	93.27	52.66
B2-85	57622032	8.6	97.35	0.03	97.47	93.09	52.38
B3-85	50045008	7.5	97.65	0.03	97.84	93.83	52.42
B1-75	53129746	8.0	97.67	0.03	97.36	92.84	52.40
B2-75	47571226	7.1	97.63	0.03	97.79	93.76	52.29
B3-75	50089370	7.5	97.98	0.03	97.62	93.37	52.63
B1-50	57729558	8.7	97.74	0.03	97.58	93.30	52.69
B2-50	57968712	8.7	97.77	0.03	97.57	93.22	52.52
B3-50	42218236	6.3	97.41	0.03	97.72	93.60	52.32
B1-25	44441624	6.7	97.93	0.03	97.65	93.42	52.59
B2-25	52793746	7.9	98.23	0.03	97.51	93.14	52.68
B3-25	41942896	6.3	98.07	0.03	97.64	93.38	52.41

[2] Sample labelling: **B1, B2 and B3** - Biological replicates, **100** – 100% RWC, **85** – 85% RWC, **75** – 75% RWC, **50** – 50% RWC, **25** – 25% RWC

Table S2 – Read-mapping statistics. Alignment rates for the of *S. lepidophylla* dehydration time course samples.[3]

Sample ID	Total seqs (millions)	Reads Mapped (millions)	Reads mapped (%)
B1-100	63.3	59.2	93.60%
B2-100	51.9	48.6	93.60%
B3-100	40.2	37.9	94.20%
B1-85	50.1	47	93.80%
B2-85	57.6	54.3	94.30%
B3-85	50	47.2	94.30%
B1-75	53.1	49.9	94.00%
B2-75	47.6	44.1	92.70%
B3-75	50.1	47.3	94.40%
B1-50	57.7	53.8	93.20%
B2-50	58	54.5	94.10%
B3-50	42.2	39.7	94.10%
B1-25	44.4	41.9	94.30%
B2-25	52.8	49.9	94.50%
B3-25	41.9	39.6	94.50%

[3] Sample labelling: **B1, B2 and B3** - Biological replicates, **100** – 100% RWC, **85** – 85% RWC, **75** – 75% RWC, **50** – 50% RWC, **25** – 25% RWC

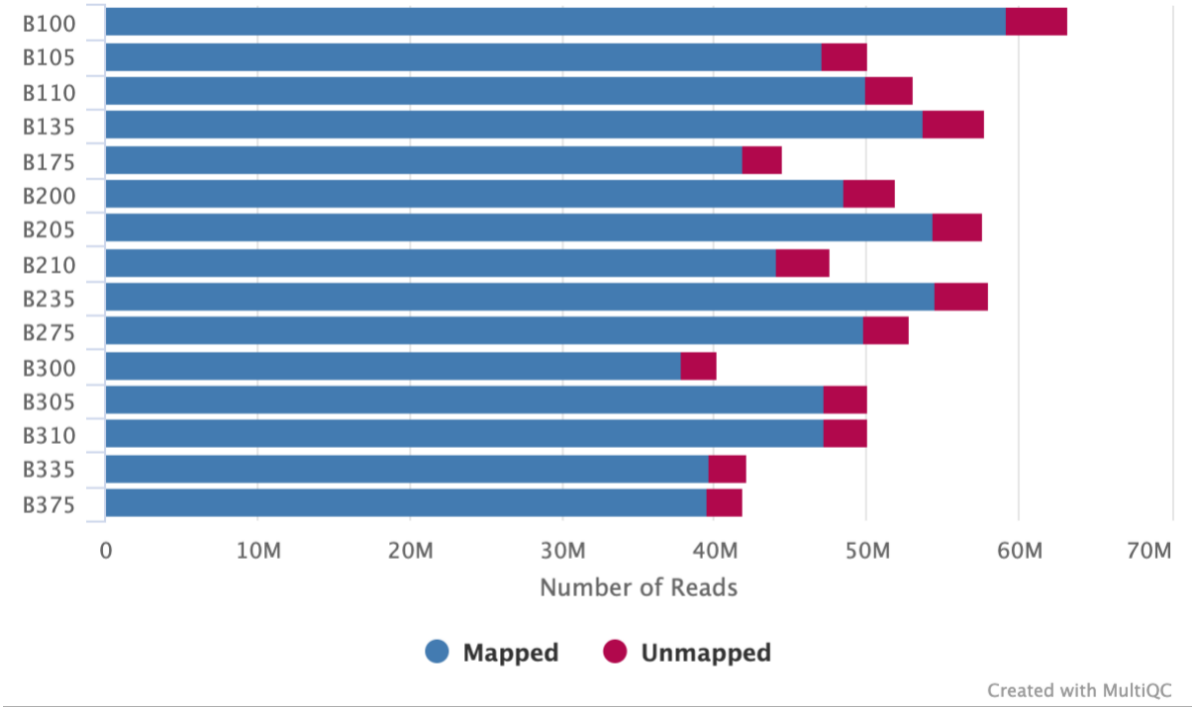

Figure S.1 – Precent Mapped. Alignment metrics from samtools stats; mapped vs. unmapped reads[4].

[4] Sample labelling: **B1, B2 and B3** - Biological replicates, **00** – 100% RWC, **05** – 85% RWC, **10** – 75% RWC, **35** – 50% RWC, **75** – 25% RWC